

A. Shibuya

ISSN 0385-2520

Rock Magnetism and Paleogeophysics

**volume 9
1982**

Published by the

ROCK MAGNETISM AND PALEOGEOPHYSICS RESEARCH GROUP IN JAPAN

PREFACE

This volume is an annual progress report of the Rock Magnetism and Paleogeophysics Research Group in Japan for the year 1982. As the previous reports were so, this volume contains a collection of summaries, extended abstracts or brief notes of the research works carried out in our group this year. Many of the reports contain materials which may undergo a significant revision or may be updated as the research activity continues. In this respect, the readers are warned to regard them as tentative, and also requested to refer from a complete paper if such is published as a final result.

One of the active areas in the recent paleomagnetic researches is that concerning accretion tectonics and the origins of the exotic terranes. This year's volume contains some papers in this field. Izu Peninsula, about a hundred kilometers from Tokyo, is generally thought to represent a portion of Philippine Sea Plate, now actively colliding to the Honshu Arc. Many of the tectonic problems in the Central Japan are directly or indirectly related to this collision. One of the chief objectives of the Japanese Lithosphere Project (dubbed DELP, for Dynamics and Evolution of the Lithosphere Project), which presumably starts in 1984 with a special Government grant, is to clarify the nature of the geologic bodies forming the Japanese islands, and a lot of allochthonous terranes are expected in them. The studies in this direction will undoubtedly prosper in the coming years.

This volume contains a list of fission-track ages obtained in Japan. This was included by a special request from the compilers. Although it has not been the custom of this Annual Report to publish a review or compiled material, such a list may be quite useful to paleomagnetism and paleogeophysics community at large. We hope that this volume is a useful reference for the current and recent researches in the fields of rock magnetism and paleogeophysics in Japan.

Tokyo
December 1982

Masaru Kono

Editor

TABLE OF CONTENTS

Preface	i
Table of Contents	ii
Rock Magnetism and Paleogeophysics Symposium 14	iv
M. Torii, A. Dharma, and T. Yokoyama Thermal Demagnetization Experiments of Welded Tuff, Sigura-gura Formation, Sumatra, Indonesia	1
Y. Onda, S. Sugihara, T. Furuta, and T. Akimoto Paleomagnetic Results of the Ofuna Formation, Miura Peninsula	4
H. Tsunakawa, and Y. Hamano Paleomagnetism of the Ashitaka Dike Swarm	9
T. Nakajima Blake Polarity Episode in a Volcanic Ash Layer with the Fission Track Age of 0.12 Ma	13
E. Kikawa, T. Akimoto, H. Kinoshita, and T. Furuta Paleomagnetism of Daruma Volcano and Adjacent Areas, Northwest Izu Peninsula, Japan	17
H. Ito, K. Tokieda, and Y. Notsu Remanent Magnetization of The Koyama Intrusive Complex, Yamaguchi Prefecture, Southwest Japan	24
H. Ito Correlation of Igneous Activities of Granitic Rocks with Geomagnetic Field Reversals during Late Tertiary	27
H. Domen On a Paleo/Rock Magnetic Study of the Metamorphic Rocks from Susa District, Northeastern Yamaguchi Prefecture, Japan	33
H. Domen, and H. Muneoka A Paleomagnetic Study of the Cenozoic Rocks from the Amakusa Islands, Westcentral Kyushu, West Japan	36
Y. Otofujii, and T. Matsuda Paleomagnetism of Igneous Rocks of Late Cretaceous to Miocene Age from The Go River Area -- Clockwise Rotation of Southwest Japan --	41
H. Domen Thermomagnetic Analysis of the Cretaceous Rock from Taikazan District, Tokuyama City, Yamaguchi Prefecture, West Japan	49

Y. Notsu and H. Ito		
	Paleomagnetism of Cretaceous Granitic Rocks from Okushiri Island, West Hokkaido	53
T. Tosha		
	Paleomagnetic Measurement of the Miyako Group in the Kitakami Massif, Northeast Japan	56
H. Domen		
	A couple of Paleomagnetic Data of the Cretaceous Rocks from Yamaguchi and Shimane Prefectures, West Japan	61
M. Kono, Y. Fukao, Y. Hamano, K. Heki, H. Kinoshita, Y. Onuki, A. Taira, T. Ui, and L. Ocola		
	Geophysical Studies of the Central Andes	66
K. Heki, Y. Hamano, and M. Kono		
	Paleomagnetic Study in Andean Peru: Cretaceous Sediments and Volcanics	72
M. Funaki		
	Natural Remanent Magnetizations of Beacon Group in McMurdo Sound, Antarctica	80
M. Funaki		
	A Preliminary Investigation of Basement Complex in Wright Valley, McMurdo Sound, Antarctica	88
H. Domen		
	On Thermomagnetic Property of So-called "Magnetic Stone" from Ii-no-Ura District, Masuda City, West Japan	96
H. Muneoka and H. Domen		
	Errors in Analyses of NRM Using Magnetic Dipole Models	99
O. Oshima		
	Reduction Decomposition of Hemimagnetite in a Cooling Magma and Its Relation to the Changes of Magnetization of Rocks	102
K. Kobayashi, T. Furuta, and T. Ishii		
	Reconnaissance Paleomagnetic and Rock Magnetic Investigation of Basaltic Rocks from Ponape Island, East Carolines	106
I. Kaneoka		
	K-Ar Age Determination of the Late Tertiary and Quaternary Andean Volcanic Rocks, Southern Peru	111
Y. Amano and S. Nishimura		
	The List of Fission-Track Ages (1) (1970-1978)	117
Author Index		126

ROCK MAGNETISM AND PALEOGEOPHYSICS SYMPOSIUM 14

The fourteenth Rock Magnetism and Paleogeophysics Symposium was held on 15 and 16 July, 1982 at Arima Hot Spa, Hyogo Prefecture. The following papers were presented.

15 July, Morning

1. S. Uchiyama, T. Date and K. Hirooka (Toyama Univ.)
Paleomagnetic study in the Hida Belt, Central Japan.
2. Y. Morinaga and Y. Fujiwara (Hokkaido Univ.)
Magnetic properties of some Paleozoic rock in the southern Kitakami terrane.
3. H. Shibuya (Kyoto Univ.)
A paleomagnetic study on red cherts in Inuyama area, Central Japan -- Polarity change frequency in Triassic.
4. Y. Maeda (Kyoto Univ.)
Paleomagnetic study on acidic tuffs in the Shimanto Belt.
5. A. Hayashida (Kyoto Univ.)
Paleomagnetism of the Miocene Ichishi Group.
6. M. Kono (Tokyo Inst. Tech.)
On the Development and Exploration of the Lithosphere Project (DELP).

15 July, Afternoon

7. M. Koyama and N. Niitsuma (Shizuoka Univ.)
Preliminary report on paleomagnetism of the Matsuzaki area in the western part of Izu Peninsula, Central Japan.
8. K. Hirooka, T. Takahashi and H. Sakai (Toyama Univ.)
Paleomagnetic study in Izu Peninsula.
9. H. Sakai, A. Takeuchi and K. Hirooka (Toyama Univ.)
Paleomagnetic study of Tertiary dykes in the southern North-East Japan.
10. M. Torii (Kyoto Univ.)
Paleomagnetic study of core samples from Lake Biwa (Preliminary report).
11. M. Funaki (Nat. Inst. Pol. Res.)
Cenozoic paleomagnetism in McMurdo Sound, Antarctica.
12. I. Katsura (Kyoto Univ.)
Post-depositional remanent magnetization of artificial sediment during normal/reversed boundary.
13. S. Okada (Tottori Univ.)
Post-DRM fixed in the Pleistocene diatomite.
14. H. Tanaka (Tokyo Inst. Tech.)
Unstable thermoremanent (?) magnetization in the baked stones of the Paleolithic age.

15. M. Yoshida (Hokkaido Univ.)
Mode of remanent magnetization of the pyroclastic flow deposit.
16. E. Kigawa (Chiba Univ.)
Chemical composition of titanomagnetites including red and blue grains and its possible effect on the thermomagnetic curve.
17. K. Kobayashi (Tokyo Univ.)
Paleomagnetism of Neogene ophiolites in Japan.

16 July, Morning

18. K. Tokieda (Shimane Univ.)
Paleomagnetism of granites from Mahe Island, Seychelles.
19. M. Kono (Tokyo Inst. Tech.), K. Heki and Y. Hamano (Tokyo Univ.)
On the tectonics of the Central Andes.
20. K. Heki (Tokyo Univ.)
On the mechanism and the timing of the bending of the Central Andes.
21. N. Niitsuma (Shizuoka Univ.)
Subduction of the Philippine sea plate and magnetostratigraphy in the southern part of Boso Peninsula and Tanzawa area, Central Japan.

16 July, Afternoon

22. H. Ito (Shimane Univ.)
A correlation of igneous activities and field reversals in Tertiary.
23. S. Yoshida (Kyoto Univ.)
Paleomagnetism in Boso Peninsula -- its relation with tectonic movement of Miura Peninsula.
24. H. Domen (Yamaguchi Univ.)
Some problems of thermomagnetic analysis.
25. H. Muneoka and H. Domen (Yamaguchi Univ.)
On analytical errors of NRM measurement of rocks as a magnetic dipole.
26. N. Niitsuma (Shizuoka Univ.)
Ring core fluxgate spinner magnetometer.
27. S. Sasajima (Kyoto Univ.)
Paleomagnetic relation between Chinese blocks and Southwest Japan.

THERMAL DEMAGNETIZATION EXPERIMENTS OF WELDED TUFF,
SIGURA-GURA FORMATION, SUMATRA, INDONESIA

Masayuki TORII*, Agus DHARMA** and Takuo YOKOYAMA***

* Department of Geology and Mineralogy, Kyoto University, Kyoto 606, Japan

** National Institute of Geology and Mining, Bandung, Indonesia

*** Laboratory of Earth Sciences, Doshisha University, Kyoto 602, Japan

A large volume of acidic volcanic materials are distributed around Lake Toba in northern Sumatra, Indonesia (Fig. 1). These volcanic products, so-called "Toba Tuff", are stratigraphically subdivided into three units; namely TukTuk Dacite, Older Toba Tuff, and Younger Toba Tuffs in ascending order (Yokoyama et al., 1980, Yokoyama and Hehanusa, 1981). Among them, Younger Toba Tuffs are divided into two formations. The upper one is Sigura-gura Formation, and the lower one is Haranggaol Formation.

Radiometric age determination of the Sigura-gura Formation has been carried out by Ninkovich(1976) and Nishimura et al(1978). The value is 75,000 years B.P. in K-Ar age and 0.1 ± 0.02 Ma in fission-track age respectively. Reversed paleomagnetic polarity of the Sigura-gura Formation has been also reported by Sasajima et al.(1980) and Yokoyama and Dharma(1982). Sasajima et al.(1983) has made a precise discussion on the reversed polarity record at the age of 0.1 Ma in Japan and Indonesia, and they concluded the Sigura-gura Formation to be a land-section recording the Blake Event.

Main purpose of this short report is to present a result of a thermal demagnetization experiment which was not performed in the previous works. Three types of specimen were collected from the Sigura-gura Formation along Asahan River for this study. Type 1 is a densely welded, black, glassy tuff from the basal part of the formation. Type 2 is a densely welded, white, devitrified tuff sampled at horizon of 50 m above the base. Type 3 is a slightly weathered welded tuff collected from the uppermost part of the formation. Though the vertical distance from type 1 to 3 is about 400 m, all specimens are presumed to belong with a single flow unit.

Result of an alternating field demagnetization up to 1600 Oe of type 1 specimen is shown in Fig. 2. Only a little portion of soft component, which was magnetized parallel to the present geomagnetic field, was removed up to 200 Oe. The median destructive field value is about 900 Oe. The other types also show quite stable nature of remanence when alternating field is applied as same as type 1.

Thermal demagnetization experiments were carried out on each type of rocks as typically shown in Fig. 3. Same as the case of alternating field demagnetization, very small secondary component parallel to the present field was removed up to 300°C. Then dominant phase of the remanence was reduced smoothly toward the origin in orthogonal projection diagram. The blocking temperature is identical with that of magnetite. There is no significant directional change of remanent vector in any case. Both alternating field and thermal demagnetization experiments show that the natural remanent magnetization of the rocks from Sigura-gura Formation are quite stable and reliable.

In order to test the possibility of self-reversal phenomenon and also to determine paleointensity, the Thellier experiment was

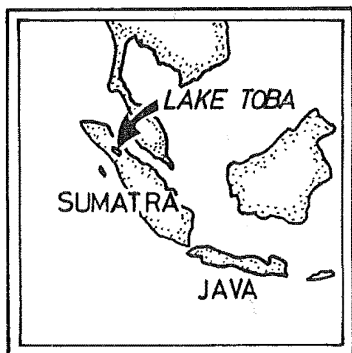


Fig. 1 Index map

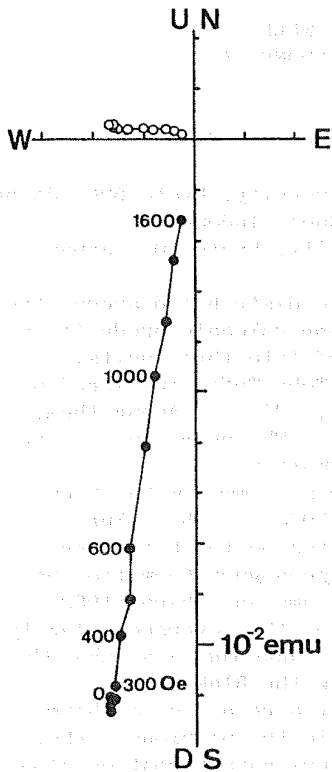
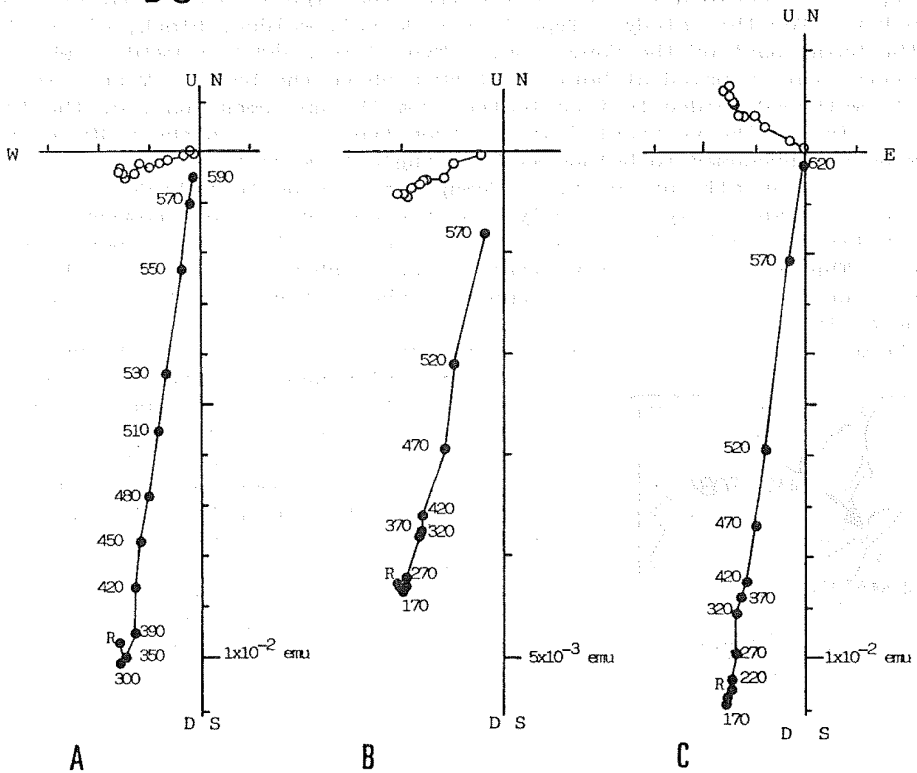


Fig. 2(left) Progressive alternating field demagnetization of type 1 rock. Solid circles indicate the projections on the horizontal plane; open circles the projections on the vertical EW plane. Numbers denote successive peak alternating filed value in Oe.

Fig. 3(below) Progressive thermal demagnetization of type 1 (A), type 2 (B), and type 3 (C). Method of projection is same manner as Fig. 2. Numbers denote successive demagnetization temperature in degrees Celsius. "R" indicate room temperature.



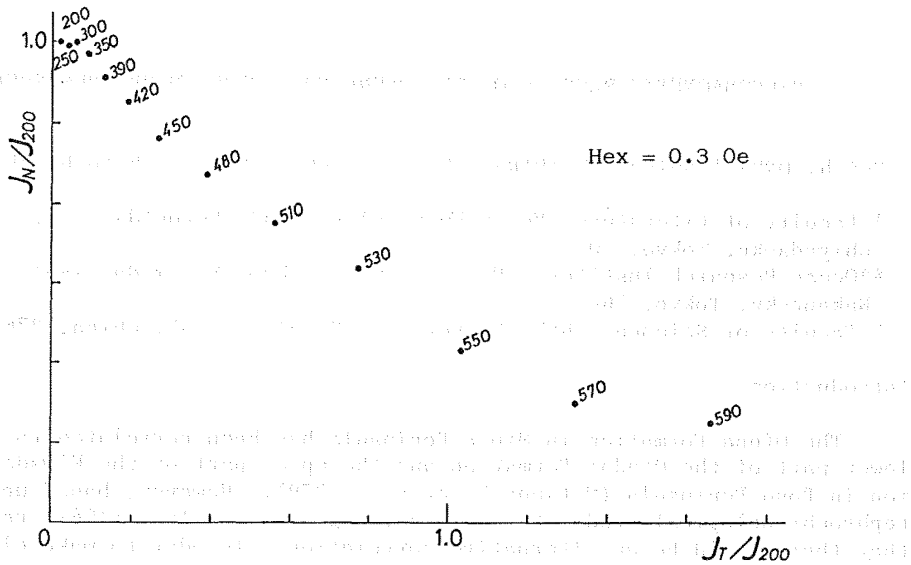


Fig. 4 NRM-TRM plot determined by the Thellier's method for type 1 rock. NRM and TRM value are divided by the NRM value of 200°C demagnetization to ignore initial soft component. Numbers denote temperature of treatment in degrees in Celsius.

carried out preliminarily. Though the possibility of self-reversal was not found, NRM-TRM plot did not make a straight line. As shown in Fig. 4, the line is concave-down curvature over the entire temperature range. This may mean a continuous increase of TRM acquisition ability in the higher temperature range. The cause of the behavior may be attributed to the high-temperature oxidation of homogeneous titanomagnetite into Ti-poor titanomagnetite and ilmenite during the course of heating experiment. The presence of such a homogeneous titanomagnetite was inferred from the result of thermomagnetic analysis. For example, type 1 rock specimen showed the Curie point at 460°C and 580°C on heating cycle. Lower Curie point was not observed on smooth cooling curve and an increase of magnetization was recognized. Though the type 1 rock is very fresh in its appearance, it is not favorable sample for Thellier experiment. We are now trying to perform Thellier experiment for the type 3 rock whose Js-T curve looks rather reversible in spite of its weathered appearance.

References:

Ninkovich, D. (1976) *Earth Planet. Sci. Lett.*, 29, 269.
 Nishimura, S., S.Sasajima, K.Hirooka, K.H.Thio and F.Hehuwat (1978) On the study of physical geology of the Sunda Island Arc (ed. S.Sasajima), Kyoto University, 38.
 Sasajima, S., S.Nishimura and K.Hirooka (1980) *Rock Mag. Paleogeophys.*, 7, 90.
 Sasajima, S., S.Nishimura and K.Hirooka (1983) *J. Geomag. Geoelectr.*, in press
 Yokoyama, T., S.Nishimura, E.Abe, Y.Otofujii, T.Ikeda, S.Sparka and A.Dharma (1980) *Phys. Geol. Indonesian Island Arcs* (ed. S.Nishimura), 122.
 Yokoyama, T. and P.E.Hehanussa (1981) *Paleolim. Lale Biwa Jap. Plei.*, 9, 177.
 Yokoyama, T and A. Dharma (1982) *United Nations ECAFE, CCOP Tech. Bull.*, 14, in press

PALEOMAGNETIC RESULTS OF THE OFUNA FORMATION, MIURA PENINSULA

Yuichi ONDA,* Shigeo SUGIHARA,* Toshio FURUTA,** and Takatoshi AKIMOTO^o

* Faculty of Literature, Meiji University, Kanda Surugadai 1-1,
Chiyoda-ku, Tokyo, 101

**Ocean Research Institute, University of Tokyo, Minamidai 1-51-1,
Nakano-ku, Tokyo, 164

^o Faculty of Science, Chiba University, Yayoicho 1-33, Chiba, 276

Introduction

The Ofuna Formation in Miura Peninsula has been correlated to the lower part of the Otadai Formation and the upper part of the Kiwada Formation in Boso Peninsula (Mitsunashi et al., 1979). However, based upon tephrochronological study of this area, Sugihara and Arai (1981) revealed that there could be an alternative correlation. In order to make clear the correlation between Miura Peninsula and Boso Peninsula, paleomagnetic study has just been started. This is the first report of the result.

Samples

Location of outcrops for this study is in Kamariya area, south of Yokohama, at $35^{\circ}18'30''$ N, $139^{\circ}36'27''$ E (Fig 1).

Marine sediment named Kazusa Group from Pliocene to Pleistocene in age is distributed over the northern part of Miura Peninsula. The Kazusa Group has thickness of about 500m in this area, and is geologically divided into the following five formations; Nojima-Urago Formation, Ofuna F., Nakazato F., and Hama F.. The Ofuna Formation consists of lump mudstone and is intercalated by many tephras some of which are good key beds. According to the correlation to the type formation in Boso Peninsula, the tephras in Ofuna Formation from the lower to the top, are Kd 23, Kd 19, O 27, and O 26, respectively (Mitsunashi et al., 1979). According to Sugihara and Arai (1981), this correlation of tephras is insufficient.

All of the samples were collected using a portable rock drill. Specimens (2.54 cm in length and diameter) were measured by means of Schonsted spinner magnetometer at the Ocean Research Institute, University of Tokyo. After measurement of NRM, all of 57 specimens were used for stepwise AF demagnetization with the peak demagnetization field of 10, 25, 50, 75, 100, 150, 200, 300, Oe. Each specimen was also used for measurement of initial magnetic susceptibility and Qn-ratio, and thermomagnetic analysis. In the thermomagnetic analysis, magnetic minerals were separated from the specimens by hand magnet in acetone.

Location of Sampling site

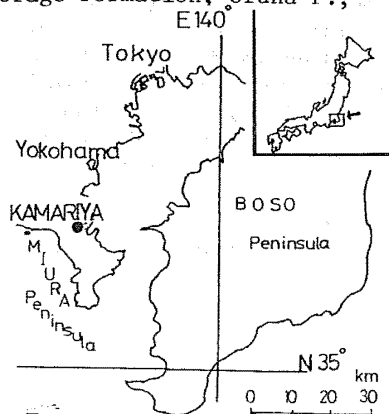


Fig 1

Results

41 specimens show a good stability in AF demagnetization, while the

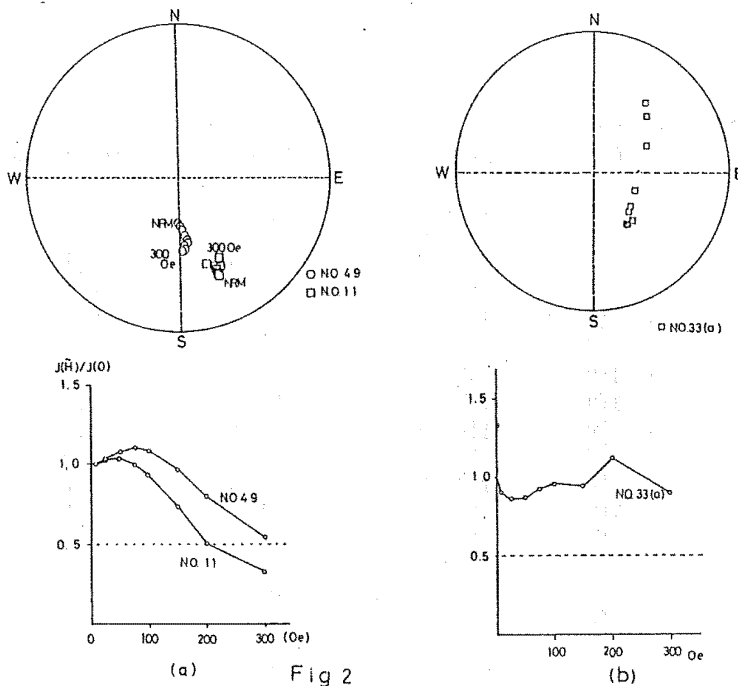


Fig 2
Typical examples the result of
AF demagnetization

rest 16 specimens have unstable components. Typical examples of the results of AF demagnetization are shown in Fig.2. Thermomagnetic analysis was performed on one specimen in vacuum (10^{-4} - 10^{-6} torr) and in a strong magnetic field of 4.5kOe and at a heating and cooling rate of $6^{\circ}/\text{min}$. As shown in Fig.3, almost reversible thermomagnetic curve was obtained. This result indicates the presence of Ti-poor Titanomagnetite. So, the secondary remanent magnetization produced by oxidation of titanomagnetite is considered to be very small.

The mean directions of NRM are listed in Table 1, and shown in Fig.4. All of the specimens have reversed NRM. Virtual geomagnetic poles (VGP) were also calculated and their changes are shown in Fig.5.

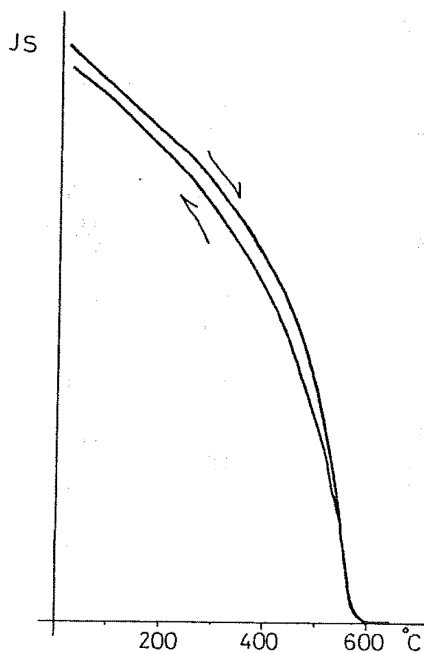


Fig 3
Result of thermomagnetic
analysis; Specimen NO.57

Sample NO. AC-field Declination Inclination Intensity Qn
 (Oe) (Degree) (Degree)(x10E-5:emu/g)

1	(50)	163.9	-31.5	2.0	0.04
2	(75)	163.8	-19.8	2.1	0.03
3	(100)	167.1	-29.0	1.8	0.02
4	(75)	156.3	-39.5	1.7	0.01
5	(50)	166.4	-38.3	1.5	0.02
6	(25)	-179.3	-53.7	2.0	0.05
7	(100)	-176.4	-55.2	2.0	0.04
8	(100)	179.3	-50.8	2.2	0.04
9	(50)	159.8	-49.3	2.5	0.05
11	(75)	157.7	-32.7	3.1	0.11
12	(50)	149.5	-31.4	3.6	0.11
15	(100)	156.3	-35.7	2.5	0.04
16	(100)	156.3	-59.6	1.9	0.05
18	(150)	171.9	-36.5	2.1	0.03
20	(50)	166.8	-40.4	3.0	0.09
21	(150)	155.3	-40.3	2.6	0.07
23(a)	(100)	-176.2	-46.2	2.3	0.03
24	(75)	170.6	-38.9	2.7	0.07
30(a)	(75)	-178.2	-48.9	1.5	0.02
32	(50)	159.3	-42.7	1.5	0.03
33(a)	(100)	143.3	-50.2	1.2	0.04
34	(50)	162.5	-34.5	1.7	0.03
37(a)	(75)	175.1	-33.3	2.1	0.02
38(a)	(75)	-143.8	-53.2	2.4	0.03
39	(100)	171.9	-57.0	2.4	0.04
41	(100)	-166.0	-57.2	2.8	0.09
42	(75)	-179.0	-38.8	2.2	0.07
43	(150)	176.5	-40.8	3.1	0.11
44	(100)	165.6	-56.6	3.0	0.07
46	(50)	178.5	-47.1	2.8	0.07
47	(75)	179.3	-46.3	2.8	0.10
48	(100)	-178.0	-43.9	2.7	0.06
49	(200)	174.1	-49.1	2.8	0.13
50	(150)	-167.1	-48.2	2.0	0.04
51	(150)	170.2	-40.7	1.8	0.04
52	(75)	-169.1	-48.7	3.3	0.08
53	(50)	164.7	-50.6	3.9	0.11
54	(100)	-177.2	-47.8	3.2	0.08
55(a)	(100)	178.3	-39.3	2.2	0.07
56	(50)	173.6	-39.0	2.3	0.07
57(a)	(75)	168.5	-43.9	2.5	0.08

Table 1
 Summary of the measurement

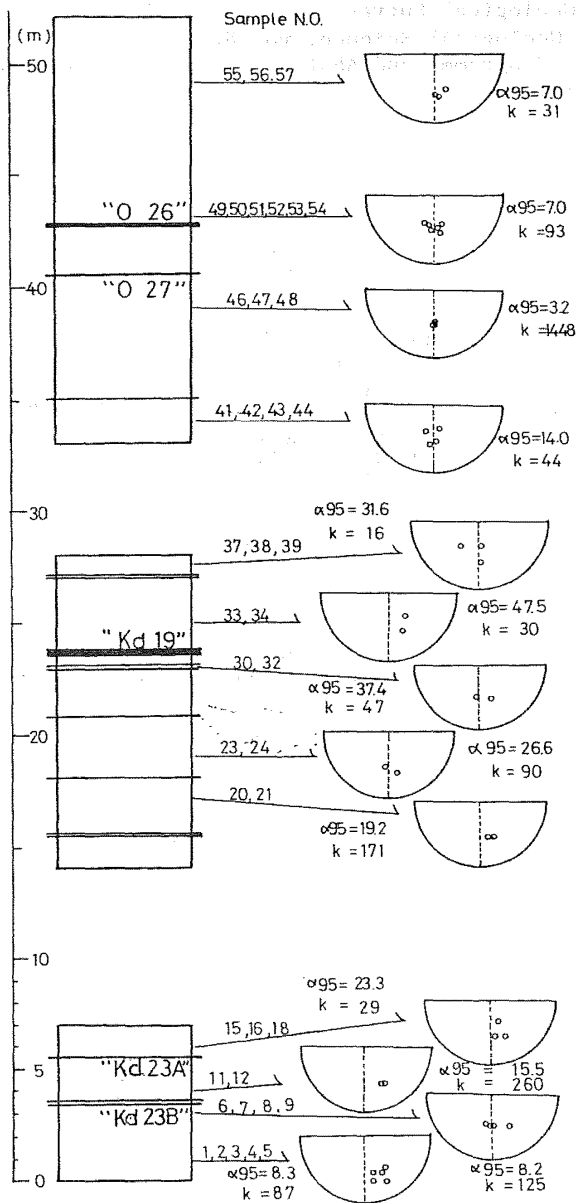


Fig 4

Picture of reversed NRM

Discussion

In this study no normal NRM was found, whereas according to Niitsuma (1976, Fig 6) several normal NRM were deduced from his paleomagnetic stratigraphy of the formations in Boso Peninsula corresponding to Ofuna formation (upper Kiwada F., lower Otadai F.). The following three reasons are considered why no normal NRM was found in the present study; 1) Samples having normal NRM were not collected because of the difficulty in the field survey. 2) Correlation of the critical formation of both Boso and Miura Peninsula are insufficient. 3) Another unknown reason. In order to make clear the problem suggested by this study, more detailed paleomagnetic investigation are essential.

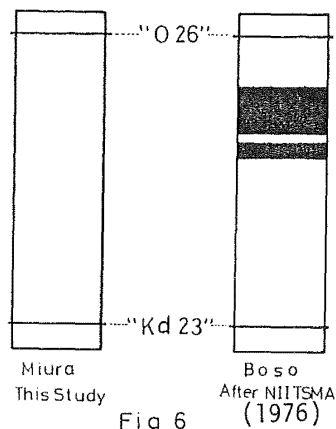


Fig 6

Paleomagnetic stratigraphy between "Kd 23" and "O 26".

References

- T. Mitsunashi et al., 1979; Explanatory Text Of The Geological Map Of Tokyo Bay and Adjacent Areas.(Geological Survey of Japan) p.91
N. Niitsuma., 1976; Journal of Geological Science, vol 82
S. Sugihara and F. Arai., 1981; Programme and Abstracts, Japan Association for Quaternary Research, vol 11

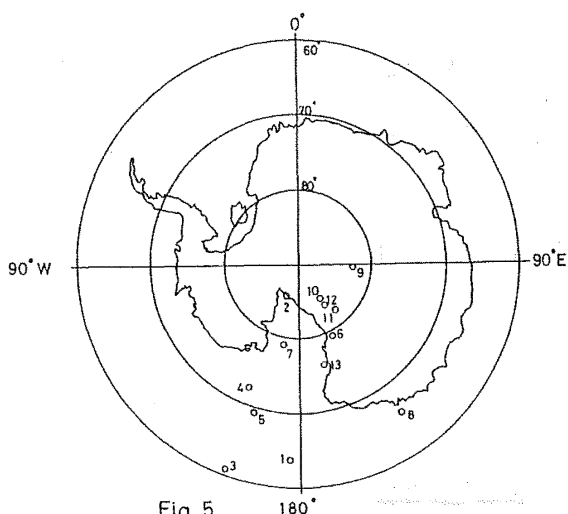


Fig 5
Change of VGP

PALEOMAGNETISM OF THE ASHITAKA DIKE SWARM

Hideo TSUNAKAWA and Yozo HAMANO

Geophysical Institute, University of Tokyo,
Tokyo 113, Japan

1. Introduction

We have performed paleomagnetic studies on Miocene dike swarms in Japan (Heki and Tsunakawa, 1981; Tosha and Tsunakawa, 1981; Tsunakawa, 1982). The activity duration of a dike swarm, which occurs usually as more than one hundred intrusions, is regarded as almost similar to that of a stratovolcano, 10^5 years (Nakamura, 1977). A dike swarm, therefore, possibly records the paleosecular variation of the geomagnetic field during sufficient time span to average out it and yields a reliable mean field direction. In order to examine on this assumption, we have carried out paleomagnetic study on the Pleistocene dike system, the Ashitaka dike swarm.



Fig.1 Ashitaka volcano and adjacent area.

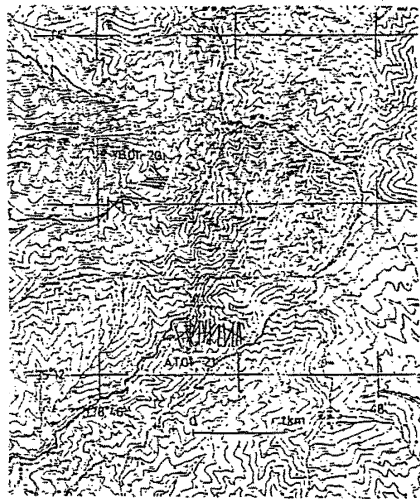


Fig.2 Localities of the AT01-21 and YB01-20 dikes. Direction of solid bar denotes a strike of dike.

2. Geological outline of the Ashitaka dike swarm

The Ashitaka volcano is located in the southward of Mt. Fuji and situated near the plate boundary between the Philippine Sea plate (Izu Peninsula) and the Eurasian plate (Central Japan) as shown in Fig.1. The Ashitaka volcano is constructed with three strata; (1) the older basaltic ejecta, a lowermost stratum, (2) the younger andesitic ejecta, and (3) the Ashitaka loam, an uppermost stratum (Sawamura, 1955). The

Ashitaka dike swarm, which intruded into the Ashitaka volcanic edifice, has been investigated geologically by Ishida(1981). According to Ishida(1981), the Ashitaka dike swarm has more than two hundred outcrops and shows a radial pattern. The width of dikes ranges from 0.2 to 5m. The dikes consist of three types of rocks: (1) basalt, (2) pyroxene andesite, and (3) hornblende andesite. The dike intrusions would have occurred as related to the eruption of the older basaltic and younger andesitic lavas. The volcanism of the Ashitaka region probably took place in the Pleistocene as well as those of the Hakone and Fuji volcanoes.

Three to six specimens of dike rocks were orientated with a magnetic compass and collected by hand sampling from each of about forty dikes, which are exposed along the dissected valley (Fig.2). As shown in Fig.2, most dikes of the AT01-21 series in the southern valley intruded in the N-S trend and the YB01-20 series in the E-W trend. Judged from the direction of strikes of dikes, each of these intrusions presumably occurred at the independent time. The remanent magnetization of the samples was measured under the AF demagnetization stepwisely until the intensity decreased up to one tenth of NRM. A site mean direction of remanences for each step of the AF demagnetization was calculated with the Fisherian statistics (Fisher, 1953), those of which with the largest value of k were taken for the representative ones.

3. Results and discussion

Paleomagnetic results of the samples AT01-21 are summarized in Table 1. These samples are quite stable against the AF demagnetization. An example of the result in the AF demagnetization is shown in Fig.3. MDFs of the samples range from 5 to 80mT, most of which are within 10 to 40mT. Site mean directions of remanences are projected in the equal area net of Fig.4 and their corresponding VGPs in that of Fig.5. In Fig.4, all of the AT 01-21 dike rocks are found to be of normal polarity. As mentioned earlier, the Ashitaka dike swarm probably occurred in the Pleistocene. The normal polarity of these remanences suggests that the AT01-21 dikes might have intruded during the Brunhes epoch. Mean field direction among sites are calculated to be of Inc.= 51.3° and Dec.= -1.4° with a radius of 95% confidence circle of 5.4°. This mean field direction well coincides with the geomagnetic field direction assuming the geocentric axial dipole (Inc.= 54.7°) at this region. Angular standard deviation of the VGPs (ASD) between sites is calculated to be 14.6° \pm 3.9° -2.5°. This

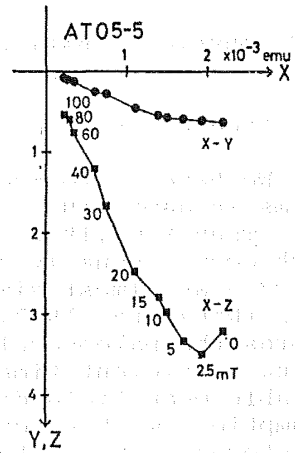


Fig.3 Demagnetization diagram of the AT05-5 dike rock. X: north, Y: east, and Z: down component, respectively.

Site	N	Inc.	Dec.	k	α_{95}	ODP	VGP	
							Lat.	Long.
AT 01	3	49.9°	-15.3°	41	19.4°	5mT	78.0°N	30.6°E
02	3	45.1	9.0	106	12.1	15	78.5	-85.7
03	3	66.5	8.2	343	6.7	15	75.0	160.1
04A	2	33.6	-15.9	56	33.9	0	68.1	2.8
04B	2	52.3	-3.9	401	12.5	20	86.1	14.4
05	3	62.7	21.9	639	4.9	20	71.0	-165.8
06	3	37.0	3.2	79	14.0	10	75.2	-52.8
07	4	27.7	-21.3	496	4.1	15	62.0	-52.8
08	4	41.5	-3.2	92	9.6	15	78.3	-26.6
09	4	48.3	8.9	83	10.1	15	80.4	-95.5
10	4	70.4	-7.6	80	10.3	15	70.0	125.9
11	3	56.2	20.7	458	5.9	20	73.5	-142.6
12	3	44.5	-10.5	125	11.1	10	77.2	6.7
13	4	48.3	21.4	71	11.0	20	71.0	-119.2
14	4	58.5	-6.5	91	9.7	30	83.4	88.6
15	4	53.1	-3.0	83	10.1	5	87.1	18.4
16	4	63.3	-11.7	102	9.2	10	76.9	99.3
17	4	60.2	9.8	104	9.1	40	80.3	-171.5
18	4	55.9	-19.7	96	9.5	5	74.0	59.0
19	4	51.8	-3.3	170	7.1	10	86.1	4.7
20	4	33.9	-9.4	126	8.2	5	71.4	-12.2
21	3	52.5	16.0	253	7.8	40	76.6	-126.8

Mean field direction		51.3	-1.4		5.4			
Axial geocentric dipole		54.7	0					
Mean VGP					5.9		87.9	21.8
					(ASD = 14.6° ± 3.9° -2.5°)			

Table 1. Paleomagnetic results of the AT01-21 dikes.

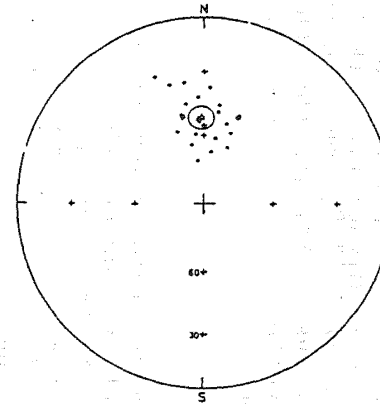


Fig.4 Equal area projection of the site mean direction for the AT01-21.

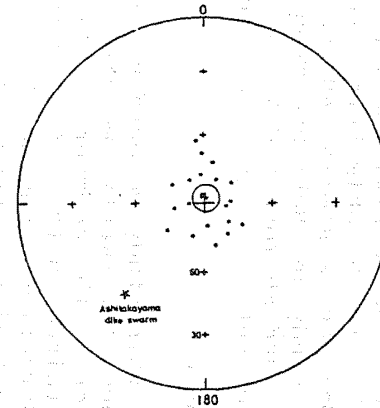


Fig.5 Equal area projection of the VGPs for the AT01-21.

value of ASD agrees well with that at the similar latitude during the Brunhes epoch obtained by using the world-wide data (McElhinny and Merrill, 1975). Hence, it is likely that the remanences of the AT01-21 dike rocks recorded the paleosecular variation during enough time interval to average out it. These paleomagnetic results imply that this region have undergone no tectonic movements since the occurrence of the Ashitaka dike swarm.

According to Heki and Tsunakawa(1981), remanences of fifteen dikes in the Shimokura dike swarm in Miyagi Pref. (K-Ar age= 8Ma) gave a similar ASD value of $14.1^{\circ} \pm 4.8$. The results in this study and Heki and Tsunakawa(1981) indicate that the Ashitaka and Shimokura dike swarms reflect the paleosecular variation sufficiently to average out it.

4. Summary

In this study we obtained the mean field direction of the remanences for twenty-two dikes which average out the secular variation of the geomagnetic field. As the mean field direction obtained in this study coincides with the geomagnetic field direction assuming the geocentric axial dipole, the Ashitaka region is suggested to have undergone no tectonic movements since the formation of the Ashitaka dike swarm. The ASD values obtained for twenty-two Ashitaka dikes in this study and for fifteen Shimokura dikes by Heki and Tsunakawa (1981) indicate that these dikes recorded the paleosecular variation during enough time interval to average out it. Hence, Remanent magnetization of not more than twenty dikes of a dike swarm can probably show the nature of paleosecular variation sufficiently to average out it. Paleomagnetic study of dike swarms will, therefore, yield useful data on the paleosecular variation of the geomagnetic field and on the tectonic movement.

References

- Fisher, R.A. (1953) Proc.Roy.Soc., Ser.A, 217,295.
Heki, K. and H. Tsunakawa (1981) Rock Mag.Paleogeophys., 8,17.
Ishida, T. (1981) Mem.Fac.Lib.Educ., Yamanashi Univ., No.32, 88.
McElhinny, M.W. and R.T. Merrill (1975) Rev.Geophys.Space Phys., 13,687.
Nakamura, K. (1977) J.Volcanol.Geotherm.Res.,2,1.
Sawamura, K. (1955) Explanetary text of geological map,Geol. Surv.Japan.
Tosha, T. and H. Tsunakawa (1981) Rock Mag.Paleogeophys.,8,28.
Tsunakawa, H. (1982) Doctoral Thesis,Fac. of Sci.,Univ. of Tokyo.

BLAKE POLARITY EPISODE IN A VOLCANIC ASH LAYER
WITH THE FISSION TRACK AGE OF 0.12 MA

Tadashi NAKAJIMA

Geological Laboratory, Faculty of Education,
Fukui University, Bunkyo, Fukui 910

About 100,000 years ago, a brief geomagnetic departure from purely normal polarity occurred. The record has been observed as an indisputable polarity reversal in normally magnetized sediments recovered at several sites in the western North Atlantic region. This geomagnetic event is called the Blake polarity event or episode (Smith and Foster, 1969; Denham, 1976; Denham et al., 1977). Also in the Japanese Islands, the possible Blake episode was recognized by Kawai et al. (1972), Manabe (1977) and Sasajima et al. (1980). Quite recently, the author discovered a geomagnetic reversal comparable to the Blake episode in a volcanic ash whose age was determined by the fission track method. This new observation is described in this paper.

The volcanic ash layer about 10 cm thick crops out along the sea cliff at Jyoshinden, Awara-cho, Fukui Prefecture, central Japan (Yoshizawa, 1982). This layer is intercalated in the Awara Formation composed of well-sorted, coarse-grained sand accumulated in a near-shore environment during the Late Pleistocene (Hokuriku Quaternary Research Group, 1969). Zircon crystals separated from the volcanic ash were dated to be 0.12 ± 0.02 Ma by the fission track technique (Danbara, 1982). This corresponds to the inferred age of the Blake episode. Therefore, paleomagnetic study on the volcanic ash layer has carried out in order to recognize the Blake polarity episode.

For the paleomagnetic measurement, eight samples oriented with a magnetic compass were collected from the ash layer. The geographic coordinates of the site are $36^{\circ} 15' 49''$ N and $136^{\circ} 10' 52''$ E. To know precisely the geographic north, the present-day declination of the geomagnetic field at the site was determined by observing the azimuth of the sun by means of a theodolite. The result gave the present-day declination of $5.56 \pm 0.008^{\circ}$ W.

The remanent magnetizations of the samples were measured by means of an astatic magnetometer. After the measurement of original NRM, all samples were demagnetized progressively in the alternating field (AF) with peak fields of 50, 100, 150, 200, 300 and 400 Oe. The directions of the residual magnetization cleaned at each step of the AF demagnetization are tabulated in Table 1.

As illustrated in Fig. 1, the volcanic ash samples exhibit remarkable change in the directions of NRM through the AF demagnetization up to 100 Oe. In a higher field, however, no detectable migration of the magnetic direction was observed. This result means that an unstable component was removed from original NRM by the AF demagnetization with a peak field of 100 Oe. Therefore, all samples were demagnetized in the fields higher than 100 Oe and densely-concentrated reverse directions

Table 1 Results of the paleomagnetic measurement.

AF peak field (Oe)	N	Dm (°E)	Im (°)	k	α_{95} (°)	Int. \pm s.d. ($\times 10^{-6}$ emu/g)
NRM	8	191.5	45.0	1.9	58.0	7.7 \pm 2.9
50	8	196.5	18.1	2.6	43.6	8.7 \pm 4.3
100	8	195.9	-38.5	19.8	12.7	7.7 \pm 3.4
150	8	188.9	-44.8	28.1	10.6	6.8 \pm 2.2
200	8	191.3	-40.4	31.7	10.0	6.1 \pm 2.4
300	8	190.5	-38.7	23.3	11.7	6.0 \pm 2.9
400	8	191.1	-40.2	35.0	9.5	5.4 \pm 2.6

Virtual Pole Position (after AF demagnetization of 400 Oe)

Lat. (°S)	Lon. (°E)	δp (°)	δm (°)
73.6	97.6	6.9	11.4

emerged. Fig. 2 shows the change in the relative intensity of NRM through the stepwise AF demagnetization. The intensity increased by 10 to 20 % until 100 Oe. This behavior is attributed to the removal of a secondary component whose direction is parallel to the present earth's field. The intensity decreased gradually in the stepwise demagnetization higher than 100 Oe. A median destructive field of each sample, however, is very high (> 400 Oe).

As mentioned above it was clarified that the reliable directions of NRM from the volcanic ash samples can be obtained by the AF cleaning. As the paleomagnetic direction of the ash layer, that of residual remanence after the 400 Oe cleaning was selected because the precision parameter (k) is largest. Judging from the stable remanence and the fission track age (0.12 \pm 0.02 Ma) of the samples, it may be reasonable to conclude that the ash layer was deposited during the Blake episode. The obtained inclination (-40.2°) of NRM is, more or less, lower than the expected one (55.7°) from the geocentric axial dipole field and thus the virtual pole position (73.6°S,

97.6 °E) calculated based on the result described in this report deviates slightly from the geographical south pole. The feature of this observation is very similar to that of the Blake episode reported from Keno and Kogashira pyroclastic flows in South Kyushu, Japan, by Sasajima et al. (1980).

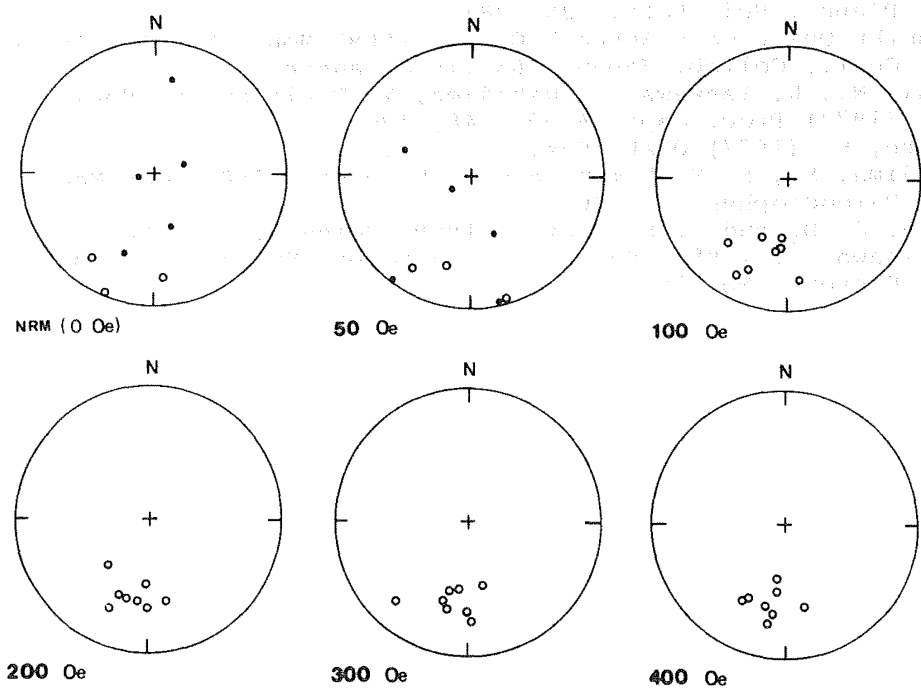


Fig. 1 Directions of the remanence cleaned at each step of the AF demagnetization. (Open circles; upper hemisphere. Solid circles; lower hemisphere.)

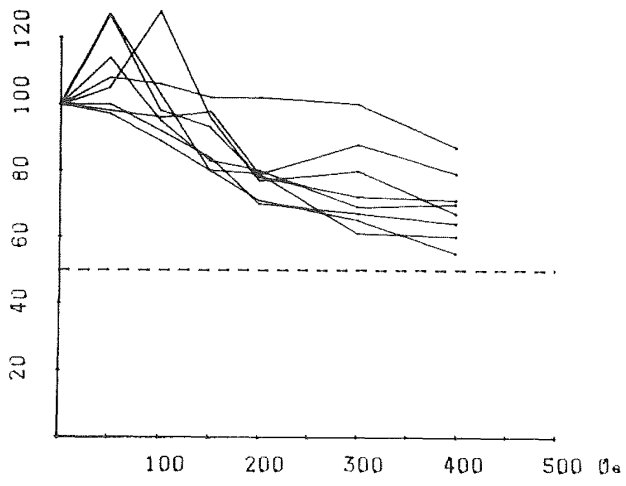


Fig. 2 Change in the relative intensity.

References

- Danhara, T. (1982) Rep. Soil Engineering Lab. Co., Ltd. (in Japanese).
- Denham, C. R. (1976) Earth Planet. Sci. Lett., 29, 422.
- Denham, C. R., R. F. Anderson and M. P. Bacon (1977) Earth Planet. Sci. Lett., 35, 384.
- Hokuriku Quaternary Research Group (1969) Mon., No. 15, Assoc. Geol., Collab. Japan, 263 (in Japanese).
- Kawai, N., K. Yaskawa, T. Nakajima, M. Torii and S. Horie (1972) Proc. Japan Acad., 48, 186.
- Manabe, K. (1977) Quat. Res., 7, 372.
- Sasajima, S., S. Nishimura and K. Hirooka (1980) Rock Mag. Paleogeophys., 7, 90.
- Smith, J. D. and J. H. Foster (1969) Science, 163, 565.
- Yoshizawa, Y. (1982) Rep. Fukui Municipal Museum of Natural History, No. 15, 1.

PALEOMAGNETISM OF DARUMA VOLCANO AND ADJACENT AREAS
NORTHWEST IZU PENINSULA, JAPAN

KIKAWA. E°, T. AKIMOTO°, H. KINOSHITA° and T. FURUTA°

° Department of Earth Sciences, Faculty of Science,
Chiba University, Yayoicho 1-33, Chiba

°° Ocean Research Institute, University of Tokyo, Minamidai
1-15-1 Nakano-ku Tokyo

1. Summary

Detailed paleomagnetic studies have been carried out on the Daruma volcano. It is clarified through the present study that Wakamatsuzaki andesites and Ida volcanic materials are normally magnetized, whereas Daruma volcanic materials show both normal and reversed NRM (natural remanent magnetization Fig6, Table1). Detailed sequences of normal and reversed NRM occurrence were investigated between Heda and Odoi sites (Fig7b). The normal-reversed structures resemble that of Brunhes-Matuyama boundary. K-Ar age of reversed sample near Funayama is about 0.8Ma.

Assuming that the paleogeomagnetic field of that time had the same features as the present one, the tectonic motion of this area can be estimated based upon the difference between the mean paleomagnetic direction (NRM) and the present geomagnetic one (Fig9a). Thus about 15° clockwise rotation and approximately northwest tectonic tilting are obtained (Fig8C, Fig9b). These results are in good harmony with seismological, geodetic and geographical data which have been deduced until now (Nakamura et al. 1981, Murauchi et al. 1982)

2. Samples

Daruma volcanic body lies in the northwest part of Izu Peninsula. The locality and the geologic map of this area are shown in Fig 1. This area is geologically divided into following three parts (Sawamura 1955, Shirao 1981).

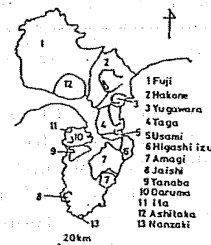
I) Wakamatsuzaki andesites non-porphyrific andesites, stratigraphically the lowest part of this area

II) Ida volcanic products olivine-augite andesites, basaltic andesites, intermediate part

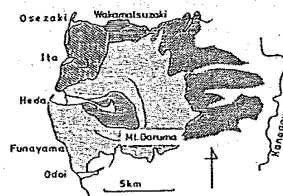
III) Daruma volcanic products olivine bearing two pyroxine andesites, consisting of two sections (early and late lava flows), uppermost part

Outcrops have thickness of 1-150m (mainly 2-8m) and fresh surface. Samples were collected from all these geologic sections. Locations of sampling sites are shown in Fig2.

3. Laboratory procedures



Distribution of quaternary volcanoes of Izu-Hakone area.



Geology map of Daruma volcano and adjacent areas.

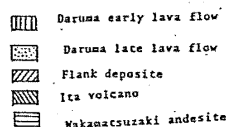


Fig 1

Six hundreds and fifty specimens about 2.5cm in diameter and height were measured by means of a Schonsted spinner magnetometer at the Ocean Research Institute, University of Tokyo. After the measurement of NRM, two or more specimens from each site were used for stepwise alternating field (AF) demagnetization. Others were used for other studies (measurement of Qn-ratio and initial magnetic susceptibility etc.). Chips of specimens were used for thermomagnetic analyses.

4. Magnetic behaviors

Almost all the specimens show a good stability of NRM in AF demagnetization. Typical examples of the changes of direction and demagnetization curves are shown in Fig 3. Intensity of magnetization decreases smoothly with the increase of the peak alternating field (maximum up to 8000e).

Thermomagnetic analyses were carried out in vacuum of 10^{-5} - 10^{-6} torr and in a magnetic field of 4.5k Oe. The results, J_s (saturation magnetization) versus T curves are irreversible except one example and can be classified into two types (type I, II) as follows: Type I; The heating curves show a single phase and the J_s values are always higher than cooling curves. Type II; The heating curves demonstrate two substantially different phases, whereas cooling curves show only a single phase. Type I is a dominant case in this study. These results indicate the presence of titanomaghemite (γ phase) produced by low temperature oxidation of titanomagnetite (β phase, Furuya 1981, Inoue 1979).

However because of the relatively small difference in J_s between the heating and cooling curves and results of AF demag, the total effect of the presence of γ phase on the NRM is considered to be very small. Detailed interpretations of the irreversible thermomagnetic curves obtained from this study are carried out in another paper of this volume. On-ratio, initial susceptibility and intensity of NRM are summarized in Fig 5.

5. Results and discussions

The mean directions of NRM are listed in Table I and shown in Fig 6. In the first place it is shown from the results that Wakamatsuzaki andesites and Ida volcanic products have normal NRM, and early and late Daruma volcanic products have both normal and reversed NRM. The ages of two rock samples from late Daruma lava showing

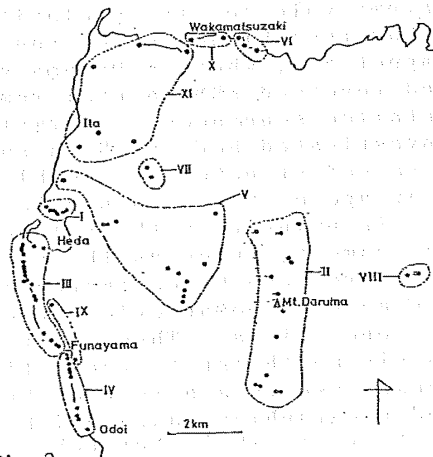


Fig 2

Sampling locality map. I. Takui-buraku II. Nishi-Ito Skyline III. Ohama-Funayama IV. Funayama-Odoi V. Inner wall of caldera of Daruma volcano VI. Yōjinsaki VII. Sanagiya VIII. Shuzenji side IX. Ohama-Odoi road X. Wakamatsuzaki XI. Ita Volcano

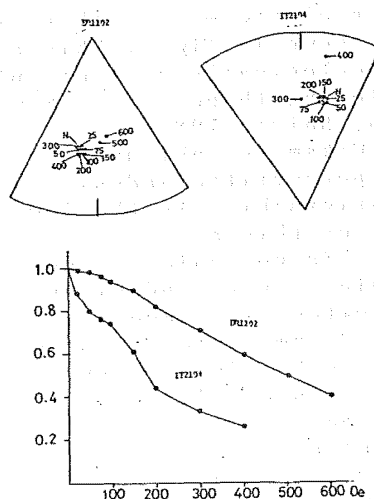


Fig 3 Progressive alternating demagnetization paths for certain specimens having a stable component and normalized alternating field decay curves of the natural moment.

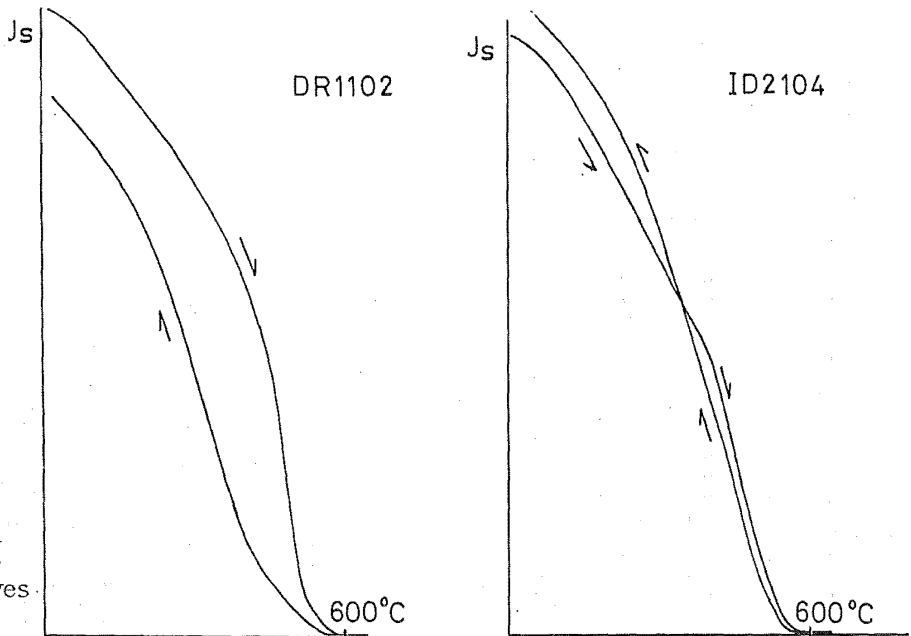


Fig 4
Example
of typical
thermomag-
netic curves.

reversed NRM(DR11,13) were determined by means of K-Ar method to result in to be about 0.8 Ma(Kaneoka; personal communication). Combining the age, geological data of this area and the general magnetic time scale, we can deduce a chronology of this area(Fig7a).

Detailed geomagnetic polarity changes were obtained along the western coast of this area(from Heda to Odoi, Fig7b). Lava flows sampled between Heda and Odoi site are stratigraphically lower than Odoi site. A series of successive lava flow outcrops shows up in between these two sites. From this geological observation, we worked on finding the changes of paleomagnetic inclination from Heda to Odoi. The feature of normal-reversed polarity changes resembles that of Brunhes-Matuyama boundary(Fig7b).

There is about 10° difference between the northside and southside of this area with respect to paleomagnetic declination. The mean direc-

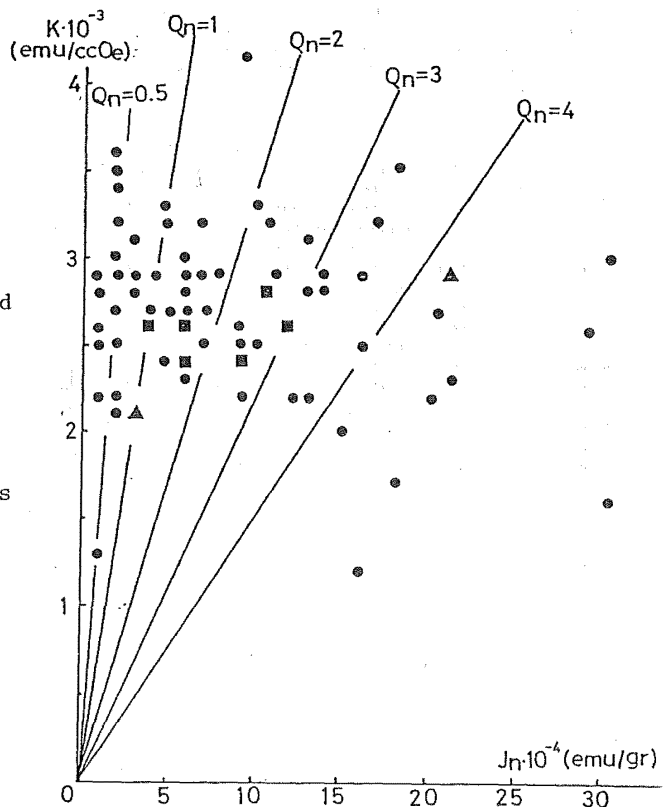


Fig 5
Summary of Q_n -ratio, initial magnetic susceptibility and intensity of NRM.
Solid circle; Daruma volcano
Solid square; Ida volcano
Solid triangle; Wakamatsuzaki andesites

Table I

Site	N	Inc	Dec	K	α_{95}	Ω_n	MDF (Oe)
Takumi-buraku (late lava)							
DR 40	5	-48.5	-154.8	405	3.8	0.7	160
41	6	-49.2	-178.7	164	5.3	1.3	150
42	4	-49.1	-162.9	333	4.2	6.0	375
43	5	-54.7	-170.3	203	5.4	1.5	75
44	5	58.6	24.8	430	3.8	3.1	225
45	5	55.7	31.2	1231	2.2	3.2	110
46	6	84.4	148.1	109	6.5	1.3	175
Nishizuku Skyline (late lava)							
DR 01	20	-46.2	178.8	51	9.4	0.9	50
61	12	37.9	7.2	88	4.7	1.5	140
93	6	-10.0	-43.3	1213	1.9	5.9	90
94	6	-80.6	167.5	43	11.5	0.9	150
95	6	-34.7	166.9	317	3.8	1.2	225
96	9	-15.3	-163.3	16	13.4	2.8	25
97	5	-2.2	-173.2	56	10.3	0.7	125
98	5	27.8	-114.0	40	12.3	51.0	80
99	12	-62.7	160.7	226	2.9	3.5	125
13	3	-14.2	-160.0	54	9.9	-	125
14	4	64.0	-10.3	250	5.8	4.4	350
15	25	20.6	-12.8	12	12.3	0.3	80
16	21	-45.6	-173.5	13	12.4	0.9	140
17	9	48.5	29.7	163	5.3	0.9	
Ohama-Funayama (late lava)							
DR 10	8	-55.8	-157.3	225	3.2	3.2	180
78	6	5.3	42.3	16	17.4	0.4	60
79	4	45.0	24.8	405	4.6	2.7	275
80	5	36.1	-26.6	89	8.2	0.5	125
62	5	72.7	2.1	7	30.6	1.9	275
63	2	56.2	6.6	7	-	4.4	240
68	14	43.3	1.9	282	3.3	1.4	120
69	5	51.7	-5.9	1290	2.1	2.8	130
81	2	-43.2	-125.7	-	-	0.3	
70	6	5.4	-8.2	17	16.8	0.2	40
71	6	13.4	-19.7	60	8.7	0.2	75
72	6	49.6	-38.2	101	6.7	0.4	150

Table I (continued)

Site	N	Inc	Dec	K	α_{95}	Ω_n	MDF (Oe)
DR 82	5	14.7	18.1	84	8.4	0.3	130
73	6	-43.0	-135.0	32	12.1	0.7	225
83	4	-46.6	-170.8	1773	1.8	7.1	800
84	6	-63.6	-133.3	58	8.9	0.3	400
85	6	-60.9	175.5	487	3.0	1.7	160
86	6	-59.8	-171.7	250	4.3	2.6	475
11	15	-48.7	-174.6	169	3.5	3.1	300
88	6	-59.0	120.9	60	10.3	0.3	50
89	4	-57.1	141.5	29	17.4		
Funayama-Odoi (late lava)							
DR 30	6	54.0	16.3	391	3.4	4.1	225
31	6	50.7	22.2	280	4.0	2.3	175
32	6	50.8	4.2	633	2.7	3.4	225
33	8	45.6	-3.3	350	2.8	1.8	130
34	6	54.0	25.2	79	8.7	1.0	90
35	4	63.2	24.6	287	5.4	5.1	275
36	6	60.2	27.3	1107	2.0	10.5	300
37	5	56.5	28.1	281	4.6	4.4	275
38	3	45.9	-0.2	289	4.0	1.4	160
12	13	-35.8	169.7	54	6.3	1.1	600
Inner wall of the caldera of Daruma Volcano (early lava)							
DR 18	6	54.3	31.7	10	22.4	0.4	175
20	19	51.3	1.7	58	8.9	1.2	160
64	6	32.8	-113.8	16	17.2	0.3	260
65	12	44.1	-36.0	4	26.9	0.3	70
66	16	-29.5	-164.2	1161	2.7	1.2	600
50	4	55.4	36.1	147	7.6	1.2	160
51	4	56.7	10.7	566	3.9	1.5	700
52	4	76.0	37.9	114	8.6	0.5	200
53	6	2.6	27.7	29	11.4	0.3	100
21	8	35.8	45.6	4	27.4	0.3	150
22	11	-22.1	177.0	5	21.8	0.2	800
23	4	-23.2	171.4	115	8.6	0.2	800
Yōjinsaki (late lava)							
DR 75	6	13.6	-3.3	1960	1.5	2.7	90
76	5	51.2	10.3	482	3.5	2.0	85

Site	N	Inc	Dec	K	α_{95}	Ω_n	MDF (Oe)
DR 77	6	48.7	11.0	304	3.9	2.4	85
Sanagiyama (late lava)							
SA 01	6	29.3	15.9	143	5.6	2.5	225
02	5	11.0	12.4	283	4.6	2.3	80
Shuzenji side (late lava)							
DR 23	9	-58.7	-163.7	56	7.0	0.7	250
24	8	-64.1	-163.3	135	4.8	0.5	400
Ohama-Odoi road (late lava)							
DR 90	6	46.3	22.3	348	3.6	1.4	130
91	6	-12.9	137.2	688	2.6	0.9	75
Ita Volcano							
IT 02	9	54.7	-3.9	57	6.9	1.6	125
03	8	29.8	-0.8	28	10.6	1.5	250
04	3	60.3	6.8	28	10.2	2.1	250
11	5	63.2	26.2	144	6.4	1.0	140
20	5	48.2	3.4	2287	1.6	2.8	125
21	4	45.4	4.4	66	11.4	2.2	110
Nakamatsuzaki							
NK 01	6	56.8	1.9	287	4.0	4.2	95
02	4	60.6	-29.8	127	8.2	0.8	220

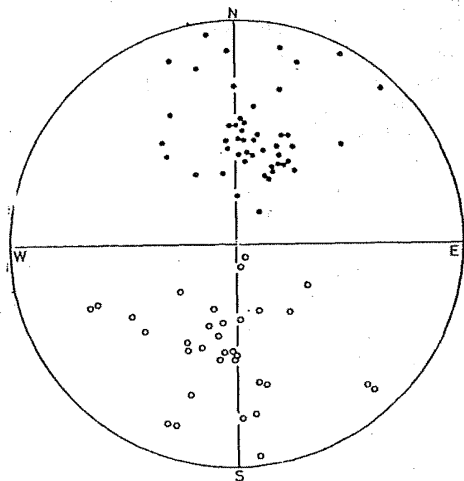


Table I

Mean direction of NRM of the igneous rocks of the area for this study represented by Schmidt projection. Solid circle means normal magnetization and open circle means reversed magnetization.

Summary of Table I

tion of northside is $D = 3^\circ$, $I = 53^\circ$ with a 95 % confidence radius (α_{95}) of 12° , while the mean direction of southside is $D = 14^\circ$, $I = 55^\circ$ with α_{95} of 10° . Boundary between two blocks can be introduced by a deep valley running westward from the central part of Daruma volcanic body (Hedaokawa river). The structure continues further deep into the submarine valley in the Suruga Bay (Heda Canyon, Fig 8a,b). Although the effect of paleogeomagnetic secular variation cannot be ruled out, it is well inferred from the deflected declinations of this area that this area may have been affected by about 15° clockwise tectonic rotation around the vertical axis.

Another finding of the paleomagnetic studies is that inclinations are often deeper than that expected from the present location of Izu Peninsula ($I = 49^\circ$, $D = -7^\circ$). Considering these deeper inclinations and eastward deviation in declinations, northwest tectonic tilting of this area could be inferred (Fig 9b). That is, if the difference between paleomagnetic direction and present one were due to a certain tectonic tilting of this area, the direction (of the motion) and total amount of the tectonic tilting could be induced resulting from a procedure shown in

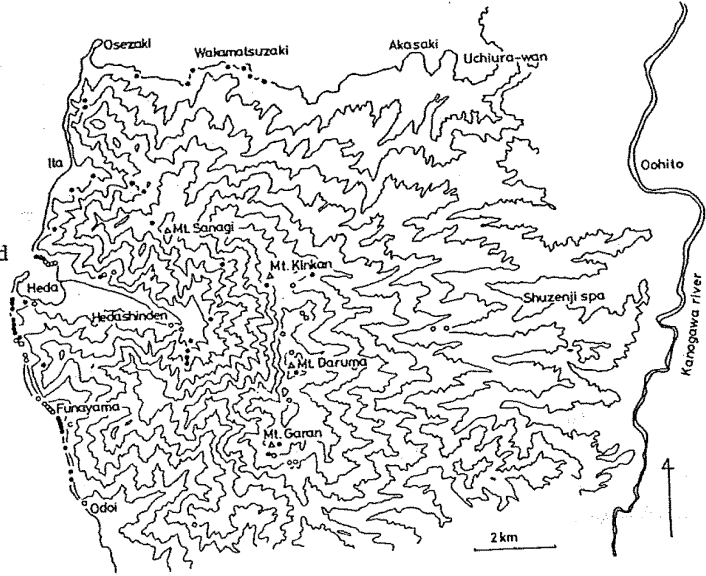


Fig 6

Topographic map and sampling site for present study. Contour intervals : 100m. Solid circle means normalized magnetization and open circle means reversed magnetization.

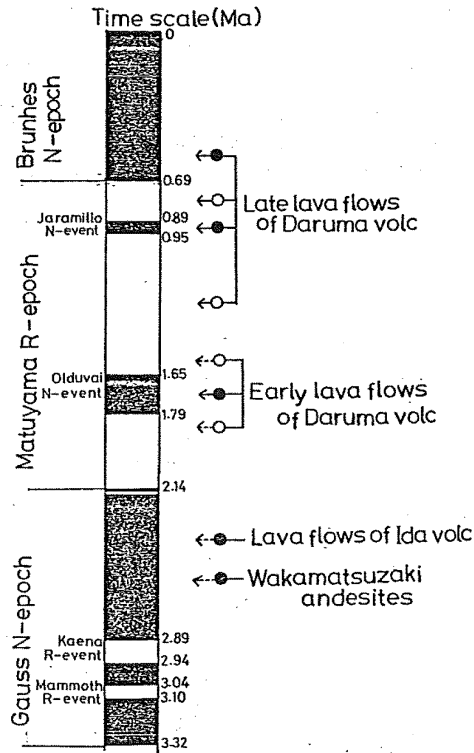


Fig 7a

A possible correlation of igneous rocks of this study to general magnetic stratigraphy

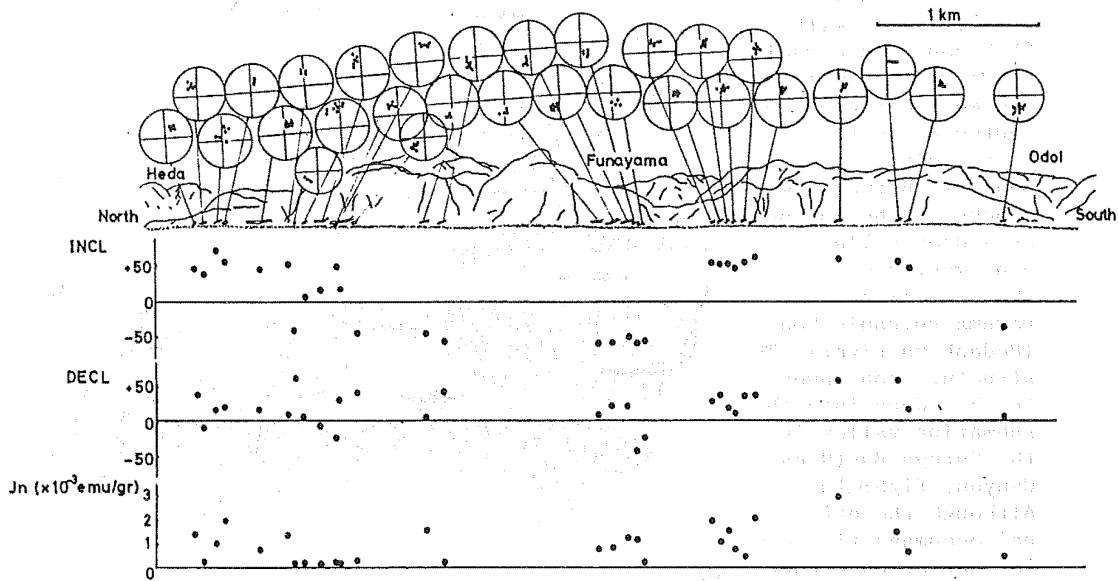


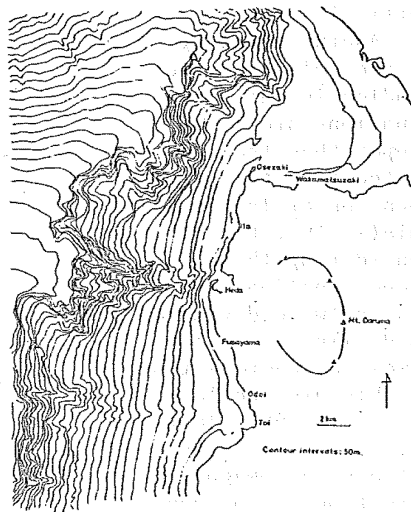
Fig 7b Picture of geomagnetic polarity changes

Fig9a.

This result may indicate a possible tectonic motion of Izu Peninsula since last at least 2.0 Ma.

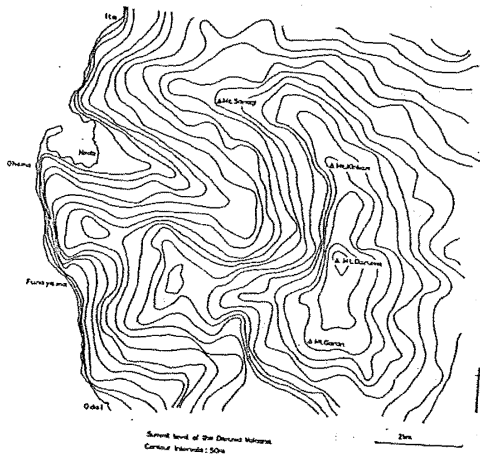
References

Inoue.Y., 1979; Master thesis of Shinshu Univ (in Japanese)
 Kuno.H., 1938; Bull. Earthq. Res. Inst 16, 763-771
 Shirao.M., 1981; Jour of Geol Soc of Japan vol 87 641-655 (in Japanese)
 Sawamura.K., 1955; Explan Text of Geol map of Shuzenji, Japan scale 1:50000 Geol Surv of Japan (in Japanese)
 Nakamura.K et al., 1981; Science vol 51 490-498 (in Japanese)
 Furuya.J., 1981; Graduation thesis of Chiba Univ (in Japanese)
 Murauchi.S et al., 1982; Program and Abst Seismol Soc of Japan No.2 165 (in Japanese)



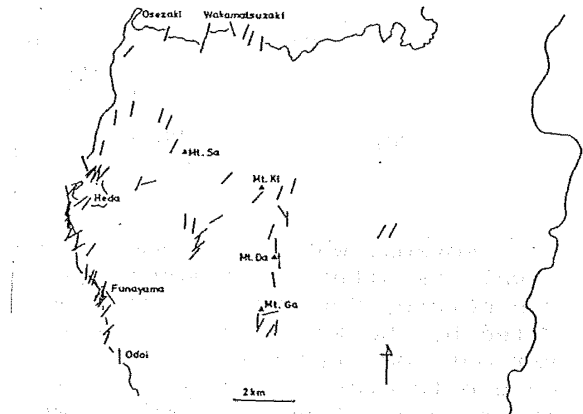
The line structure of the inner wall of the caldera of Daruma volcano continues further into the deep submarine valley in the Suruga Bay.

Fig 8a



Summit level of Daruma volcano shows that the inner wall of the caldera of Daruma volcano opens unnaturally toward north-west direction.

Fig 8b



Projection of Declination. This reveals the clockwise rotation of declinations of remanent magnetization.

Fig 8c

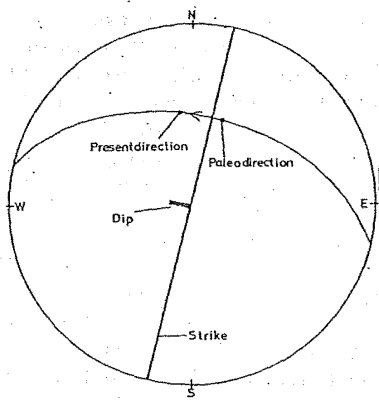


Fig 9a

The above procedure was carried out in order to reveal the motion of the igneous rocks of this area. This example shows northwestward tilting.

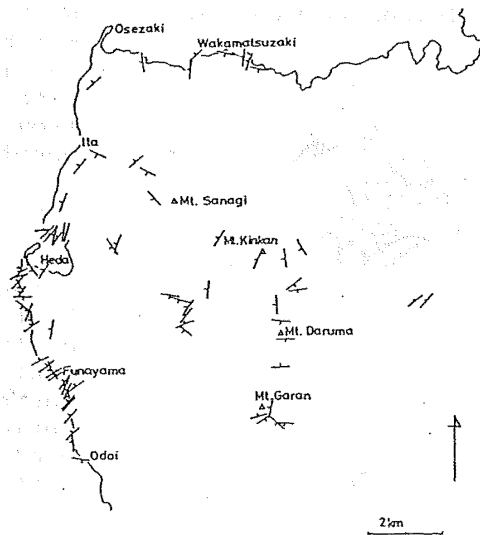


Fig 9b

Projection of the result of the procedure shown in Fig 9a. this reveals the north-westward tectonic tilting.

REMANENT MAGNETIZATION OF THE KOYAMA INTRUSIVE COMPLEX,
YAMAGUCHI PREFECTURE, SOUTHWEST JAPAN

Haruaki ITO, Katsuyasu TOKIEDA
and
Yukio NOTSU

Department of Physics, Faculty of Science,
Shimane University, Matsue 690, Japan

Koyama, which is a small mountain of 533 meters above sea level, is situated in Koyama peninsula of Susa-cho, Yamaguchi Prefecture, Southwest Japan. Most of the Koyama area is blanketed by the Koyama intrusive complex which is composed of various rock types varied with gradual relations from quartz gabbro to granite. A part of anorthositic quartz gabbro in the Koyama intrusive complex, which is typically exposed at the summit of Koyama, is well known as the "Jishakuishi" strongly magnetized and the "Jishakuishi" is designated as a natural monument.

The Koyama intrusive body intrudes into the Susa Formation which has been correlated with the early Miocene strata in Northeast Japan by molluscan fossils found in fine sandstone (Yamazaki, 1967). According to Yamazaki (1967), the shape of Koyama intrusive body is semi-elliptical and its longer and shorter axes are about 3 and 2 kilometers respectively. It is also considered to be boss-like in profile and the present exposures are likely to be only the uppermost part of the body.

Geochronologic age of the Koyama intrusive complex has

not been reported, but the age of the intrusion is estimated to be late Miocene or early Pliocene from geological evidences of the country rocks (Yamazaki, 1967).

Magnetic investigations on the Koyama intrusive complex were first carried out by Domen (1958). According to Domen's results, the intensity of NRM of samples collected at the summit of Koyama is of the order of 10^{-2} emu/gr and that of samples from the foot of the mountain was 10^{-4} emu/gr. The Curie point of ferromagnetic minerals in samples investigated is consistent with that of magnetite. Paleomagnetic directions after alternating field or thermal cleaning are not described in the Domen's paper.

Thirty four hand samples were collected from only three sites in gabbro and quartz gabbro region which occupies most part of the complex as shown in Fig. 1. The sampling sites were approximately

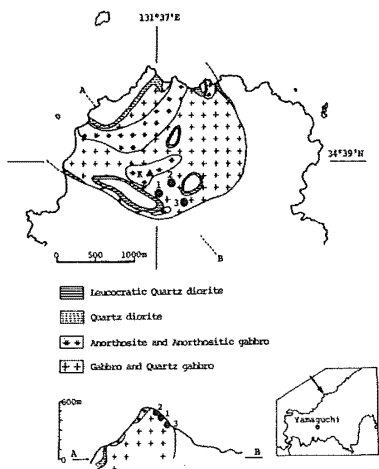


Fig. 1. Geological map of the Koyama intrusive complex and its schematic profile (after Yamazaki, 1967). Sampling sites are shown by numbered dots. K represents the summit of Koyama (533 meters).

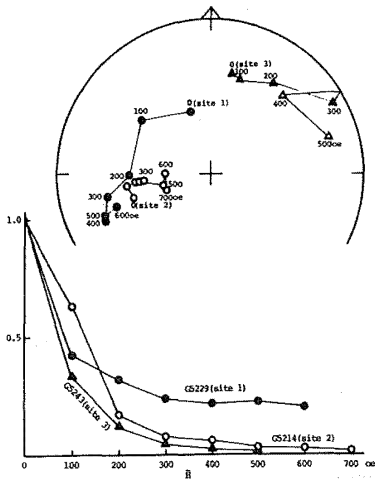


Fig. 2. Alternating field demagnetization of NRM for typical samples at each sampling site.

located on 360, 440 and 480 meters above sea level. Anorthositic quartz gabbro exposed at the summit (533 meters), which has strong remanent magnetization, was not sampled for this study.

Magnetic cleaning in progressive alternating field up to 600 or 700 oe was done for all core samples. The intensity and directions of magnetization of typical core samples after partial demagnetization in alternating field are shown in Fig. 2. Directions of magnetization after alternating field cleaning are also shown in Fig. 3. Results of measurements are summarized in Table 1. As seen in Fig. 3, paleomagnetic directions from the three sites are extremely deviated from the present geomagnetic field direction and their mean directions are significantly located on a great circle in the equal area net.

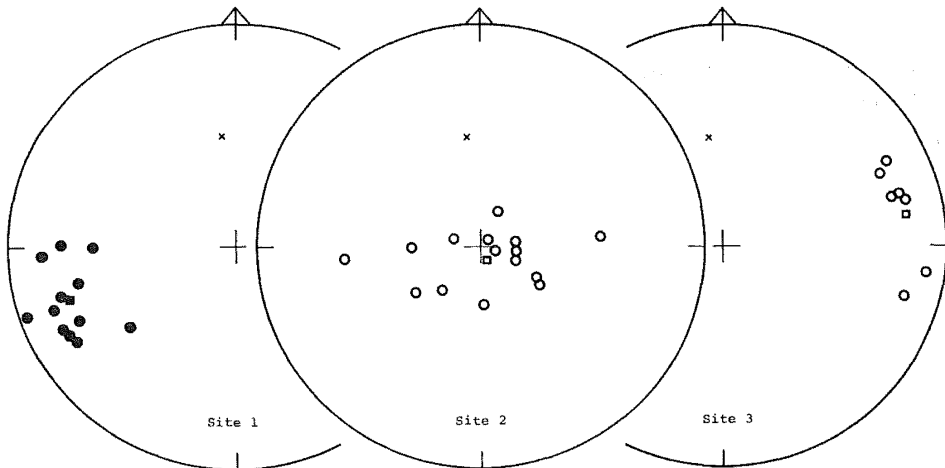


Fig. 3. Paleomagnetic directions after alternating field demagnetization. Cross mark indicates the present direction of the geomagnetic field. Squares indicate site mean directions, solid one, downward inclinations; open one, upward inclinations. Cross mark is the present field direction.

Table 1

Site	N	Mean direction D(°) I(°)	K	α_{95} (°)	J_r (emu/gr)	Cleaning field (oe)
1	12	252.6 23.5	29.8	8.1	3.84×10^{-5}	400
2	15	158.1 -84.9	10.9	12.1	2.57×10^{-5}	600
3	7	79.9 -18.3	25.0	12.3	3.38×10^{-6}	500

Furthermore, the site mean directions for the sites 2 and 3 are nearly antipodal with each other. Such antipodal magnetic directions within a body have been frequently found in small-sized intrusive bodies of the Tertiary (e.g., Ito et al., 1979).

In case of the Koyama intrusive body, it is difficult to consider that the between-site scatter in magnetic directions was only due to extremely local deformation within the body after the emplacement. The reason is that the boundary of the intrusive body and country rocks shows a very sharp pattern and no evidences of assimilation, and that the dip of Susa Formation which was intruded by the Koyama intrusive body is about 10° and disturbance of the stratum is very small (Yamazaki, 1967). Therefore, it will be expected that the Koyama intrusion records a change in direction of the ambient geomagnetic field during cooling of the body after the intrusion. There may be, however, a possibility that the Koyama intrusive body has been tilted as a rigid block during uplift from original level of the emplacement to the present one. An apparent amount of tilting may be estimated by comparing paleomagnetic directions of the Koyama intrusion with those of late Miocene or early Pliocene rocks in Southwest Japan (Ito, 1970).

References

- Domen, H. (1958) Bul. Fac. Edu. Yamaguchi Univ., 7, 35.
Ito, H. (1970) J. Geomag. Geoelectr., 22, 273.
Ito, H., K. Tokieda and Y. Notsu (1980) Mem. Fac. Sci., Shimane Univ., 14, 85.
Yamazaki, T. (1967) Sci. Rep. Tohoku Univ., 3rd Ser., 10, 99.

CORRELATION OF IGNEOUS ACTIVITIES OF GRANITIC ROCKS
WITH GEOMAGNETIC FIELD REVERSALS
DURING LATE TERTIARY

Haruaki ITO

Department of Physics, Faculty of Science,
Shimane University, Matsue 690, Japan

1. Introduction

Granitic rocks are clearly consolidated at a few hundred meters or more below the surface of the earth (Raguin, 1965). The time required for cooling of such bodies emplaced below the surface is generally hard to established. However, rough estimates of the temperature and the time in cooling intrusive bodies have been reported by some workers (e.g., Carslaw and Jaeger, 1959; Dodson et al., 1978).

According to Dodson et al. (1978), for example, the time required for the cooling of intrusive bodies with a few kilometers in diameter is estimated to be of the order of 10^3 or 10^4 years. On the other hand, the time required for a transition between polarity epochs is sometimes given by the paleomagnetic studies of volcanic rocks, intrusive rocks or ocean sediments (Harrison and Somayajulu, 1966; Cox and Dalynple, 1967; Dunn et al., 1971; Opdyke et al., 1973). Most probable estimates tend to give times of the order of 10^3 or 10^4 years. Thus the time for a transition in direction during field reversals corresponds closely with that for the cooling of intrusive bodies. This good correlation between the times indicates that, if an intrusive body intruded at the time of a polarity transition and cooled slowly enough to record the transition, part or all of a continuous record of the field reversal are found in such a body.

A few examples of field reversals recorded in intrusive rocks have been reported by some workers (Ito and Fuller, 1970; Dunn et al., 1971; Dodson et al., 1978). I actively undertook paleomagnetic survey of late Tertiary granitic rocks in Japan to get reliable records of field reversals. Subsequently, intrusive bodies with both the normal and reversed polarity are not rare, but such bodies were rather usually found in granitic rocks of late Tertiary.

2. Granitic rocks in Japan and K-Ar ages

According to the geological map and K-Ar age map of Japan by Nozawa (1975), late Tertiary granitic rocks are widely scattered in Hokkaido, Honshu, Shikoku, Kyushu and the other small islands. Exposures of late Tertiary granitic rocks in Japan is poor as compared with Cretaceous granitic rocks. Small-sized granitic masses sampled for this study are mainly exposed in the Hidaka mountains, Uetsu province, Fossa Magna area, the Outer Zone of Southwest Japan, Goto Islands and Tsushima.

K-Ar age data determined in late Tertiary (25-5 Ma) are about sixty according to Nozawa (1975) and Shibata (1978). The histogram of number of age determinations for granitic rocks in Japan is shown in Fig. 1. Fig. 1 indicates that the age

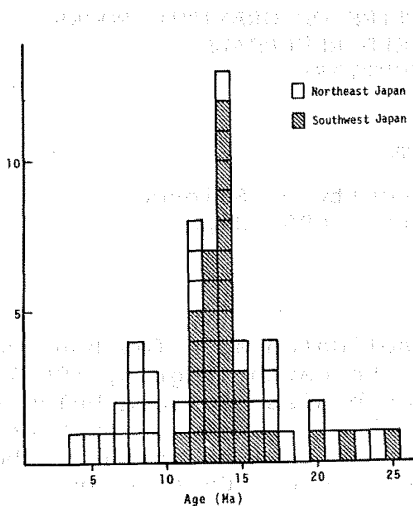


Fig. 1. Histogram of age determination (after Nozawa, 1975 and Shibata, 1978).

rock and K-Ar mineral ages is generally observed in granitic masses with slow and complex cooling history, Shibata and Ishihara (1979) concluded that small-sized granitic masses with simple cooling history in Japan indicate the concordance or slight discordance between both the ages. It implies that remanent magnetizations of small-sized granitic masses were almost acquired at the time calculated by K-Ar biotite system. Fortunately, most of late Tertiary granitic rocks in Japan appears to be small-sized masses which were rapidly cooled after the emplacement.

3. Samples and laboratory procedure

A large number of hand samples were taken from the Hidaka mountains and the southwestern part of Hokkaido, Northeast Honshu, Fossa Magna, Chugoku district, the Outer Zone of Southwest Japan, Goto Islands, Tsushima and Koshiki-jima. Oriented hand samples were always collected from two or more sites within a single body and about ten samples were usually taken at a site. One or two core samples were drilled from a hand sample in the laboratory.

Measurements of remanent magnetization were mainly made on a spinner magnetometer having a noise level of $<10^{-7}$ emu and sometimes an astatic magnetometer of high sensibility ($\sim 10^{-8}$ emu). Pilot samples for each group of cores were subjected to progressive stepwise alternating field demagnetization and the remaining samples were demagnetized at a steady field level. Thermal demagnetization was done on one or two cores of each sample in an ambient field of 30 gamma or less. The stably and consistent sites were selected by both alternating field and thermal demagnetization treatments.

4. Results

After alternating field and thermal cleaning, samples

distribution is concentrated in the ranges of about 17 to 11 Ma and 9 to 5 Ma. Shibata (1978) concluded, however, that the Tertiary granitic rocks in the Outer Zone of Southwest Japan are almost always dated at 14 ± 1 Ma. On the other hand, the closing temperature for Rb-Sr Whole-rock and K-Ar biotite systems are estimated to be 500°C and 300°C respectively (Shibata and Ishihara, 1979). It has been, therefore, expected that the Rb-Sr ages indicate the time of emplacement and the K-Ar ages the time uplift and cooling. This suggests that the time of acquisition of magnetization in granitic masses should be more closely connected with Rb-Sr ages than K-Ar ages. Although discordance between Rb-Sr whole

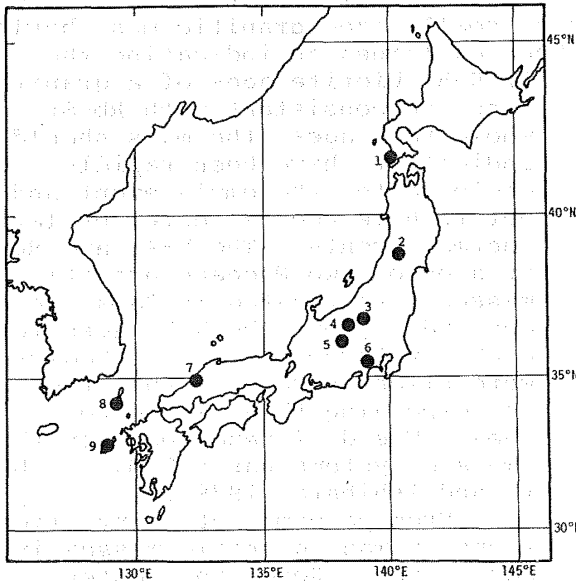


Fig. 2. Locality of granitic masses having both normal and reversed polarity in Japan. 1, Kaminokuni; 2, Dai-yama; 3, Tanigawadake; 4, Suzaka; 5, Utsukushigahara; 6, Wada; 7, Tanzawa; 8, Kawamoto; 9, Tsushima; 10, Hisaka-jima.

collected from about 30 granitic masses were found to have stable components of magnetization and to display within-site consistency in directions. Samples from the Hidaka mountains of Hokkaido and the Outer Zone of Southwest Japan have nearly always contained pyrrhotite with Curie point of about 300°C as magnetic carrier. Although magnetic directions of samples that contained pyrrhotite were stable in lower alternating field than about 150 oe, within-site scatter in directions were frequently observed in higher field than 200 oe. Such samples were more complex for thermal demagnetization. However, some granitic bodies from the Outer Zone of Southwest Japan are likely to have recorded both normal and reversed polarity in a single body.

Finally ten granitic bodies as shown in Fig. 2 and Table 1 were recognized to display both normal and reversed polarity within a body, but granitic masses from the Outer Zone of Southwest Japan are rejected from these data because there are some uncertain factors in the stability and reliability of magnetization. The remaining masses with stable and reliable magnetizations have recorded only normal or reversed polarity.

Fig. 3 shows the mean directions for the normal and reversed samples in a body. The normal and reversed directions are nearly antipodal with each other in a body and intermediate directions suggesting a transitional process of the geomagnetic field were not found in the bodies measured. Only the paleomagnetic directions for the Kawamoto granodiorite mass (Locality 8) are considerably deviated from the present direction of the geomagnetic field and their directions seem to be intermediate. However, assuming that the Kawamoto mass have moved as a rigid block at the time of post-cooling tectonic movements in Southwest Japan, the deviation in directions can be successfully explained.

5. Discussion

The fact that only normal and reversed polarity were found in ten small-sized masses may indicate that intermediate directions of magnetization showing a transitional process of the field were not stably recorded. It may suggest that the geomagnetic field abruptly changed its direction during cooling of their masses.

According to Shibata and Ishihara (1979), the difference between Rb-Sr and K-Ar ages of small-sized granitic mass having simple thermal history has been explained as indicating the cooling time of the masses. If K-Ar biotite ages of a granitic mass are consistent with Rb-Sr whole rock ages, the mass should indicate to have been rapidly cooled after the emplacement and not to have been affected by later thermal events. The K-Ar and Rb-Sr ages of two Neogene granitic masses investigated in Japan were concordant, but the K-Ar ages for eight Cretaceous granitic bodies were slightly younger than the corresponding Rb-Sr whole rock ages. The difference between the two age systems was 4-9 Ma (Shibata and Ishihara, 1979).

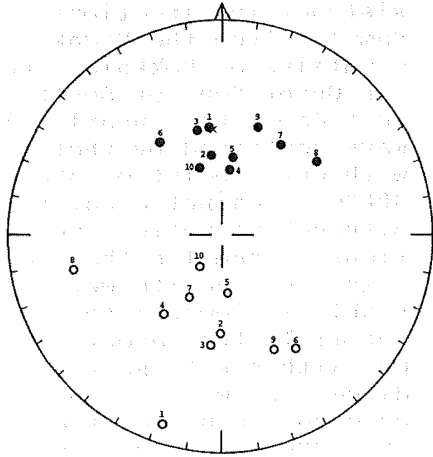


Fig. 3. Mean directions of normal and reversed magnetizations in each mass. Numbered solid circles are directions of normal polarity and numbered open circles directions of reversed polarity. Cross mark is the present direction of the geomagnetic field.

From paleomagnetic investigations of many granitic masses in Japan, South Korea and western part of USA, granitic masses which show concordant ages are expected to correspond with granitic bodies having stable components of magnetization and a part of each mass with discordant ages is considered to be characterized by unstable components of magnetization. Granitic rocks of late Tertiary in Japan are mostly of small-sized masses, with the exception of granitic rocks in the Outer Zone of Southwest Japan (Nozawa, 1978).

Thus data of radiometric age determinations and paleomagnetic surveys of late Tertiary granitic rocks in Japan indicate that small-sized masses were rapidly cooled after the intrusion and also that they have stable components of magnetization. On the other hand, K-Ar age data on late Tertiary granitic rocks suggest that igneous activity was particularly intensive in the ranges of 17-11 Ma and 9-5 Ma (Nozawa, 1968, 1975; Shibata, 1978) and granitic bodies with both normal and reversed polarity were found in small-sized masses dated at late Tertiary. The ages of such granitic masses can be roughly divided into two groups of older and younger ages. It is indeterminate whether these ages correspond exactly with the ages of intensive igneous activities (17-11 Ma and 9-5 Ma) because of uncertainty of age determinations.

The polarity transitions of the geomagnetic field have been observed about 60 times in the range of 25 and 5 Ma (Tarling and Mitchell, 1976; LaBrecque et al., 1977). The time required for a polarity transition is of the order of 10^3 or 10^4 years (Harrison and Somayajulu, 1966; Cox and Dalrymple, 1967; Dunn et al., 1971; Opdyke et al., 1973) and the time for cooling of small-sized granitic bodies is approximately consistent with that of a polarity transition (e.g., Dodson et al., 1978). These results imply that there is not much probability that a granitic mass encountered with a geomagnetic field

reversal during the cooling of the mass. However, the ten granitic masses with both normal and reversed polarity were found in late Tertiary granitic rocks in Japan. This result was more than I expected. The presence of a number of granitic bodies with both normal and reversed magnetizations may be explained by presuming that igneous activities of granitic rocks were exceptionally concentrated in the period of geomagnetic field reversals.

References

- Carslaw, H. S. and J. R. Jaeger (1959) *Conduction of Heat in Solids*, Charendon Press, Oxford.
- Cox, A. and G. B. Dalynple (1967) *J. Geophys. Res.*, 72, 2603.
- Dodson, R., J. R. Dunn, M. Fuller, I. Williams, H. Ito, V. A. Schmidt and Yee-Ming Wu (1978) *Geophys. J. R. Astr. Soc.*, 53, 373.
- Dunn, J. R., M. Fuller, H. Ito and V. A. Schmidt (1971) *Science*, 172, 840.
- Harrison, C. G. A. and B. L. K. Somayajulu (1966) *Nature*, 212, 1193.
- Ito, H. and M. Fuller (1967) *Palaeogeophysics* (ed. S. K. Runcorn), Academic Press, London and New York, 133.
- LaBrecque, J. L., D. V. Kent and S. C. Cande (1977) *Geology*, 5, 330.
- Nozawa, T. (1968) *J. Geol. Soc. Japan*, 74, 485.
- Nozawa, T. (1975) *Radiometric Age Map in Japan*, Geol. Surv. Japan.
- Opdyke, N. D., D. V. Kent and W. Lowrie (1973) *Earth Plan. Sci. Letters*, 20, 315.
- Raguin, E. (1965) *Geology of Granite*, Interscience Publishers, London.
- Shibata, K. (1978) *Bull. Geol. Surv. Japan*, 29, 551 (in Japanese).
- Shibata, K. and S. Ishihara (1979) *Geochem. J.*, 13, 113.
- Tarling D. H. and J. G. Mitchell (1976) *Geology*, 4, 133.

Table 1. Paleomagnetic data for granitic rocks with both normal and reversed polarity

Locality	Size	Age (Ma)	Distance between N and R	Number of site	Mean direction		K	α_{95} (°)	J_r (emu/gr)
					Decl. (°E)	Incl. (°)			
1 Kaminokuni Hokkaido	3 x 4 km	17	800 m	N = 3	353.0	49.3	12.3	9.0	1.11×10^{-4}
				R = 3	197.7	-8.1	48.1	4.2	1.24×10^{-5}
2 Dai-yama Yamagata Pref.	3 x 6 km	Upper Miocene	1.8 km	N = 1	351.2	58.7	105.0	6.0	1.02×10^{-4}
				R = 1	180.5	-51.9	232.6	3.4	2.98×10^{-4}
3 Tanigawadake Gunma Pref.	3 x 8 km	5.9, 20, 24	400 m	N = 1	346.3	48.5	59.2	8.8	2.52×10^{-5}
				R = 5	184.9	-47.2	143.3	3.3	1.61×10^{-4}
4 Suzaka Nagano Pref.	3 x 5 km	21	100 m	N = 2	6.6	65.1	32.8	5.4	3.13×10^{-5}
				R = 2	217.2	-52.0	63.0	4.5	2.23×10^{-4}
5 Utsukushigahara Nagano Pref.	4 x 8 km	Upper Miocene	6.0 km	N = 2	8.2	59.7	8.6	12.9	3.06×10^{-5}
				R = 4	173.1	-68.3	28.8	4.7	8.84×10^{-6}
6 Wada Nagano Pref.	3 x 6 km	7.3 8.6	200 m	N = 1	324.8	46.3	17.7	9.7	9.31×10^{-5}
				R = 1	145.6	-37.0	85.0	8.3	3.21×10^{-5}
7 Tanzawa Kanagawa Pref.	5 x 20 km	4.3 5.2	200 m	N = 6	34.0	48.0	9.7	9.4	3.79×10^{-5}
				R = 2	207.0	-63.0	11.9	16.7	5.46×10^{-5}
8 Kawamoto Shimane Pref.	3 x 6 km	25	400 m	N = 4	53.1	42.3	19.4	7.8	9.20×10^{-4}
				R = 2	257.1	-29.1	19.5	11.9	4.53×10^{-5}
9 Tsushima Nagasaki Pref.	3 x 5 km	12	300 m	N = 1	18.8	45.5	43.3	14.1	1.05×10^{-5}
				R = 3	153.8	-41.2	18.2	9.5	1.82×10^{-5}
10 Hisaka-jima Nagasaki Pref.	3 x 7 km	Upper Miocene	4.5 km	N = 1	340.5	63.0	84.1	5.3	3.79×10^{-5}
				R = 1	214.7	-75.6	20.8	10.9	5.81×10^{-6}

N: Normal polarity.

R: Reversed polarity.

K: Fisher's precision parameter.

α_{95} : Semi-angle of cone of 95 percent confidence for the mean direction.

J_r : Intensity of remanent magnetization after AF cleaning of 100-500 oe.

ON A PALEO/ROCK MAGNETIC STUDY OF THE METAMORPHIC ROCKS COME FROM SUSA DISTRICT, NORTHEASTERN YAMAGUCHI PREFECTURE, JAPAN

Haruo DOMEN

Institute of Physical Sciences, Faculty of
Education, Yamaguchi University, 753 Japan

Susa Tertiary layer was metamorphosed by the gabbroic intrusion, then a part of the Tertiary layer became hornfers. Along the coast line of the Japan sea, the zone thus altered mentioned above was recently studied geologically and also petrologically by Nishimura (Nishimura 1979). And he offered several fist-sized rock samples to the present author. Those samples are now under examination from the paleo/rock magnetic stand points.

In this report, NRM of these samples offered is briefly reviewed. The map (Fig. 1) is showing the sampling sites. The directions of NRM of the test specimens, which were drilled out in cylindric having 2.5cm in both diameter and long, was determined by means of a spinner magnetometer (Schonstedt's, SSM-1A; see Domen 1978). The mean NRM data obtained are roughly shown together with the cleaned RM plots in the map shown above, and those numerals are sited in Table 1. Some data previously obtained (Domen 1953) are also plotted in the stereograms in the same map and are entered in the table respectively.

It seems rather difficult to give any conclusion refering the thermal effect to the NRM directions of those examined samples due to the gabbroic intrusion.

Now the thermomagnetic analysis has been carried out. Further discussions with the data of the analysis will be made in the near future.

References

- Domen, H. (1953) B.Sc. Thesis, Yamaguchi University.
- Domen, H. (1978) Rock Magnetism & Paleogeophys. 5, 40.
- Nishimura, I. (1979) see the report published by Yamaguchi Prefectural Board of Education.

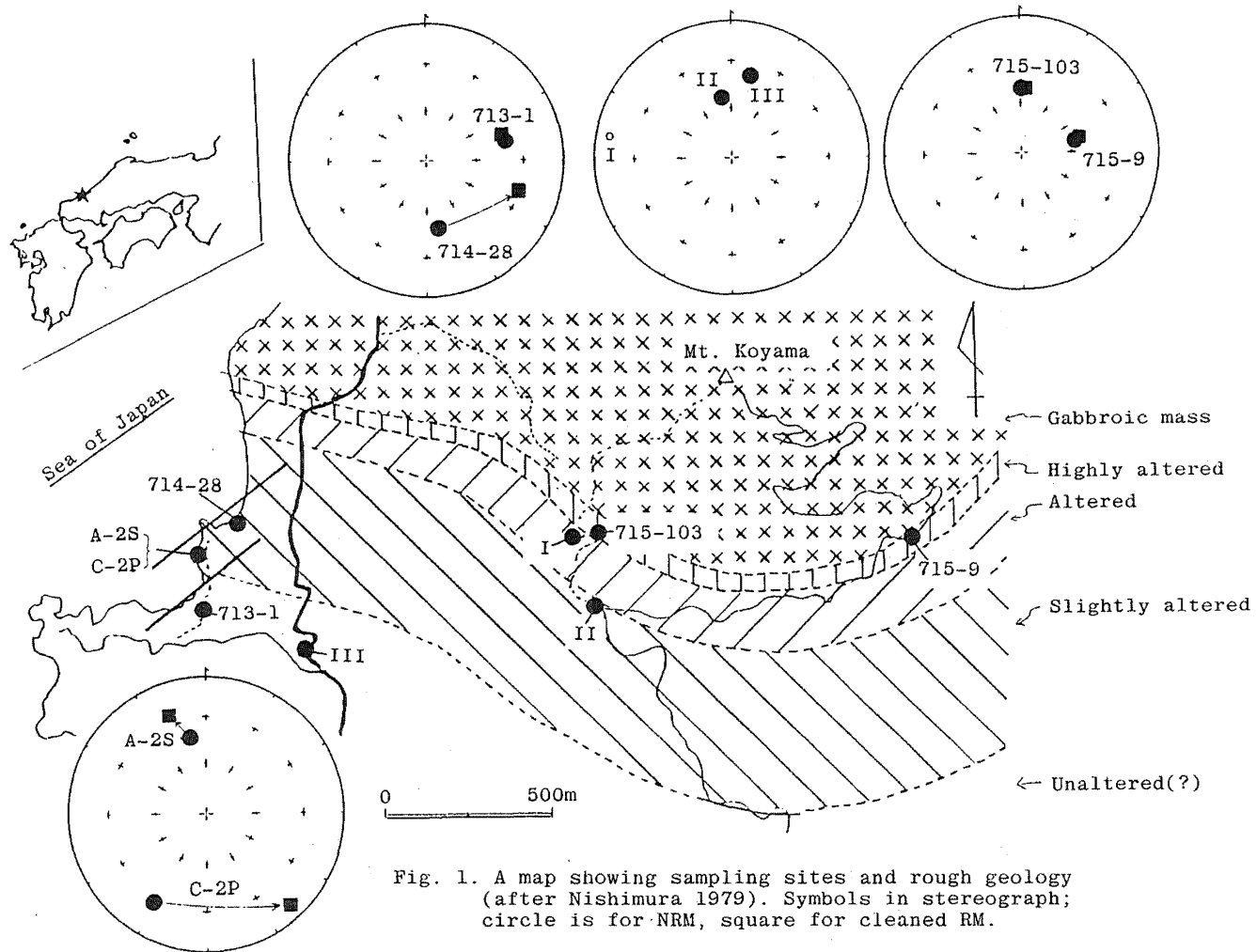


Table 1. Paleomagnetic data of Susa Tertiary layer metamorphosed by gabroic intrusion, Yamaguchi, Japan.

Site	N	N R M				Cleaned R M					Degree of Alteration
		D(E)*	I(D)	K	$\alpha_{95\%}$	D(E)*	I(D)	\tilde{H}	K	$\alpha_{95\%}$	
Present data											
713-1	1	84.5 ^o	40.4 ^o	-	-	74.8 ^o	44.2 ^o	210 ^{Oe}	-	-	Unaltered(?)
A-2S	1	-12.1	41.9	-	-	-23.4	25.4	"	-	-	Slightly
C-2P	7	-149.1	27.2	5	28.5 ^o	147.9	6.2	270	42	12.0	"
714-28	3	169.1	48.1	widely scattered		109.4	29.5	200	398	12.6	"
715-9	4	78.1	57.2	1562	2.3	74.3	54.7	420	297	5.3	Highly
715-103	4	0.5	51.2	692	3.5	4.0	51.6	280	1255	2.6	"
1953 data											
III	13	12.7	39.3	13	12.1	-	-	-	-	-	Unaltered(?)
II	13	-8.0	53.4	36	7.0	-	-	-	-	-	Slightly
I	9	-78.5	-9.4	widely scattered		-	-	-	-	-	Altered

N: Numbers of specimens, *: form the astronomical north.

A PALEOMAGNETIC STUDY OF THE CENOZOIC ROCKS FROM THE
AMAKUSA ISLANDS, WESTCENTRAL KYUSHU, WEST JAPAN

Haruo DOMEN* and Hiroshi MUNEOKA**

* Institute of Physical Sciences, Faculty of
Education, Yamaguchi University, 753 Japan

** Ozuki Air Base, M. S. D. F., Shimonoseki,
750-11 Japan

During this summer(1982), a few samples of Cenozoic rocks have been collected at the Amakusa Islands, westcentral Kyushu Island, west Japan, and those of collected samples are now being examined paleomagnetically. Fig. 1 is a sketch map showing the sampling sites. Table 1 shows NRM data obtained up to this time, by means of an astatic magnetometer. The samples are also submitted to AF demagnetization and Js-T analysis. A couple of examples for AF demagnetization have been seen their directions in Table 2, together with that of the successive demagnetizations(in spite of only two specimens). Typical examples of Js-T curves obtained on the bulk-flakes of specimens come from each site are illustrated on Fig. 2.

When more data such as mentioned above accumulate, discussions will be made in the elsewhere.

Table 1. Temporary paleomagnetic data on the Cenozoic rocks from Amakusa Islands, westcentral Kyushu.

Site, Age, Rock Type	n	N R M			α _{95%}	Polarity [#] Class
		D(E)*	I(D)	K		
1. Mt. Misumi-Dake Pliocene, Hornblende Andesite	32	39.5°	25.9°	10	8.5°	-III, (N)
2. Tobi-Dake Miocene, Andesitic Lava	18	171.0	-55.8	49	5.0	-III, R
3. Kura-Take, Miocene, Liparite						(not available yet)
4. Shimokochi, Miocene, Welded Tuff						(' ')
5. Saitsu, Pleistocene, Welded Tuff						(' ')
6. Itsuwa Machi Pleistocene, Welded Tuff	15	-4.1	42.2	53	5.3	I, N
7. Naga-Shima, Neogene, Augite Andesite						(not available yet)

* from astronomical north, # see Domen, 1978.

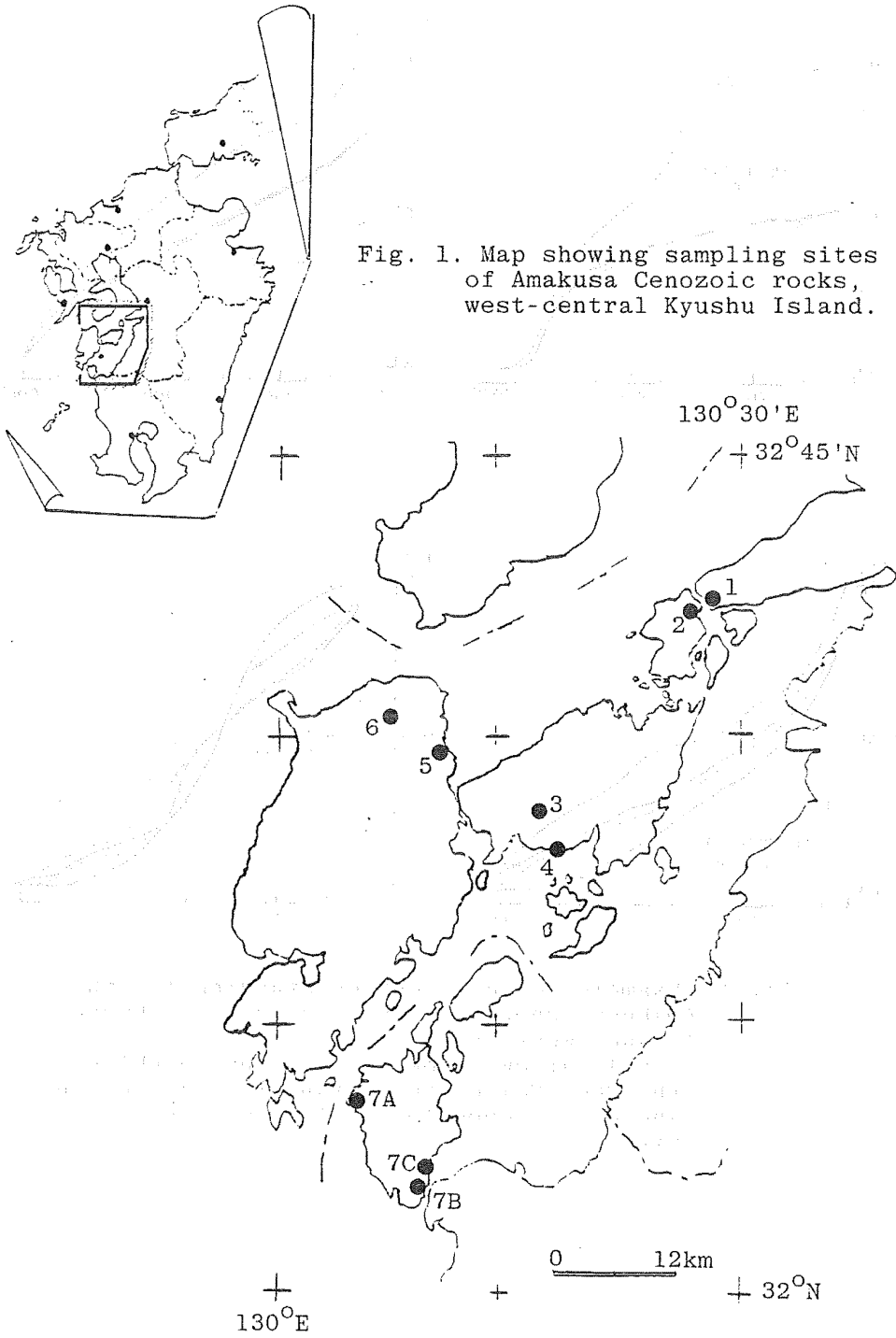


Fig. 1. Map showing sampling sites of Amakusa Cenozoic rocks, west-central Kyushu Island.

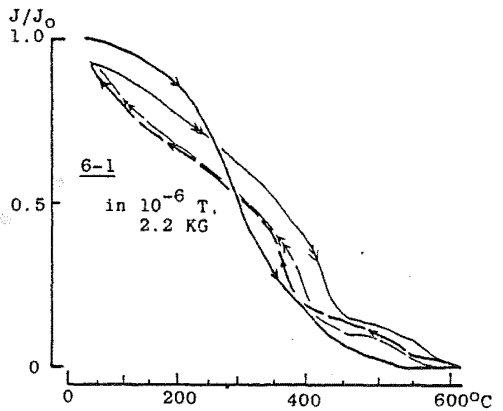
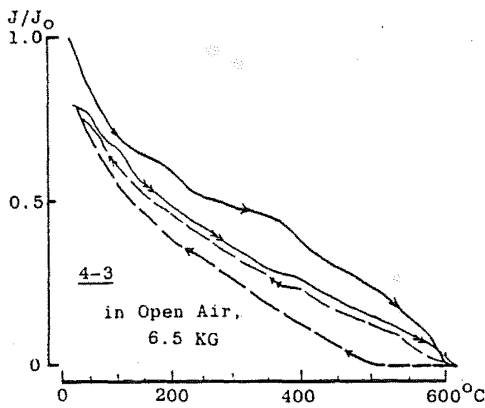
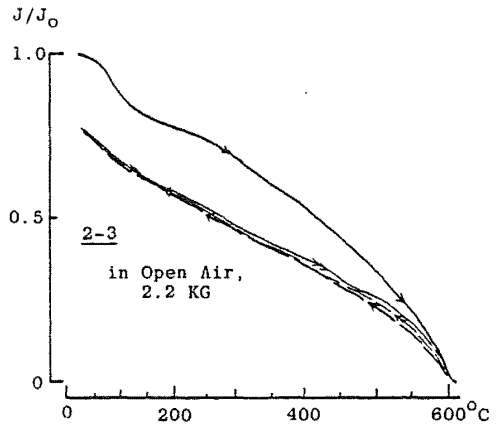
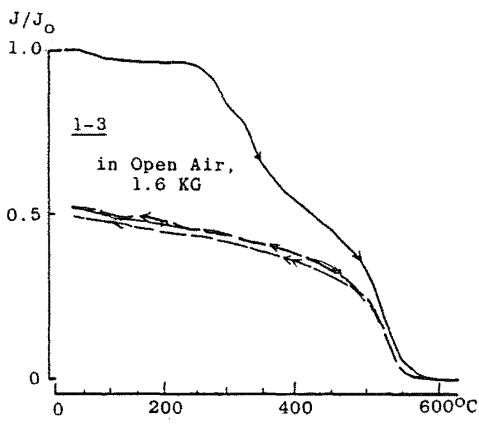


Fig.2. Examples of J_S - T curves standing for the Amakusa Cenozoic rocks, westcentral Kyushu Island, west Japan. Single arrows show the 1st run, doubles the 2nd. Solid lines stand for the heating and dotted ones for cooling process respectively.

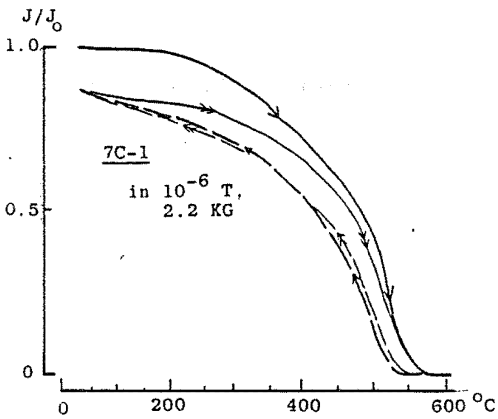
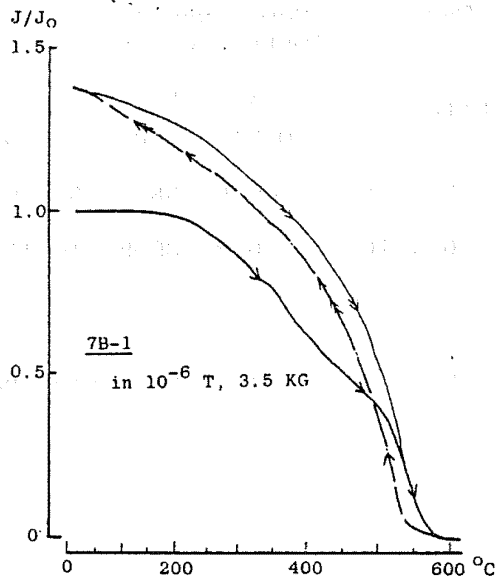
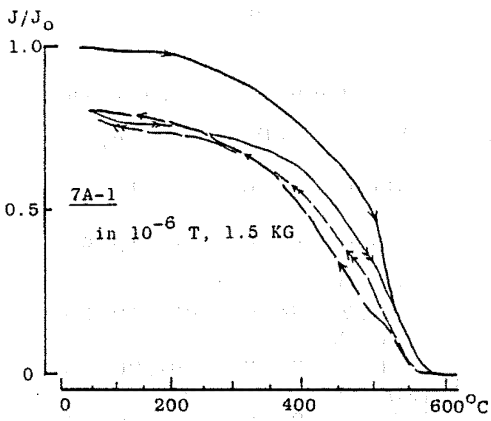


Fig. 2.(contd.) Exsamples of J_S -T curves of Amakusa rocks.

Table 2. Some examples of AF demagnetization data of Amakusa Cenozoic rocks.

Site	n	N R M				Cleaned R M (150 Oe)			
		D(E)*	I(D)	K	$\alpha_{95\%}$	D(E)*	I(D)	K	$\alpha_{95\%}$
2	8	169.9°	-58.3°	35	9.5°	164.9	-57.9°	27	10.9°
6	10	0.9	39.9	10	16.5	0.6	41.0	10	15.9
2	2	4.4	33.9	(107, 24.4)		100 Oe	6.7	34.0	(587, 10.3)
						150 Oe	6.7	33.3	(156, 20.1)
						200 Oe	17.1	39.8	(173, 19.1)
						250 Oe	6.6	37.0	(52, 35.2)

Reference

Domen, H. (1978) Bull. Fac. Educ., Yamaguchi Univ., 28 (Part 2), 33.

PALEOMAGNETISM OF IGNEOUS ROCKS OF LATE CRETACEOUS TO
MIOCENE AGE FROM THE GO RIVER AREA
-- CLOCKWISE ROTATION OF SOUTHWEST JAPAN --

Yo-ichiro OTOFUJI* and Takaaki MATSUDA**

* Department of Geology and Mineralogy, Faculty of Science,
Kyoto University, Kyoto 606, Japan

** Department of Geology, Himeji Institute of Technology,
Himeji 671-22, Japan

Introduction

Paleomagnetic studies of Cretaceous rocks of Southwest Japan (Kawai et al., 1971; Yaskawa, 1975) have established that the directions of Cretaceous sedimentary and volcanic rocks have shown clockwise deflection from the expected paleofield direction. This anomalous direction is explained by a clockwise rotation of Southwest Japan associated with the opening of the Japan Sea (Uyeda and Miyashiro, 1974; Kobayashi and Isezaki, 1977). Similar easterly declination data are reported from the Paleogene rocks (Sasajima et al., 1968). These facts leave little doubt that the clockwise rotation mainly occurred during the latter part of the Tertiary. The aim of the present work is to measure the process of clockwise rotation of Southwest Japan by paleomagnetism in an attempt to assess the timing and the amount of the rotation.

Felsic igneous rocks of Late Cretaceous to Miocene age are common over large areas of the Inner zone of Southwest Japan. These rocks are ideal for studying the tectonic rotation of Southwest Japan, because these rocks of Cretaceous and Paleogene age have easterly characteristic direction of

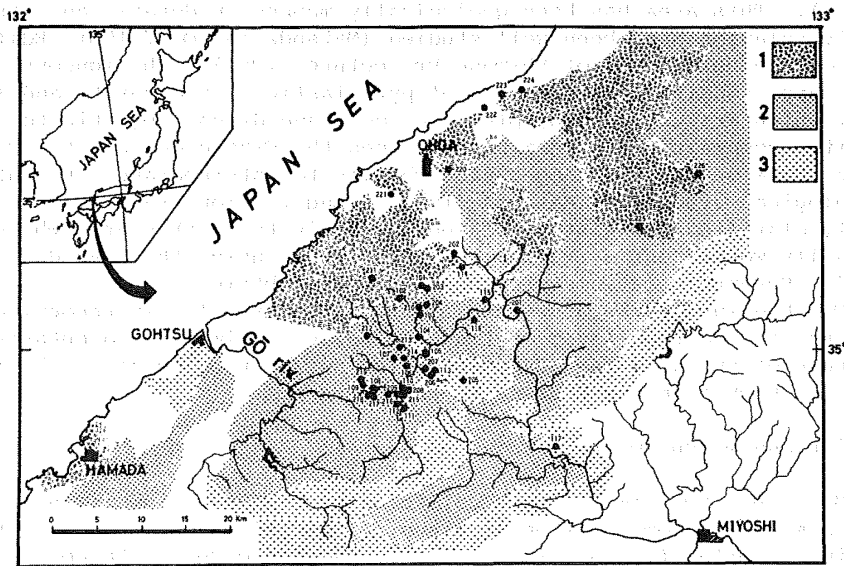


Fig. 1 Map showing the sampling localities together with distribution of the Cretaceous to the Tertiary felsic rocks. 1. Neogene rocks; 2. Paleogene rocks; 3. Cretaceous rocks.

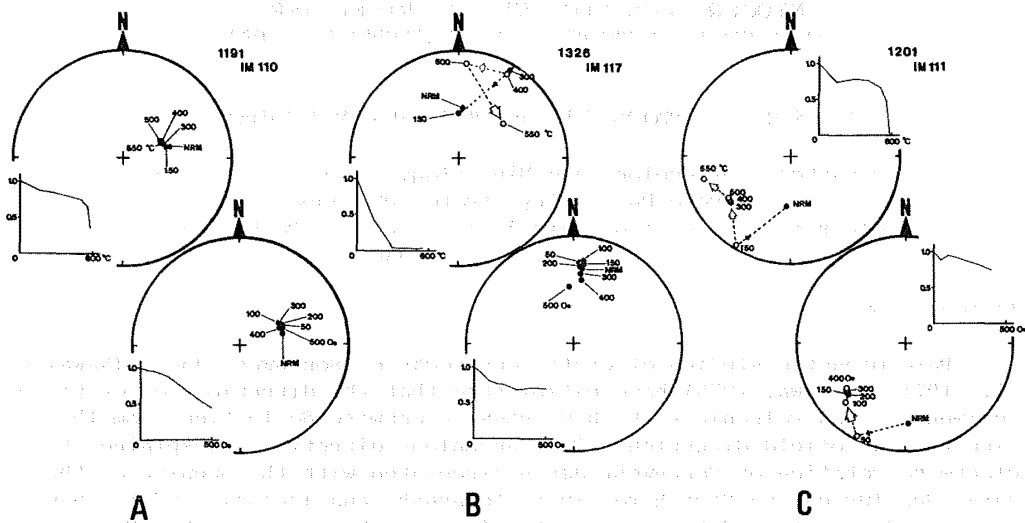


Fig. 2 Demagnetization data for specimens in three categories. A, B and C correspond to the three categories A, B and C in text, respectively. Thermal demagnetization steps are indicated by the temperature in °C while alternating field demagnetization steps are indicated by the value of the peak field in Oe. Projections are equal area, solid symbols on the lower hemisphere, open symbols on the upper hemisphere.

Southwest Japan (Sasajima et al., 1968; Kawai et al., 1971). These igneous rocks are extensively exposed along the Gō River and the neighbouring region in the central part of Southwest Japan, where this study was carried out (Fig. 1). This area has been geologically mapped in detail, and its stratigraphic relation have been well studied (Matsuda and Oda, 1981; Editorial Board of Geological Map of Shimane Prefecture, 1982): The igneous rocks of the area consist of a sequence of pyroclastic flow deposits and lava flows, which are intruded by plutonic rocks and dykes. Dacitic to rhyolitic compositions predominate between the Cretaceous and the Paleogene. During the Miocene, the composition changes to intermediate. Recently chronological studies by Matsuda (1982) using fission-track methods have greatly clarified the history of igneous activity in this area which was originally worked out by Kawano and Ueda (1966) using the K-Ar dating method. Seventeen radiometric ages have been obtained.

The bedding planes of strata of this area are clearly recognized from the intercalated thin layer of fine tuffaceous sediments and eutaxitic structure of the granules of pumice. The declination change with time can be traced back from the Miocene to the Cretaceous.

Sampling and measurements

More than 500 samples were collected by hand sampling oriented blocks using a magnetic compass from 45 sites. These sites included all the sampling sites for fission-track dating. Samples cover Cretaceous to Miocene in age. Sampling sites are shown in Fig. 1. Dips of the strata at all sites were observed in the field except for plutonic rocks. Uncertainty of a few degrees was introduced in determining the dip.

Two cylindrical specimens were drilled from each oriented hand sample in the laboratory. Remanent magnetization was measured with a Schonstedt

Table 1. Paleomagnetic results for the G3 River region

Geological Sequence		Age (Ma)	Site	Category	DT	N	D	I	α_{95}	k	Rock Type	
Izumo Group	Omori Fm.	(12) ^{α}	221	C	500°C	8	-165.2	-58.7	8.7	41.8	andesite lava	
			222	A	400°C	12	164.5	-39.6	3.0	210.3	andesite lava	
			223*	A	400°C	12	148.5	-65.9	2.8	242.9	dacite welded tuff	
			224*	C	400°C	12	-3.0	57.2	16.6	7.8	andesite lava	
Iwami Group	Kuri Fm.	(14) ^{α}	220	C	500°C	12	25.0	50.9	12.0	14.0	dacite lava	
			Hata subgroup	202*	C	550°C	9	-104.2	-64.1	6.1	72.3	andesite lava
				203*	C	550°C	12	-2.3	44.8	5.2	69.5	andesite lava
		23	226*	A	500°C	11	-177.5	-52.1	2.7	283.3	gabbro	
Kawauchi Group	Ringdyke Sorajo Fm.	29	104*	A	500°C	10	-118.6	30.5	5.5	77.4	rhyodacite dyke	
			103*	C	500°C	10	-83.5	64.5	9.8	25.1	dacite welded tuff	
			210*	C	500°C	11	-101.8	52.1	3.6	165.6	"	
			204*	C	500°C	11	-96.1	30.5	11.2	17.2	"	
	Sasahara Fm.	28	107*	A	400°C	10	52.4	15.9	3.6	185.6	dacite welded tuff	
			212*	A	500°C	11	83.5	21.6	5.8	63.2	"	
			213*	A	500°C	12	42.0	30.9	1.8	552.1	"	
			214*	A	500°C	11	35.6	35.1	3.6	164.1	"	
Kawamoto granodiorite	29 (25) ^{β}	105	C	400°C	9	61.4	39.5	11.5	21.1	granodiorite		
		33	110	A	400°C	8	64.3	55.4	3.2	305.0	"	
		207	C	550°C	10	68.3	57.5	11.0	20.3	"		
		208	C	400°C	5	59.6	56.8	5.0	230.7	"		
		209	C	500°C	12	54.0	60.5	2.6	273.4	"		
		215	A	400°C	12	56.3	46.8	2.0	463.8	"		
		219	C	500°C	10	-116.4	-43.4	5.0	95.4	"		
Sakurae Group	Nakano Fm.	N4 N3 N2 N1	216*	C	500°C	9	-115.8	-56.0	18.9	8.4	dacite welded tuff	
			106*	A	500°C	12	-100.2	-27.0	8.9	22.5	"	
			108*	B	500°C	8	-107.7	-15.8	16.3	12.5	dacite welded tuff	
			218*	A	500°C	11	98.8	10.9	3.4	181.1	"	
			109*	A	400°C	10	-64.4	-72.9	2.7	325.3	rhyodacite lava	
Ochi Group	Yadani Fm.	80 < 92	111*	C	500°C	11	-131.5	-44.7	6.7	47.1	rhyolite tuff	
			111'*	B	500°C	6	-91.1	-36.4	13.5	25.6	mud stone	
			205*	C	500°C	12	-119.7	-63.1	2.2	377.2	rhyolite welded tuff	
	Ichiihara Fm.	92	112*	C	500°C	8	-72.7	-53.4	4.9	130.6	rhyolite welded tuff	
			206*	C	500°C	11	-137.4	-35.8	6.4	51.5	"	
		1137*	B	550°C	9	-99.3	-18.2	9.7	29.0	"		

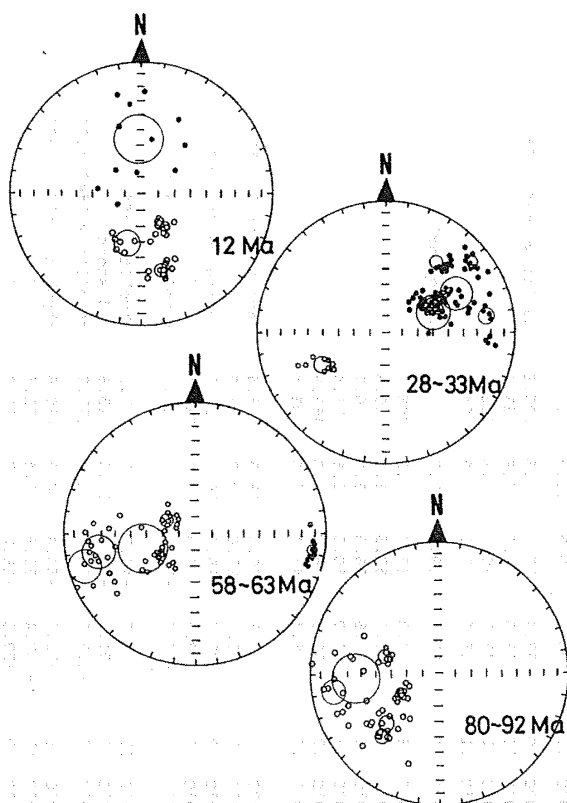


Fig. 3 Summary of characteristic directions of magnetization of samples with site mean directions and α_{95} confidence circles for four periods; 80-92 Ma (Cretaceous), 58-63 Ma (Paleocene), 28-33 Ma (Oligocene) and 12 Ma (Miocene). Projections are equal area, solid symbols on the lower hemisphere, open symbols on the upper hemisphere.

direction of a primary magnetization with both treatment (Fig. 2; C); in general thermal treatment was more successful in isolating a coherent magnetization than AF treatment.

The optimum demagnetization temperature to produce minimum dispersion was selected from three pilot specimens for each site of the category (A), and the other specimens from the site were demagnetized at its temperature. All specimens in the other categories were progressively treated with thermal demagnetization so that the primary component was recognized in individual specimens. The mean direction at the demagnetization level yielding the highest value of Fisher precision parameter, k , (Fisher, 1953) was

SSM-1A spinner magnetometer. Three specimens from each site were progressively demagnetized in alternating field (AF) in steps of 50 Oe up to a maximum field of 500 Oe. Progressive thermal demagnetization was also undertaken on three specimens from each site in steps of 100 °C or 150 °C to the Curie temperature with increment steps reduced to 30 °C or 50 °C near the Curie temperature.

Treatment in progressive AF and thermal demagnetization for three pilot specimens from each site divided the sites into three categories (see Fig. 2): (A) Natural remanent magnetization (NRM) shows little change in direction with either AF or thermal treatment (Fig. 2; A); (B) NRM directions moved after each thermal treatment step and ultimately converged about a mean direction which was assumed to be that of the primary magnetization, but directions were quite stable under AF treatment (Fig. 2; B); and (C) NRM directions moved toward a

Table 1. Data are after tilting correction. (*) denotes a site where dip of the strata were observed. Kawamoto granodiorite is estimated to be subjected to little regional movement. The ages are fission-track data after Matsuda (1982). (α) Age estimated based on paleontology (Tai and Kato, 1979; Takenouchi et al., 1982); (β) K-Ar data from Kawano and Ueda (1966). Category: Behaviour of NRM direction during demagnetization (see text). DT is the magnetic cleaning temperature, N is the number of samples in site mean computation, D is the site mean declination, I is the site mean inclination, and α_{95} and k are Fisher statistic parameter.

generally accepted to be that of the primary magnetization.

Loss of specimens occurred during thermal demagnetization, as specimens exploded at about 400 °C. The following criteria were adopted to determine the reliability of each site; An acceptable site has at least five specimens cut from individual oriented samples and a mean direction from them has a mean circle of 95 percent confidence of less than 20°.

Results

Thirty five sites survived the criteria. The paleomagnetic data and the categories of magnetic behaviour of samples during demagnetization of each site are listed in Table 1, corrected for geological dip.

The reliable paleomagnetic data cover the age between 92 Ma and 12 Ma. Radiometric age indicates that the paleomagnetic data can be divided into four stages; (80 Ma-92 Ma), (58 Ma-63 Ma), (28 Ma-33 Ma) and (12 Ma-23 Ma). The cleaned paleomagnetic directions of each stage are shown in Fig. 3.

80 Ma - 92 Ma (Late Cretaceous):

Samples from all sites have a reversed polarity. Their directions show a clockwise deflection of declination by more than seventy degrees. The reliability of this direction is ascertained by agreement between directions of sediments and tuffs, although there is only a single polarity in magnetization. All the samples may have acquired their magnetization during the reversed interval between magnetic anomalies 33 and 34 (Lowrie and Alvarez, 1981).

59 Ma - 63 Ma (Paleocene):

The declination value is $81^\circ \pm 26^\circ$ with 95 % confidence. The reliability of the direction is confirmed by the presence of both normal and reversed polarities as well as high agreement between data from lavas and tuffs.

28 Ma - 33 Ma (Oligocene):

The directions from granodiorite (29 Ma and 33 Ma) and from tuff (28 Ma) show a high degree of consistency. Evidence from eleven sites shows that the clockwise deflection of declination still persisted in the Late Oligocene.

At sites of the Sorajo Formation (sites: 103, 210, 204; 29 Ma) a partial field reversal is apparently recorded. While these sites have anomalous westerly declination (by about 90°), inclination change systematically: The younger sites have more steeply downward inclinations than the older site. The NRM of a ring dyke (site 104) may be acquired during this field reversal. These directions were excluded from the statistical

Table 2. Average Paleomagnetic directions

Stage	N	\bar{D}	\bar{I}	α_{95}	V. G. P.	∂p	∂m	Δ	Δ_{95}
12Ma	4	1.3	56.3	16.9	87.9N 161.6E	17.6	24.4	1	32
28 - 33 Ma	11	58.0	43.0	10.4	39.5N 142.8W	8.0	12.9	58	14
59 - 63 Ma	6	80.9	42.2	25.6	20.8N 153.4W	19.3	31.5	54	40*
80 - 92 Ma	6	71.3	44.2	20.3	29.1N 150.3W	16.0	25.5	45	34*

N is the number of site. \bar{D} , \bar{I} are mean declination and inclination for each period, α_{95} is circle of 95 % confidence. Δ is the difference in declination value between this area and Korean Peninsula. Data for Korean Peninsula from Otofujii et al. (1982): $D = 26.6^\circ$, $I = 62.3^\circ$ and $\alpha_{95} = 8.3^\circ$. Δ_{95} is uncertainty in declination at 95 % confidence, where $\Delta_{95} = \sin^{-1}(\sin \alpha_{95} / \cos I)$. Uncertainty of older period (*) is calculated as

follows: $\sqrt{(\Delta_{95}^2)_{\text{Korea}} + (\Delta_{95}^2)_{\text{this area}}}$

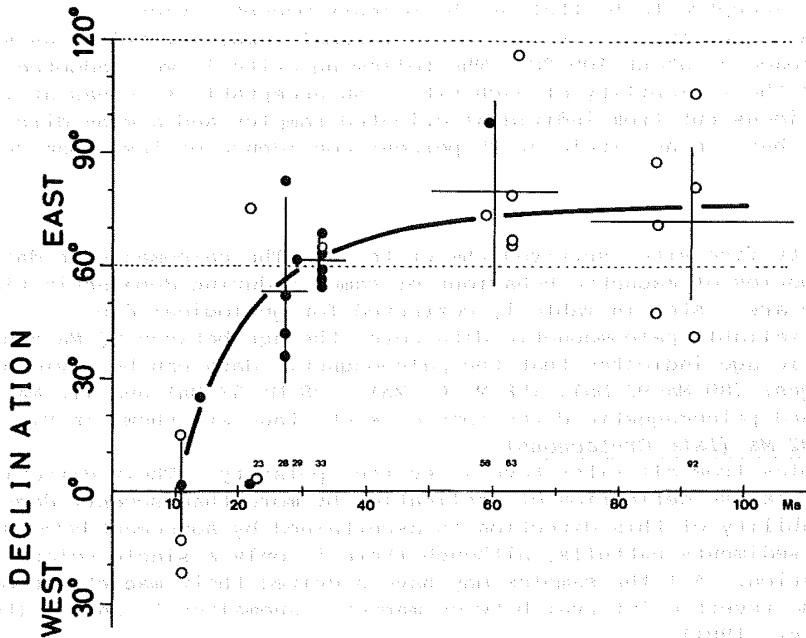


Fig. 4 Declination data of site means as a function of the age with fission-track method together with representative mean directions for five periods. The declination error bars are the α_{95} values and age error bars are the uncertainty of fission-track method of 20 %. The ages with fission-track method are shown along the abscissa of age. Closed circles show the data with normal polarity and open circles show with reversed polarity. The solid curve is presumed declination change.

computation for this stage.

12 Ma - 23 Ma (Miocene):

The paleomagnetic direction of the Omori Formation is almost the same as the axial dipole field. The Omori Formation is assigned to the Middle Miocene (about 12 Ma) from the geological correlation with the Kuri Formation of 14 Ma (Tai and Kato, 1979; Takenouchi et al., 1982).

The declination change probably occurred during the Early Miocene. Data from two sites, 220 (14 Ma) and 202 (23 Ma), may show characteristic directions during the period of declination change. The NRM's of two other sites (203, 226; 23 Ma) formed during this period are coincident with the direction of the present magnetic field, although the gabbroic rocks show a reversed polarity. It is possibly that the primary component of NRM was completely obscured by the secondary component which was acquired after the Middle Miocene. There remains, however, another possibility for the explanation of the directions during this period that declination change began at about 23 Ma and finished within one million years. Further paleomagnetic and chronological work is in progress and will hopefully enable us to refine the time of the declination change. The data from the four sites formed during the period of the declination change were excluded from the statistical computation of the Miocene.

Discussion

A statistical analysis (Fisher, 1953) is given for each stage in Table 2, together with virtual geomagnetic poles.

Comparing the pole position of the Cretaceous with previously reported data from Southwest Japan (Sasajima, 1981), the circles of 95 percent confidence overlap. This indicates that the study area appropriately rep-

resents the tectonic block of Southwest Japan since the Cretaceous. Both declination values of Cretaceous and Paleocene age are relatively larger than the previous data which were obtained without intensive thermal demagnetization (Sasajima et al., 1968; Kawai et al., 1971). The more easterly direction in this study can be attributed to successful removal of secondary component by thermal treatment. The secondary component remaining without demagnetization generally makes the remanent magnetization direction fall closer to that of the present field. The inclination value of Cretaceous seems to be shallower than previous data (Sasajima, 1981). Since the direction in this study is fairly scattered ($\alpha_{95} = 20.3^\circ$), it is difficult to postulate the northward translation of this area.

The change in declination is plotted as a function of the age determined by fission-track dating in Fig. 4. The easterly declination value decreases gradually from the Late Cretaceous of 92 Ma to the Late Oligocene of 28 Ma. While the easterly declination persists until 28 Ma, the declination at about 12 Ma coincides with that expected from axial dipole. This clearly indicates that the main part of the declination change began after 28 Ma.

The declination change is caused by both tectonic rotation and apparent polar wander. The tectonic rotation of Southwest Japan is calculated through comparison between declinations of Southwest Japan and the Korean Peninsula, since the paleomagnetic data from Korean Peninsula only show the geomagnetic effect of apparent polar wander (Otofuji et al., 1982). Differences of declinations between Southwest Japan and the Korean Peninsula were calculated only for the periods of the Paleocene and the Cretaceous, because the paleopole after 30 Ma is consistent with the present geographic north pole (Irving, 1977; Harrison and Lindh, 1982). The amount of rotation of Southwest Japan is listed in Table 2. The uncertainty in rotation at the 95 percent confidence level is the Δ_{95} value after Kellogg and Reynolds (1978) where $\Delta_{95} = \sin^{-1}(\sin \alpha_{95}/\cos I)$ with α_{95} the radius of the 95 % confidence circle and I the mean inclination. The amount of rotation scarcely decreases with decreasing age between 92 Ma to 28 Ma, although the uncertainty is quite large. The declination change during the Paleogene probably results from the effect of polar wander. The results suggest that the tectonic rotation of Southwest Japan took place abruptly after 28 Ma.

The amount of rotation of Southwest Japan was estimated from the data of the Kawamoto Granodiorite and the Sasahara Formation with fission-track ages between 28 Ma and 33 Ma, because these directions scarcely include the effect of the polar wander motion, and the geomagnetic secular-variation would be eliminated from their mean direction by averaging over enough time. It is concluded that Southwest Japan has been subjected to a clockwise rotation through $58^\circ \pm 14^\circ$. Inclination data indicate that Southwest Japan has not undergone significant north-south translation.

The reliability of the timing of 28 Ma is ascertained through the concordancy of the fission-track data within same rock unit and comparison of fission-track ages with that determined by the K-Ar method. The fission-track ages of 29 Ma and 33 Ma are obtained from the Kawamoto Granodiorite which is overlain by the Sasahara Formation with fission-track age of 28 Ma. These ages show good agreement with a K-Ar age (25 Ma) determined on biotite (Kawano and Ueda, 1966), although the K-Ar age is relatively younger than the other ages. The younger age of K-Ar may be attributed to the loss of argon from biotite because of alteration of rock samples from the Kawamoto Granodiorite (Kawano and Ueda, 1966).

Conclusion

The paleomagnetic results from the Upper Cretaceous to Miocene rocks

from Gō River area established: (1) The clockwise rotation of $58^\circ \pm 14^\circ$ of Southwest Japan took place later than 28 Ma; (2) the rotational motion terminated around 12 Ma; and (3) Southwest Japan was subjected to little rotational motion between 92 Ma and 28 Ma.

References

- Editorial Board of Geological Map of Shimane Prefecture (1982) Geological Map of Shimane Prefecture, Dept. Geol. Shimane Univ.
- Fisher, R. (1953) Proc. R. Soc. London, Ser. A, 217, 295.
- Harrison, C.G.A. and T. Lindh (1982) J. Geophys. Res., 87, 1903.
- Irving, E. (1977) Nature, 270, 304.
- Kawai, N., T. Nakajima and K. Hirooka (1971) J. Geomag. Geoelectr., 23, 267.
- Kawano, Y. and Y. Ueda (1966) Jour. Japan Assoc. Min. Petr. Econ. Geol., 56, 121.
- Kellogg, K.S. and R.L. Reynolds (1978) J. Geophys. Res., 83, 2293.
- Kobayashi, K. and N. Isezaki (1977) The geophysics of the Pacific Ocean Basin and its Margins, Am. Geophys. Union, Geophys. Monogr., 19, 235.
- Lowrie, W. and W. Alvarez (1981) Geology, 9, 392.
- Matsuda, T. (1982) Abstr. of 5th International Conf. Geochron. Cosmochron. Isotope Geol. (Nikko), 37.
- Matsuda, T. and M. Oda (1982) Jour. Geol. Soc. Japan, 88, 31.
- Otofujii, Y., J.Y. Oh, T. Hirajima, K.D. Min and S. Sasajima (1982) The tectonic and geologic evolution of Southeast Asian seas and islands, Am. Geophys. Union, Geophys. Monogr., 27. (in press).
- Sasajima, S. (1981) Paleoreconstruction of the continents, Geodynamic Ser. Vol. 2, edited by M.W. McElhinny and D.A. Valencio, pp 115 (AGU, Washington, D.C. and GAS, Colorado) p. 194.
- Sasajima, S., J. Nishida and M. Shimada (1968) Earth Planet. Sci. Lett., 5, 135.
- Tai, Y. and M. Kato (1979) Fundamental data on Japanese Neogene Bio- and chronostratigraphy, edited by R. Tsuchi, pp. 101, Shizuoka Univ., Shizuoka.
- Takenouchi, S., Y. Tai and M. Kato (1982) Hiroshima Univ. Integrated Arts and Sci. Fac., Mem. ser. IV, 7, 49.
- Uyeda, S. and A. Miyashiro (1974) Geol. Soc. Am. Bull., 85, 1159.
- Yaskawa, K. (1975) Geophys. J. R. astr. Soc., 43, 835.
- (in press in Earth Planet. Sci. Lett.).

THERMOMAGNETIC ANALYSIS OF THE CRETACEOUS ROCK FROM TAIKAZAN DISTRICT, TOKUYAMA CITY, YAMAGUCHI PREFECTURE, WEST JAPAN

Haruo DOMEN

Institute of Physical Sciences, Faculty of Education, Yamaguchi University, 753 Japan

Previously the present author reported a paleo/rock magnetic properties on some Cretaceous rocks come from Yamaguchi Prefecture, west Japan (Domen 1982), in which some examples of the J_S -T curve standing for each sampling site were shown. Those J_S -T curves are roughly classified into two types; one shows a convex type; that is rather similar to that of magnetite, another is a concave. However, the main Curie points for both types are found around 600°C. Among them, the test specimen from one sampling site; Mt. Taikazan district, Tokuyama City at the seaside of Seto Island Sea, southcentral Yamaguchi Prefecture (Site No. S-2 in the previous paper mentioned above) shows quite different mode of J_S -T curve compared with those of all other samples. The Taikazan specimen having such a rather peculiar mode of J_S -T curve has now been examined precisely, and in this report, some results obtained since the last paper was published are briefly shown.

So far as the present study concerned, the test specimen come from Taikazan rock (bulk flakes are submitted to the analysis) shows during the initial heating that the J_S value decreasing with temperature rising lose about one third of the initial intensity at ca. 200°C firstly. As has been seen in a schematic diagram (Fig. 1), the J_S intensity decreases down towards the abscissa at the point, $T \approx 350^\circ\text{C}$ (dotted line in Fig. 1), but the J_S value does not smoothly decrease in this process. The intensity once increases with temperature increasing at around 300°C then on sharply decreases, and small value of J_S still remained following up to ca. 600°C, then finally disappears. Sometimes before reaching to such the highest Curie point, J_S -T curve recovers a little. Generally speaking, such the initial decay mode of J_S -T curve

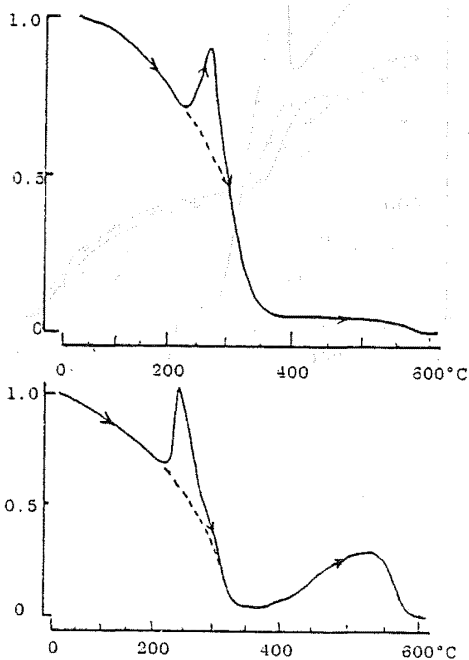


Fig. 1. Typical mode of initial heating curves of J_S -T.

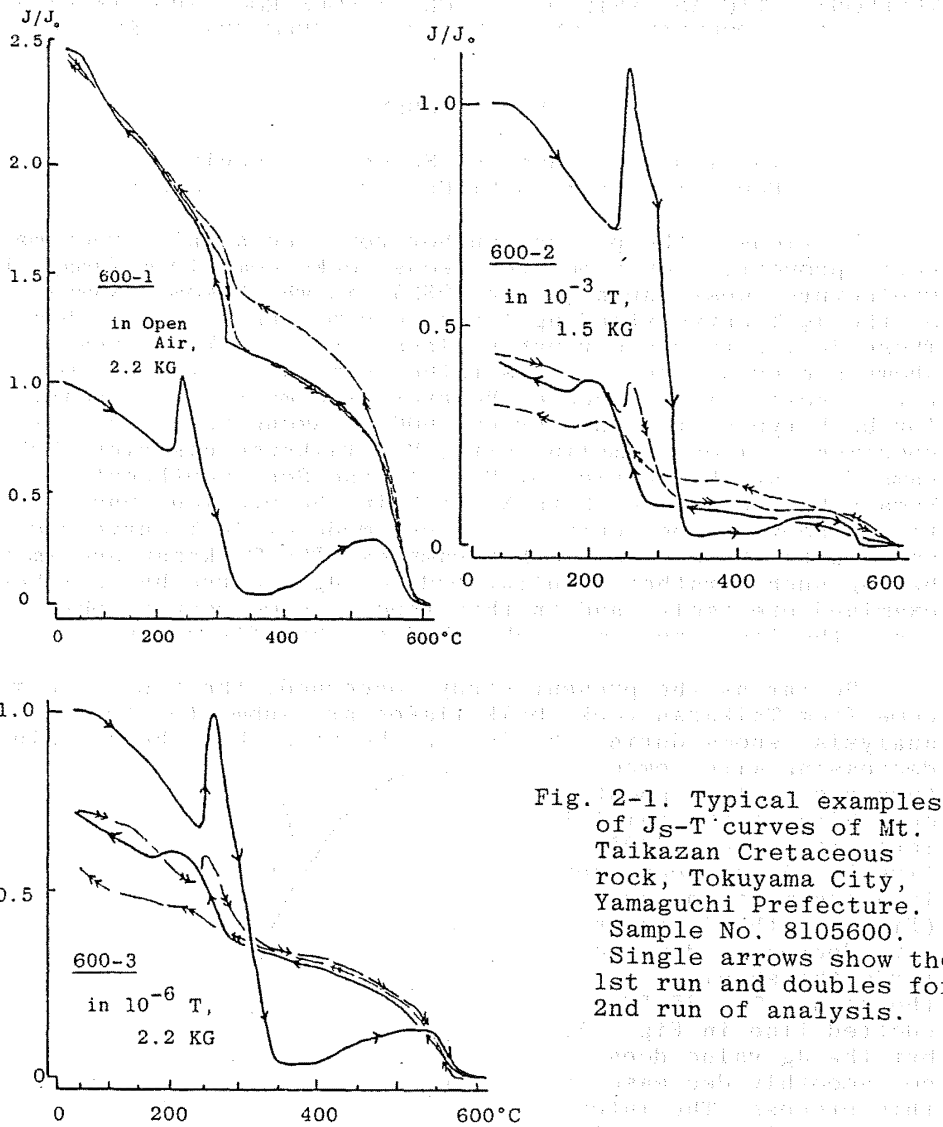


Fig. 2-1. Typical examples of J_S - T curves of Mt. Taikazan Cretaceous rock, Tokuyama City, Yamaguchi Prefecture. Sample No. 8105600. Single arrows show the 1st run and doubles for 2nd run of analysis.

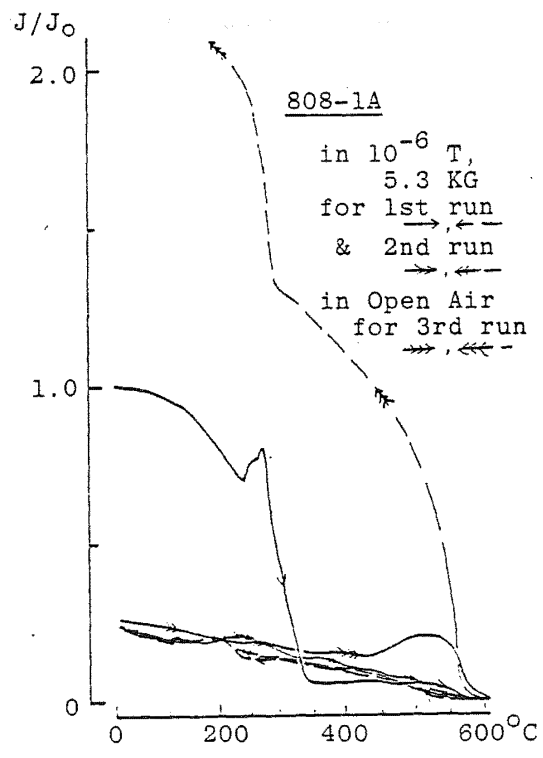
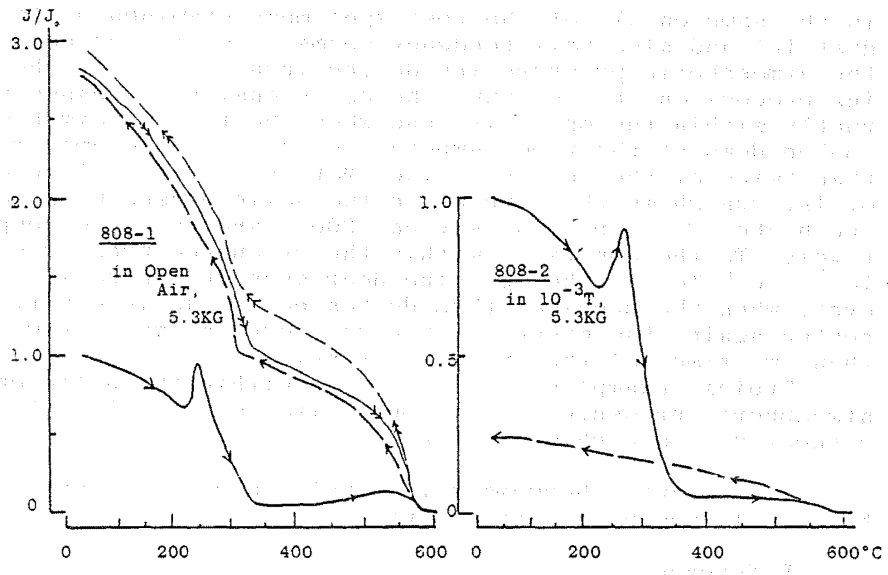


Fig. 2-2. J_S -T curves for Taikazan Creta. rock; Sample No.8105800. Symbols are same to those in Fig.2-1 otherwise noticed.

is the same on all of the test specimens examined of Taikazan district and also this tendency seems to be independent on the atmospheric pressure inside the furnace. But in the cooling process on the 1st run, the J_S intensity increases abruptly within the open air, and when the test specimen was cooled down at the room temperature, J_S value becomes more than twice of the initial value. Moreover, the cooling curve of 1st run shows that there are two solid phases with lower and higher Curie points, say ca. 300°C and ca 600°C respectively. To the contrary, within the evacuated pressures; say 10^{-3} , 10^{-6} Torrs, the J_S value decreases during cooling. However, when the specimen thus decreased of J_S intensity was heated again, the magnetization recovers as much as more than two times of the initial intensity.

Typical examples of J_S -T curves within the different atmospheric pressure; in the open air, 10^{-3} and 10^{-6} Torrs respectively are shown in Fig. 2-1, -2.

More minute thermomagnetic analysis on these specimens have still now been carried out.

Reference

Domen, H. (1982) Bull. Fac. Educ., Yamaguchi Univ., 32 (Part 2), 23.

PALEOMAGNETISM OF CRETACEOUS GRANITIC ROCKS
FROM OKUSHIRI ISLAND, WEST HOKKAIDO

Yukio NOTSU and Haruaki ITO

Department of Physics, Faculty of Science,
Shimane University, Matsue 690, Japan

Cretaceous granitic rocks in the Okushiri Island intrudes into early Cretaceous volcanic rocks and their igneous rocks are locally covered by the Neogene Tertiary formations which consist mainly of andesitic volcanic complex and lacustrine deposits (Hata, 1976). The intrusive bodies can be considered to have been emplaced at relatively shallow depth because zonal texture of plagioclase and micrographic texture of quartz orthoclase are generally observed in the rocks (Narita et al., 1980).

K-Ar age of a granodiorite sample taken from a shore reef in the west coast of the Island is obtained by Shibata and Yamada (1978). The age determined is 95.8 ± 3.1 Ma. This value is consistent with K-Ar ages (90-100 Ma) for granitic rocks from the Abukuma plateau given by Kawano and Ueda

(1965b). On the other hand, granitic rocks in the Oshima Peninsula are dated at 111 Ma for granodiorite sample taken at Setana and 124 Ma for granodiorite sample at Imagane (Kawano and Ueda, 1966). These ages from the Oshima Peninsula are clearly older than the age of the Okushiri granodiorite, but the values are well consistent with the ages (110-125 Ma) for granitic rocks from the Kitakami plateau (Kawano and Ueda, 1965a, 1967). This suggests that the time of emplacement or cooling of the granitic rocks in the Okushiri Island is correlated with that of the granitic rocks in the Abukuma plateau, and that the granitic rocks in the Oshima Peninsula are coeval with the granitic rocks in the Kitakami

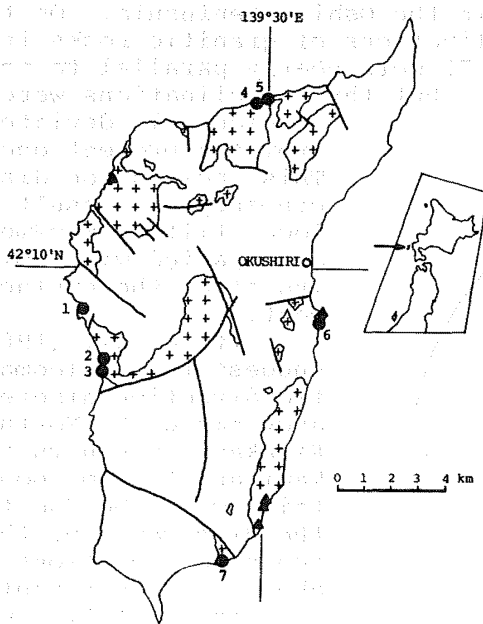


Fig. 1. Simplified map showing distribution of Cretaceous granitic rocks in the Okushiri Island. Closed circles represent sampled sites with stable magnetizations. Closed triangles represent sampled sites showing within-site scatter in directions or unstable magnetizations.

mountains.

Paleomagnetic data for Cretaceous granitic rocks of the Oshima Peninsula, Kitakami and Abukuma mountains are reported by many workers (e.g., Kawai et al., 1971; Ito et al., 1980). Ito et al. (1980) pointed out that there is a significant difference between paleomagnetic directions for granitic rocks in the Oshima Peninsula and the Kitakami plateau, despite of having similar K-Ar ages to each other as mentioned above. Paleomagnetic directions from the Oshima Peninsula were almost easterly, but those from the Kitakami plateau extremely westerly. Although paleomagnetic data for Cretaceous granitic rocks of the Abukuma plateau are insufficient, paleomagnetic directions obtained are mostly westerly.

One hundred eighteen samples were collected from 12 sites in seven bodies as shown in Fig. 1. Core samples were drilled from each hand sample in the laboratory. All but a few core samples were magnetically demagnetized and remaining cores thermally demagnetized. Consequently, samples at the seven sites were found to be magnetically stable and to display within-site consistency. Magnetic directions within the remaining five sites would never converge. Results of measurements are summarized in Table 1.

The granitic rocks in the Okushiri Island are roughly divided into two groups from paleomagnetic directions after alternating field demagnetization as shown in Fig. 2. Paleomagnetic directions of granitic rocks in the west coast (sites 1, 2 and 3) were easterly and their directions are consistent with those of granitic rocks in the Oshima Peninsula. On the other hand, paleomagnetic declinations of granitic rocks in the east coast (sites 4, 5, 6 and 7) were nearly parallel to the present earth's magnetic field, but their inclinations were

considerably deviated from the present one. This inclination discrepancy may result from local tilting movements accompanied with uplifting after the emplacement.

Ito et al. (1980) suggest that paleomagnetic direction discrepancy among the Northern Kitakami, Southern Kitakami and Abukuma mountains would be due to the difference of the amount of rotations about northwest-southeast axes, if tilt was produced by rotation about a horizontal axis. The difference between paleomagnetic directions for the granitic rocks from the Okushiri Island and the Oshima Peninsula

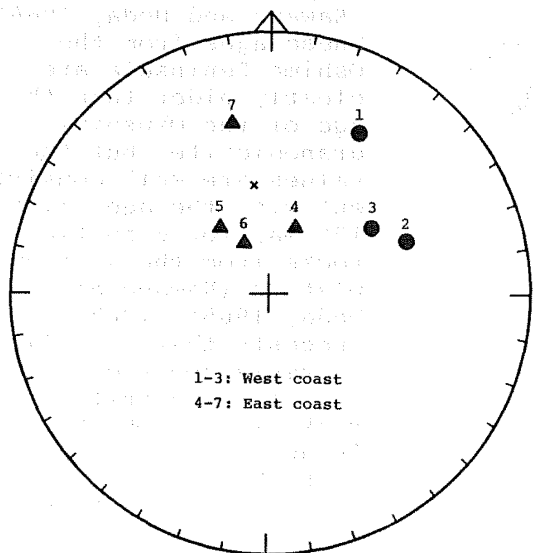


Fig. 2. Site mean directions of magnetization. Cross mark is the present direction of the geomagnetic field.

Table 1

Site	N	Mean direction		α_{95} (°)	J_r (emu/gr)	Cleaning field (oe)
		D(°)	I(°)			
1 Kamoishi tunnel	10	28.7	35.1	13.1	1.92×10^{-5}	100
2 Tsukidashi	12	69.5	42.9	11.0	0.47×10^{-5}	100
3 Tsukidashi	13	58.2	51.5	8.5	0.49×10^{-5}	100
4 Oiwaoui-gawa	9	22.5	68.1	6.6	1.96×10^{-5}	100
5 Oiwaoui-gawa	10	-37.3	64.5	5.0	1.35×10^{-5}	100
6 Akaishi-misaki	10	-26.3	73.3	11.7	0.95×10^{-5}	100
7 Matsue	12	-12.9	34.2	6.3	1.97×10^{-5}	200

N: Number of samples.

J_r : Intensity of NRM after alternating field demagnetization.

α_{95} : Semi-angle of cone of 95 percent confidence.

is not quite clear yet, but the directions are certainly different from those for granitic rocks from the Kitakami or Abukuma mountains. This result will give us an important clue to investigations of tectonic movements in Northeast Japan.

References

- Hata, M. (1976) Rep. Geol. Min. Inst. Niigata Univ., No 4, 91 (in Japanese).
- Ito, H., K. Tokieda and Y. Notsu (1980) Rock Mag. Paleogeophys. 7, 113.
- Kawai, N., T. Nakajima and K. Hirooka (1971) J. Geomag. Geoelectr., 23, 267.
- Kawano, Y. and Y. Ueda (1965a) J. Japan. Assoc. Min. Petr. Econ. Geol., 53, 143 (in Japanese).
- Kawano, Y. and Y. Ueda (1965b) J. Japan. Assoc. Min. Petr. Econ. Geol., 54, 162 (in Japanese).
- Kawano, Y. and Y. Ueda (1966) J. Japan. Assoc. Min. Petr. Econ. Geol., 56, 41 (in Japanese).
- Kawano, Y. and Y. Ueda (1967) J. Japan. Assoc. Min. Petr. Econ. Geol., 57, 177 (in Japanese).
- Narita, E., E. Ohta, E. Ohmori and S. Terashima (1980) Bull. Geol. Surv. Japan, 31, 55 (in Japanese).
- Shibata, K. and N. Yamada (1978) Bull. Geol. Surv. Japan, 29, 45 (in Japanese).

PALEOMAGNETIC MEASUREMENT OF THE MIYAKO GROUP
IN THE KITAKAMI MASSIF, NORTHEAST JAPAN

Toshiyuki Tosha

Geophysical Institute, Faculty of Science, University of Tokyo,
Bunkyo-ku, Tokyo 113

1) Introduction

In the Kitakami mountains, voluminous Cretaceous granite were intruded into the Paleozoic and Mesozoic complexes. Kawai et al. (1961) argued the deformation of the Japan islands from the paleomagnetic data in the intrusives. It is, however, difficult to estimate the tectonic tilting of intrusive rocks. In order to obtain correct paleomagnetic direction, it is necessary to assume the paleo-horizontal plane and/or to estimate a tilting angle from the geological information. On the other hand, Sedimentary rocks maintain the paleo-horizontal plane. Hence the reliable paleomagnetic directions can be obtained from sedimentary rocks.

The formations of Cretaceous sedimentary rocks are exposed along the east seacoast in the Kitakami massif. These sedimentary rocks constitute the Miyako Group. The Miyako Group is divided into following four formations in ascending order, the Raga formation, the Tanohata formation, the Hiraiga formation, and the Aketo formation. The main purpose of this study is to obtain the paleomagnetic pole position in sedimentary rocks of the Miyako Group.

2) Geological setting and sampling

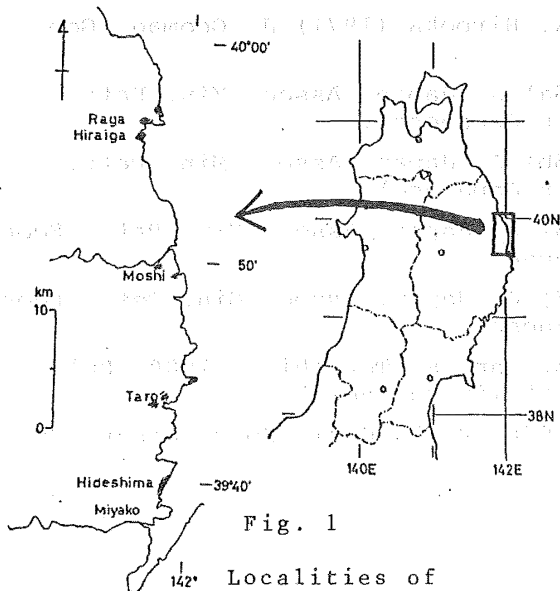


Fig. 1

Localities of
sampling site and
the distribution
of the Miyako

Group after Tanaka (1978)

Isotopic ages of the granitic rocks exposed in the Kitakami region have the range between 110 Ma and 125 Ma (e.g. Kawano and Ueda, 1965) with the only exception of the age upon Hikami granite (e.g. Shibata, 1975). This granitic activity was called Oshima Orogeny (Minato et al. 1981). A basal conglomerate of the Raga formation of the Miyako Group covers unconformably this early Cretaceous granitic rocks or the pre-Cretaceous Harachiyama formation. The Tanohata and Hiraiga formations overlie the conglomerate. They are mainly composed of alternation of sandstone and siltstone. The fossils from the alternation indicate

<u>Formation</u>	<u>rock type</u>	<u>site name</u>	late Aptian and/or early Albian (Matsumoto et al., 1982). The Raga formation contains numerous pebbles and cobbles, so they are suitable for conglom- erate test to estimate the thermal distur- bance after the deposition of the Miyako Group. The Miyako Group dips gently eastward to the Japan Trench. The distribution of the Miyako Group is shown in Fig. 1 and sampling sites are listed in Table 1.
Aketo	(sandstone)	---- HG04 ---- HG03	
Hiraiga	siltstone	---- HG02 ---- HG01	
Tanohata	siltstone	---- TN01	
Raga	conglomerate	---- RG01	
----- (unconformity) -----			
Harachiyama, intrusive rocks			

Table 1 : Stratigraphy of the Miyako

Group, rock type collected (except of sandstone), and horizon of each site performed with magnetic compass in four sites and sun compass in the other site. Six sites were selected for the paleomagnetic measurement. About eight samples were collected in each locality. The samples collected were drilled into 2.5 cm in diameter and cut 2.5 cm in length. Orientations were performed with magnetic compass in four sites and sun compass in the other sites.

3) Result and Discussion

The remanence was measured by a Spinner Magnetometer with six spin after stepwise alternating field demagnetization up to, mostly, 30 mT in a step of 2 mT. The direction of stable remanence was determined from the linear portion of progressive demagnetizing diagram (Zijderveld, 1967) as shown in Fig. 2. NRM mainly consists of one component with a small amount of secondary magnetization. Paleomagnetic directions obtained from stable remanence in each sampling site are shown in Fig. 3. The intensity of the remanence is the order of 10^{-3} to 10^{-4} A/m. Paleomagnetic results are largely scattered because of this weak NRM intensities.

No reversely magnetized rocks are found in this study. The question arises whether magnetic minerals were reheated after Oshima Orogeny. If some thermal episode were happened after deposition, the remanence of conglomerate pebbles would show the uniform paleo-direction. The directions of magnetization of the conglomerate pebbles in Raga formation are random shown in Fig. 4. As the Raga conglomerate formation is the basal layer of the Miyako Group, the result of the random direction suggests there was no thermal aligning force for magnetic minerals after the sedimentation. There was also no significant episode in this region after Oshima Orogeny geologically.

Thermomagnetic analysis of strong field magnetization

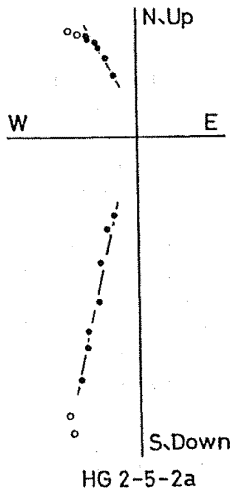


Fig. 2

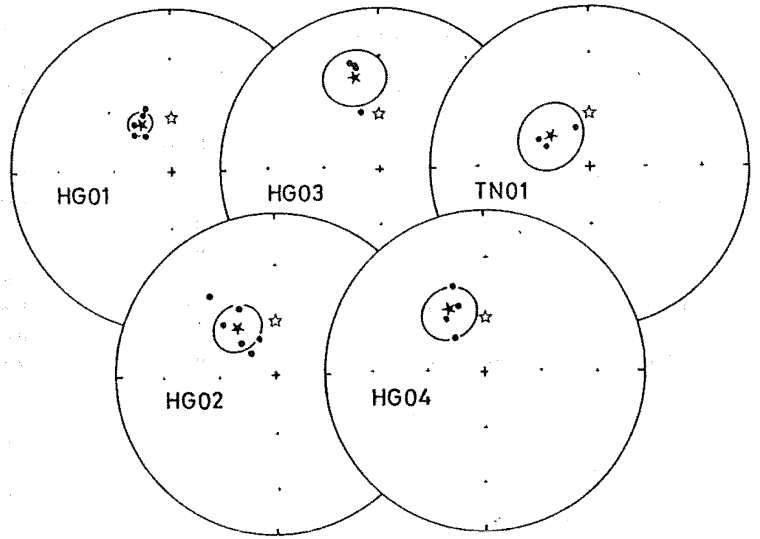


Fig. 3

Fig. 2 : An example of Zijderveld diagram. The direction is determined from the line portion of the solid line

Fig. 3 : Equal area projections showing the directions of remanence determined in Zijderveld diagram for each specimen. The closed and opened star symbols indicate mean direction and the axial geocentric dipole field at the locality, respectively. 95% confident ovals for individual mean direction are shown as solid lines.

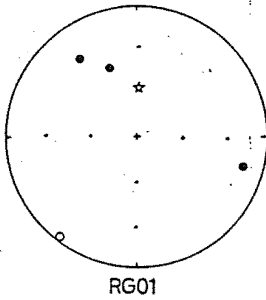


Fig. 4

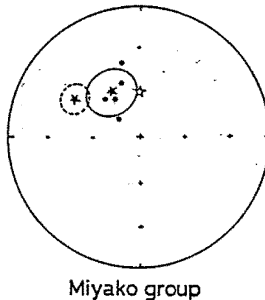


Fig. 5

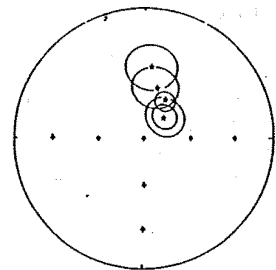


Fig. 6

Fig. 4 : The scattered direction of the conglomerate pebbles in the Raga formation, the lowest formation of the Miyako Group. Closed and open circles are represent lower and upper hemisphere, respectively. Open star symbol is as the same meaning as in Fig. 3.

Fig. 5 : Mean field directions among sites of the Miyako Group (star symbol within solid oval) and Granite studied by Ito et al. (1979) (star symbol within dashed oval). Two confident ovals overlap each other.

Fig. 6 : Site mean direction for each formation after bedding correction. Each direction is agreement with the axial dipole field.

versus temperature (J_s -T curve) was performed in a vacuum with an automatic recording valance. A chip of sample was pulvelized to separate magnetic minerals from other non-magnetic minerals. The J_s -T curve in both heating and cooling processes was similar in shape with high Curie temperature of about 580 C, indicating that magnetic minerals which carry the remanence are mainly magnetite. As the value of mean demagnetizing field is the range of 10 mT to 15 mT, the remanences are carried by depositional remanent magnetization.

The other question arises whether viscous remanent magnetization (VRM) of present field is dominant in stable magnetization. Mean direction in each site before bedding correction is different from that of the axial dipole field expected from the present location as shown in Fig. 5. The inclinations and declinations in situ are not in agreement with those from present geocentric magnetic field but with those of granite in Kitakami mountains studied by Ito et al. (1980). VRMs are not dominant in sedimentary rocks of Kitakami massif.

The age from late Aptian to early Albian was the bottom part of the long normal polarity of Earth's magnetic field (e.g. Lowrie et al., 1980). The fossils from in the Miyako Group show that it is within this age when these sedimentary rocks deposited. That is the reason why all the specimen magnetized normally.

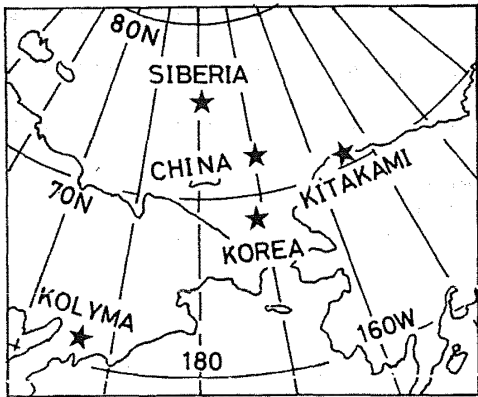


Fig. 7
Cretaceous paleomagnetic pole position for the Kitakami massif and for the other East Asia region. These poles are excellently close one another.

The magnetic directions of site mean after bedding correction are shown in Fig. 6. The directions obtained in this study are close to that of present. Paleomagnetic pole position are plotted in Fig. 7. Mean virtual geomagnetic pole position is calculated to be 71 N, 155 W. Otofujii et al. (1981) showed the pole position of the Korean Peninsula in Cretaceous and proposed no rotational movement of this region relative to the Asian continent. Pole position obtained in this study is in agreement with that from the Korean Peninsula and other East Asia. Though the paleomagnetic data for each site is not enough in number, it suggests that the Kitakami massif has

not migrated significantly after early Cretaceous. Sasajima(1981) compiled the Cretaceous pole positions for Northeast and Southwest Japan. The latitude and longitude of pole position for Southwest Japan are 45.9 N and 163.9 W, respectively. This paleomagnetic pole is far from that obtained in this study. It suggests that Southwest Japan was separated

from not only Asian platform but Northeast Japan in Cretaceous.

Table 2. Results of paleomagnetic measurement
(in situ)

Site name	Location		Inc.	Dec.	N	k	a95
	Lat.	Lon.					
HG01	39.92	141.95	61.1	-33.1	5	134.2	6.6
HG02	39.92	141.95	59.2	-38.6	6	30.4	12.3
HG03	39.93	141.95	40.6	-14.4	4	38.2	15.0
HG04	39.93	141.95	54.0	-19.2	4	43.9	14.0
TN01	39.92	141.95	72.4	-48.8	3	56.3	16.6
-----	-----	-----	-----	-----	-----	-----	-----
mean			58.1	-27.5	5	25.7	13.0

(after bedding correction)

Site name	Bedding		Inc.	Dec.	VGP	
	Strike	Dip			Lat.	Lon.
HG01	N 1 W	31 E	62.9	29.2	67.4 N	150.3 W
HG02	N S	35 E	72.6	46.8	54.9 N	175.4 W
HG03	N 5 E	22 E	44.3	5.8	76.0 N	163.0 W
HG04	N 5 E	22 E	57.2	13.7	79.4 N	128.3 W
TN01	N 7 E	32 E	72.4	46.9	55.4 N	177.1 W
-----	-----	-----	-----	-----	-----	-----
mean			62.9	22.9	70.8 N	154.6 W

N : Number of specimens
k : Precision parameter
a95: Semi-angle of 95% cone of confidence

Reference

- Ito, H. et al. (1979) *Rock Mag. Paleogeophys.*, 7, 113
- Kawai, N. et al. (1961) *Geophys. J. R. astr. Soc.*, 6, 124
- Kawano, Y. and Y. Ueda (1964) *J. Japan Assoc. Min. Petr. Econ. Geol.*, 51, 127
- Lowrie, W. et al. (1980) *J. Geophys. Res.*, 82, 3597
- Matsumoto, T. et al. (1982) *Fossils*, 31, 1
- Minato, M. et al. (1981) *In The Abean Orogeny*, (Tokai Univ. Press, Tokyo), p.395
- Otofujii, Y. et al. (1981) *Rock Mag. Paleogeophys.*, 8, 46
- Sasajima, S. (1981) *In Paleoreconstruction of the continent* (AGU, Washington, D.C.), p.115
- Shibata, K. and S. Uchiumi (1975) *Bull. Geol. Surv. Japan*, 26, 235
- Tanaka, K. (1978) *Chishitsu News*, 291, 32
- Zijlderveld, J. D. A. (1967) *In Method of Paleomagnetism*, (Elsevier Publishing Co., Amsterdam), p.254

A COUPLE OF PALEOMAGNETIC DATA OF THE CRETACEOUS ROCKS
FROM YAMAGUCHI AND SHIMANE PREFECTURES, WEST JAPAN

Haruo DOMEN

Institute of Physical Sciences, Faculty of
Education, Yamaguchi University, 753 Japan

Several samples of inkstone were collected during the summer of 1976 at the west coast of Yamaguchi Prefecture; Kojuku district, northern Shimonoseki City, and also another stock of granodiorites from the western Shimane Prefecture; Hikimi district was made in 1970.

Fig. 1 is a map roughly showing the location of those sampling sites together with some other sites for Yamaguchi Cretaceous rocks reported in the previous paper (Domen 1982). Since the samples were taken, those rock samples were stored in the laboratory in random orientation without any handling. Recently their NRM directions of both samples were determined by means of a spinner magnetometer.

The geologic age of both rocks is Cretaceous; Kojuku inkstone is belonged to the Kwanmon groups:- lower Cretaceous and Hikimi granodiorite stands for the Hikimi groups, which age seems to be slightly younger than that of former.

NRM directions of both samples are widely scattered but the fashions of the scattering of those NRM directions are rather similar each other as have been seen in Tables 1-1 and 1-2 (also see Table 2, in which these data are summarized).

Since 1953, not a few of paleomagnetic data have been published by the present author (for example, see Domen 1979). Among those, the data on inkstones, which are belonged to the Kwanmon groups, are sited, and some other Cretaceous rocks had been collected recently at the Hikimi district (Domen & Muneoka 1981) located near by the site of the present study. Moreover, another paleomagnetic result has recently been shown on the inkstone come from the place closed to the Kojuku district (Domen 1982, also see Fig. 1 of this paper as the site; K-3). The data on both inkstone and granodiorite presented here are newly appeared entirely.

The NRM directions and their dispersion are different a little in comparison with those of the Shimonoseki Cretaceous rocks mentioned above (K-3), however, the NRM of Kojuku district samples is rather similar to that of one of the middle Cretaceous rocks; andesitic welded tuff from Ogori district, near by Yamaguchi City (S-4 in Fig. 1 and Table 2. Also Domen 1982). On the other hand, the NRM directions of Hikimi granodiorite seem to be resemble to that of another andesitic welded tuff from Miné district, central Yamaguchi Prefecture (middle Creta., S-3 in figure etc. as well).

For the sake of the comparison made easy, the NRM data of S-3, -4 and K-3 are shown in Table 2 mentioned above, after the previous paper together with the present data (see Table 1-1 and -2).

Further paleomagnetic study on these rocks is being made.

Table 1-1. Paleomagnetic data of Cretaceous rock.
Kojuku inkstone, Yamaguchi Prefecture.

SITE, LONG 130.2° LAT 34.1° GEOMAG. DECLI -6.2°			
NO.	D(E)	D(E)*	I(D)
761103	-42.9°	-43.2°	59.3°
761105	31.2°	35.9°	19.1°
76110501	36.2°	30.8°	44.8°
76110502	35.3°	79.1°	38.8°
76110503	70.8°	72.4°	24.4°
761108	-160.4°	-166.6°	33.4°
761109	110.5°	104.3°	31.2°
10	177.4°	171.2°	61.2°
11	-31.7°	-37.9°	14.9°
12	59.7°	53.5°	63.2°
13	53.7°	47.5°	67.7°
14	38.6°	32.4°	38.9°
1401	48.2°	42.9°	58.6°
15	36.5°	30.3°	70.2°
17	53.2°	47.6°	49.2°
1701	61.3°	55.1°	61.6°
25	-64.5°	-70.7°	84.9°
27	138.0°	131.8°	32.4°
29	73.6°	69.4°	47.3°
35	73.1°	72.3°	62.3°
36	72.3°	66.1°	65.1°
3601	56.8°	50.6°	70.1°
37	102.4°	96.2°	47.7°
3701	105.8°	92.8°	44.9°
3702	89.4°	83.2°	55.0°
38	71.5°	65.3°	42.3°
761140	-6.7°	-12.9°	60.7°
TOTAL	MEAN		
27		68.2°	62.4°
		DEL D	DEL I
		23.8°	11.9°
K	6.5°	ALFA 95%	11.9°
M G A,	LONG -171.2°	LAT 37.6°	
	DEL P 14.4°	DEL M 18.5°	
	POLARITY CLASS IV,	DCN)	
		*R	EE.3622

Table 1-2. Paleomagnetic data of Cretaceous rock.
Hikimi granodiorite, Shimane Prefecture.

NO.	DCE	DCE*	I(D)
11	-81.8°	-87.9°	67.1°
111	-107.8°	-114.1°	49.9°
112	-72.9°	-79.2°	62.1°
611	80.1°	73.8°	61.4°
612	65.2°	58.9°	40.8°
613	84.5°	78.2°	50.8°
711	86.5°	80.2°	69.5°
712	-41.4°	-47.7°	14.3°
713	82.4°	76.1°	64.3°
714	23.9°	17.6°	65.9°
TOTAL	MEAN		
10		15.2°	77.4°
		DEL D	DEL I
		115.2°	25.1°
	K 4.7	ALFA 95%	25.1°
M G P,	LONG 143.5°	LAT 57.3°	
	DEL P 44.0°	DEL M 47.0°	
	POLARITY CLASS +III, (N)		
		*R	8.0681

Table 2. A comparison of NRM data of some Cretaceous rocks in Yamaguchi and in Yamaguchi and Shimane Prefectures.

Site	n	N		R		M		V		G		P		Polarity# Class
		D(E)*	I(D)	K	$\alpha_{95\%}$	Long.(E)	Lat.(N)							
(Present study)														
Kojuku (1976) Yamaguchi	27	68.2°	62.4°	7	12°	-171°		38°						IV, O(N)
Hikimi (1970) Shimane	10	15.2	77.4	5	25	144		57						+III, (N)
<hr/>														
(Previous Yamaguchi data: Domen 1982)														
S-3; Miné	21	-5.5	63.2	9	12	111		79						+III, N
S-4; Ogori	13	82.3	42.8	12	12	-156		20						IV, O(N)
K-3; Shimonoseki	13	23.8	48.5	3	27	-133		69						-III, N

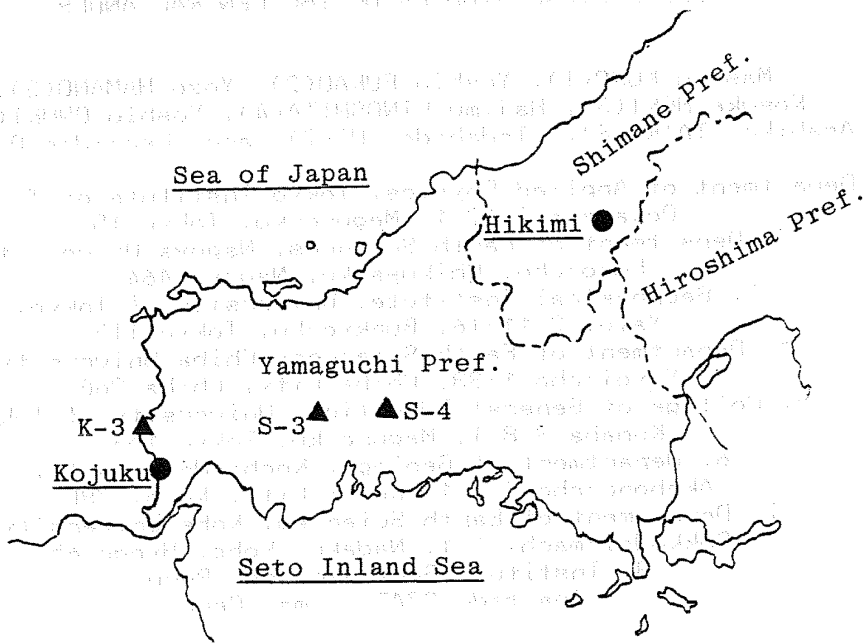


Fig. 1. Map showing sampling sites of Cretaceous rocks of Kojuku & Hikimi districts together with some other Cretaceous Yamaguchi rocks.

References

- Domen, H. (1979) Bull. Fac. Educ., Yamaguchi Univ., 29, 11.
- Domen, H. (1982) Bull. Fac. Educ., Yamaguchi Univ., 32, 23.
- Domen, H. & H. Muneoka (1981) Rock Mag Paleogeophys., 8, 38.

GEOPHYSICAL STUDIES OF THE CENTRAL ANDES

Masaru KONDO(1), Yoshio FUKAO(2), Yozo HAMANO(3),
Kosuke HEKI(3), Hajimu KINOSHITA(4), Yoshio ONUKI(5),
Asahiko TAIRA(6), Tadahide UI(7) and Leonidas Ocola(8)

1. Department of Applied Physics, Tokyo Institute of Technology,
Ookayama 2-12-1, Meguro-ku, Tokyo 152
2. Department of Earth Sciences, Nagoya University,
Furo-cho, Chikusa-ku, Nagoya 464
3. Geophysical Institute, University of Tokyo,
Yayoi 2-11-16, Bunkyo-ku, Tokyo 113
4. Department of Earth Sciences, Chiba University,
Yayoi-cho 1-33, Chiba City, Chiba 260
5. College of General Education, University of Tokyo,
Komaba 3-8-1, Meguro-ku, Tokyo 153
6. Department of Geology, Kochi University,
Akebono-cho 2-5-1, Kochi City, Kochi 780
7. Department of Earth Sciences, Kobe University,
Rokkodai-machi 1-1, Nada-ku, Kobe, Hyogo 657
8. Instituto Geofisico del Peru,
Apartado 3747, Lima, Peru

1. Introduction

The Andes is a huge mountain chain running along the western border of the South American continent and having a length of more than 10,000 km. Except the Central Asia, where the Himalayas and other mountains form the "roof of the world", the Andes is the only mountain chain which attains a height of nearly 7,000 m in a considerable area. The Andes is a place of plate subduction, just as the Japan and other island arcs in the North-western Pacific are, but differs from the latter in the fact that they form a margin to a stable continent.

The Central Andes constitutes the middle part of the Andes chain, ranging from Peru to northern Chile, and is characterized by many features typical of the subduction zones such as trenches deeper than 5 km, deep-focus earthquakes occurring at depths greater than 300 km, and existence of a numerous active and Quaternary volcanoes.

In the years 1980 and 1981, we carried out a series of field works in the Central Andes region, with a grant-in-aid for overseas scientific researches from Mombusho (the Ministry of Education, Science and Culture, Grant Nos. 504204 and 56041015). The ultimate aim of this research was to clarify and understand the processes involved in the formation of the great mountain belts such as the Andes, and in particular, to make comparisons with other collision type boundaries (such as the Himalayas) and with island-arc type consuming boundaries (such as Japan). To make an effective approach to this ultimate aim, and to perform other useful studies, we decided to make the following specific

researches on the rock samples and other data collected by the field works:

- (1) Determination of the paleomagnetic polar wander curve for the area of the Central Andes, especially for Peru.
- (2) Comparison of the polar wander curves from the Central Andes and from the stable, cratonic area of the South America.
- (3) Study of paleointensities and paleosecular variation of the geomagnetic field.
- (4) Crustal structure of the Andes based on terrain corrected Bouguer gravity anomalies.
- (5) Seismotectonic study using seismicity, mechanism solutions, and wave propagation data.
- (6) Correlation between the distances of active volcanoes from the trench axis and major element chemistry of the volcanic rocks.
- (7) Change with time in the sedimentation environment and its bearing to the tectonics.

The items (4) and (5) are carried out with the participation of Instituto Geofisico del Peru (IGP), which is contributing to the project with unpublished gravity and seismic data.

2. Field Works

A reconnaissance survey of Peru was carried out in the autumn of 1980 by Kono, Onuki and Ui, with the help of Crisolfo Perales and Isaias Vallejos of Instituto Geofisico del Peru (IGP). The route taken was Lima-Trujillo-Cajamarca-Chachapoyas-Moyobamba-Tarapoto-Juanjui in the northern Peru, and Lima-Pisco-Arequipa-Tacna-Arica-Tacna-Puno-Cuzco-Ayacucho-Huancayo-Lima in the southern Peru and Northern Chile.

In the northern route, gravity survey by LaCoste-Romberg gravimeter G-375 (curtesy of Prof. Yokoyama, Hokkaido University) was carried out at about 200 bench marks between El Cruce (near Pacasmayo) and Juanjui. Gravity connection was also done at 14 national and international standard stations including Tokyo, Los Angeles, Lima, Arequipa and Arica.

Preliminary sampling of volcanic and metamorphic rocks were also carried out in the reconnaissance trip. The route taken is shown in Figure 1. Some Pre-Inca potsherds from Cajamarca region was also collected in 1980.

The field works of 1981 were mostly dedicated to the collection of rock samples from various geologic strata in Peru and northernmost Chile. The sampling was carried out by a series of field trips starting from Lima:

(i) Northern Chile, near Cajamarca and Bagua. Kinoshita, Taira and Heki sampled extensive outcrops of limestones, shales, silts, and sandstones. Jose Machare and Julio Melgar from IGP also went to this trip to help them.

(ii) Central Peru, Lima-Huancayo and near Ayacucho. Kono, Ui and Hamano sampled "Quaternary" andesite dykes near Ocros, southwest of Ayacucho. Felix Monge and Franklin Moreno of IGP helped in this trip. They also collected various metamorphic and sedimentary formations ranging from Eocene to Precambrian in age.

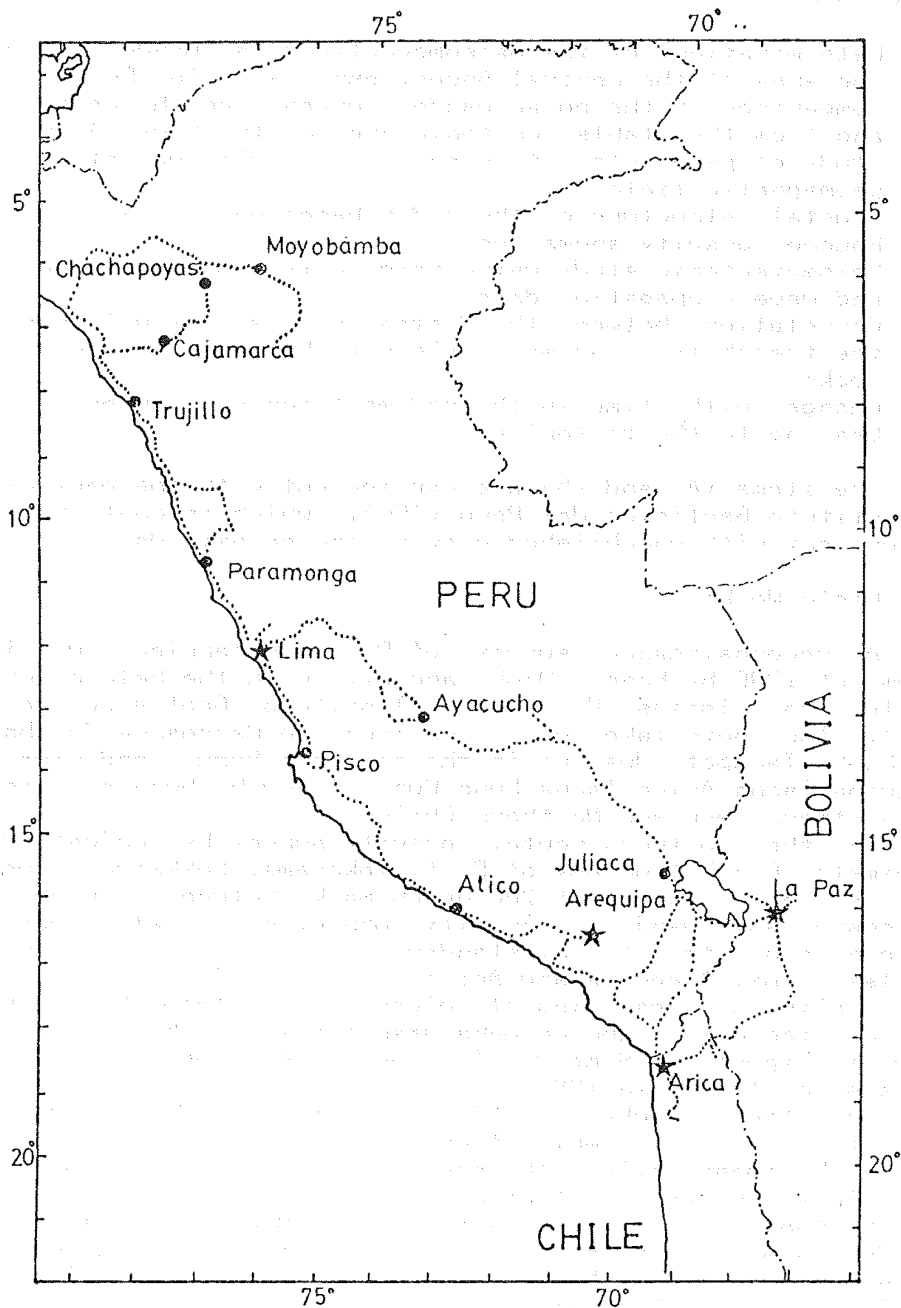


Fig. 1. The routes taken in the field works of "Geophysical Studies of the Central Andes" in 1980 and 1981. Stars and closed circles indicate IGSN71 international reference gravity stations and IGP national reference points. The total distance traveled is 30,000 km and 1.5 tons of rock samples are collected.

(iii) Northernmost Chile, near Arica. Ui, Taira, Fukao, Hamano and Heki collected Tertiary and Jurassic volcanic rocks (welded tuffs and dykes) and sediments (dolomites, sandstones and shales) in cooperation with Hugo Moreno of Departamento de Geologia, Universidad de Chile (Santiago) and Konosuke Sawamura of JICA and Departamento de Geociencia, Universidad de Norte (Antofagasta). Kono and Kinoshita sampled Jurassic dyke swarm at Cuya, south of Arica.

(iv) Central and southern Peru. Volcanic, sedimentary and metamorphic rocks of various ages near Huarmay, Nazca, Arequipa and Moquegua were collected in various occasions.

3. Previous Works in Paleomagnetism

We shall give here a very brief review of the previous paleomagnetic works in South America. Data reported in 1972 or earlier are summarized in McElhinny (1973).

Before 1970, paleomagnetic studies were mainly done to obtain the polar wander curve for South America. The samples were therefore collected from the stable, cratonic area; that is, mostly from southeastern part of the continent. Creer performed extensive studies in this period and his results are summarized

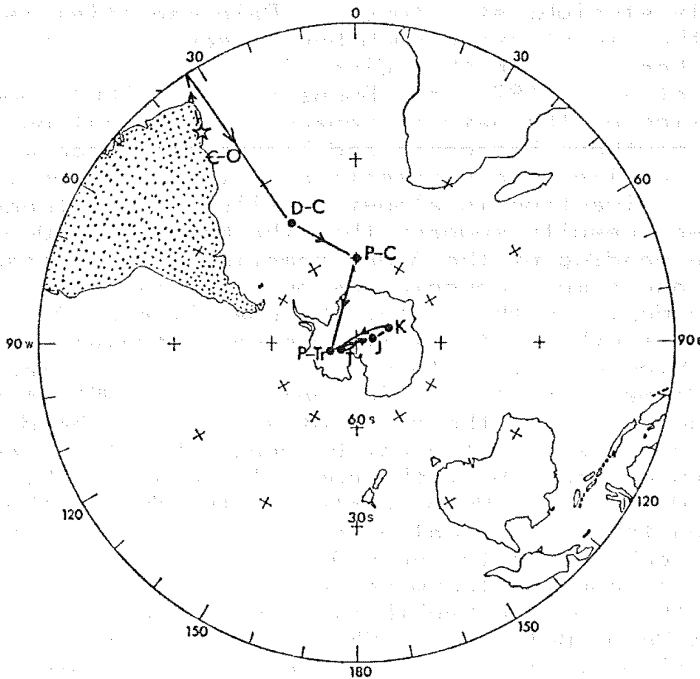


Fig. 2. Phanerozoic Apparent polar-wander path for South America. Star indicates a pole lying in the northern hemisphere. Polar stereographic projection. Reproduced from McElhinny (1973).

in Creer (1970). Figure 2 shows the polar wander path for South America, reproduced from McElhinny (1973). A very prominent feature of this curve is that the paleomagnetic pole was located near the equator in the first half of Paleozoic, but that there was a large shift of the pole before Permian, and after Permian period, the pole was quite near the present geographic pole.

With the advent of new paleomagnetic laboratories in South America, a much wider age range and more specific problems were studied especially by the workers of Argentine. For example, Valencio et al. (1980) obtained a polar wander path for the period of 400 to 1000 Ma, and Valencio et al. (1977) applied the paleomagnetic data to the problem of the opening of the South Atlantic. The idea was to see if the position of South America determined from the reconstruction based on sea-floor spreading data is compatible with the paleomagnetic directions near the time of the breakup of Gondwanaland. These studies are very promising in the future, but at present, data are only available from somewhat restricted region of Argentine, and are therefore to be substantiated by further studies.

Recent investigations are more and more directed to clarify the process in tectonically active regions. There are several places in the Andes where the general trend of the mountain chain changes rather abruptly (called oroclines). Carey (1958) was the first to suggest that these features were formed by the bending of originally straight structures. Paleomagnetism is the most effective method in studying such hypotheses, and some researches have already been done in this direction.

Dalziel et al. (1973) and Burns et al. (1980) reported that the declination of the natural remanent magnetization (NRM) in the rocks of southern Patagonia and Tierra del Fuego with ages of Cretaceous or earlier are systematically turned to west, so that the magnetic direction is almost parallel to the trend of the Andes. These results suggest that the Magallanes Orocline was formed by the bending of the Andes sometime after Cretaceous.

Another and a more conspicuous orocline is situated near the Peru-Chile border. In the north, the coastline of Peru is almost NW-SE, while south of Arica it runs very straight in the N-S direction (Figure 1). This is generally called Bolivian Orocline. Palmer et al. (1980) measured the NRM of the rocks both to the north and to the south of Arica. If the direction of NRM is systematically different between the two regions, an inference can be made about the possible rotation which produced the Bolivian Orocline. Unfortunately, the NRM of the northern rocks was unstable, and Palmer et al. (1980) report only the results from rocks collected near Arica. Their result suggest a 30 to 40 degrees counterclockwise rotation of Arica region. To substantiate the orocline hypothesis, much more studies covering wide areas in Peru, Bolivia and Chile are necessary.

A special mention should be made about paleointensity and paleosecular variation studies. Paleomagnetic data are heavily biased to the northern hemisphere. The latitude dependence of the paleosecular variation appears to have been well established (e.g., Cox, 1970). Yet, on closer examination, it is apparent that these models and conclusions are based primarily on the data obtained in the northern hemisphere. Given the large asymmetry

in the distribution of the present day non-dipole field in both hemispheres, there is no a priori reason to suppose that the model based on the northern hemisphere data are applicable to the entire earth. Studies of paleosecular variation in the southern continents should be encouraged.

Paleointensity data from South America are entirely from the potsherds and other remains of Inca and Pre-Inca civilizations in Peru. Earlier results were given by Nagata et al. (1965) and Kitazawa and Kobayashi (1968). Some new data were reported by Games (1977), Gunn and Murray (1980) and Kono and Ueno (in preparation). The availability of well dated bricks and potteries from old civilizations of Peru makes this area very attractive place to work on the archeomagnetic intensity changes. Future efforts should include volcanic rocks, so that intensity variation in a much longer time span can be studied.

References

- Burns, K.L., M.J. Rickard, L. Belbia and F. Chamalaun (1980) *Tectonophysics*, 63, 75.
- Cox, A. (1970) *Geophys. J. Roy. Astron. Soc.*, 20, 253
- Carey, S.W. (1958) *Proc. Roy. Soc. Tasmania*, 89, 255.
- Creer, K.M. (1970) *Phil. Trans. Roy. Soc. Lond.*, A267, 457.
- Dalziel, I.W.D., R. Krigfield, W. Lowrie and N.D. Opdyke (1973) in "Implications of Continental Drift to the Earth Sciences" vol. 1, p. 87.
- Games, K.P. (1977) *Geophys. J. Roy. Astron. Soc.*, 48, 315.
- Gunn, N.M. and A.S. Murray (1980) *Geophys. J. Roy. Astron. Soc.*, 62, 345.
- Kitazawa, K. and K. Kobayashi (1968) *J. Geomag. Geoelectr.*, 20, 7.
- McElhinny, M.W. (1973) *Palaeomagnetism and Plate Tectonics*, 358p. Cambridge University Press, London.
- Nagata, T., K. Kobayashi and E.J. Schwarz (1965) *J. Geomag. Geoelectr.*, 17, 399.
- Palmer, H.C., A. Hayatsu and W.D. MacDonald (1980) *Geophys. J. Roy. Astron. Soc.*, 62, 155.
- Valencio, D.A., E. Mendia, A. Giudici and J.O. Gascon (1977) *Geophys. J. Roy. Astron. Soc.*, 51, 47.
- Valencio, D.A., A.M. Sinito and J.F. Vilas (1980) *Geophys. J. Roy. Astron. Soc.*, 62, 563.

PALEOMAGNETIC STUDY IN ANDEAN PERU : CRETACEOUS
SEDIMENTS AND VOLCANICS

Kosuke HEKI⁽¹⁾, Yozo HAMANO⁽¹⁾ and Masaru KONO⁽²⁾

(1) Geophysical Institute, University of Tokyo, Hongo 7-3-1,
Bunkyo-ku, Tokyo 113.

(2) Department of Applied Physics, Tokyo Institute of
Technology, Ookayama 2-12-1, Meguro-ku, Tokyo 152.

1. Introduction

Rock samples were taken for paleomagnetic study in 1980 and 1981 as a part of the work titled "Geophysical study of the Central Andes". On these samples, paleomagnetic measurements have been in progress, from which several results are reported here.

Paleomagnetic poles of South American Plate are available for the entire Phanerozoic age, but they are usually based of the rock formations of the cratonic area such as Precambrian shields or intracratonic basins (e.g. Creer, 1970). On the other hand, there have been reported several paleomagnetic works on the rock formations of Andean orogenic belts, some of which suggest some "anomalous" paleomagnetic poles inconsistent with the "standard" polar wander path. Andean orogenic belt has several "deflections" where the trend of the structure abruptly changes within its whole length of more than 7,000km (Fig.1), and anomalous paleomagnetic results were often attributed to the "oroclinal bending" occurred around these deflections. For example, Palmer et al.(1980a) reported 30°-40° counterclockwise rotation of Jurassic Camaraca Formation, Arica at the Peru-Chile border. MacDonald and Opdyke (1972) and Burns et al.(1980) reported the anomalous declination in the Northernmost and Southernmost parts of the Andes respectively. Palmer et al's

(1980) attempt was to compare the paleomagnetic declination between the northern and southern regions of the Santa Cruz deflection, at the Peru-Chile border and to test the orocline hypothesis with paleomagnetic techniques. They, however, failed to derive any reliable paleomagnetic results from Peru due to the "unstability" of the remanent magnetization of the rock samples. Our original objective was the same as that of Palmer et al.(1980a) and we succeeded in getting several reliable paleomagnetic records of Cretaceous age from sediments of Northern Peru and volcanic rocks of coastal Central Peru.

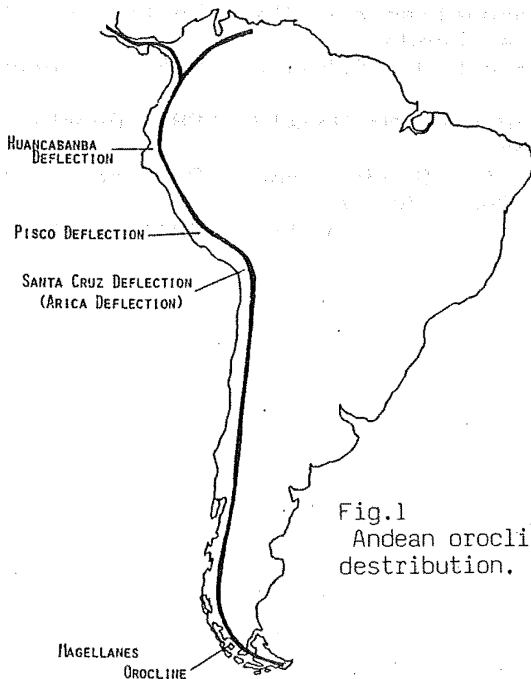


Fig.1
Andean orocline
distribution.

2. Geology

Peruvian continental

margin is characterized by Mesozoic geosynclinal pair which roughly comprises of what we call eugeosyncline and miogeosyncline, the former consists of both volcanics and sediments and the latter consists mainly of sediments. Subsidence in the eugeosyncline was most rapid during the Albian, Middle Cretaceous, and the total thickness amounts to about 7,000m. In the miogeosyncline, the age of the greatest subsidence is the Tithonian, Late Jurassic, but its subsidence continued throughout the Cretaceous to accumulate a total thickness of about 6,000m (Cobbing, 1976).

From the miogeosyncline, sedimentary samples were collected for paleomagnetism (CM, BG series) from Middle Cretaceous rock formations near Cajamarca, Northern Peru, with the time span covering from the Albian to the

Turonian. Rocks are mainly composed of shallow-sea limestone and marl and contain many fossils. Their stratigraphy and geology are reported in Reyes (1980), Bellido (1979) and some others. Rock types and sampling site localities are given in Table 1 and Fig.2.

From the eugeosynclinal area, volcanic rocks such as lava flows or dike rocks were collected (HM, AC, NZ series) along the coast between Huarmey and Nazca, Central Peru. Volcanic rocks in this region are reported to range in their composition from high-alumina basalt to andesite (Webb, 1976), which demonstrates these volcanisms are of island-arc type. Direction of maximum horizontal stress axis suggested by the dike orientation is almost north-south, which is nearly perpendicular to the present compression axis. Some lava flows show pillow structure indicating their submarine genetic environment. Geology of this region are reported by Myers (1974), Bellido (1979) and others. Rock types and sampling site localities are also given in Table 1 and Fig.2.

3. Experimental Procedure and Paleomagnetic Results

Sedimentary rocks

Each sample was taken from an outcrop as an oriented block and was cut into a core specimen in the laboratory. A cliogenic magnetometer of University of California, Santa Barbara was used in the measurement

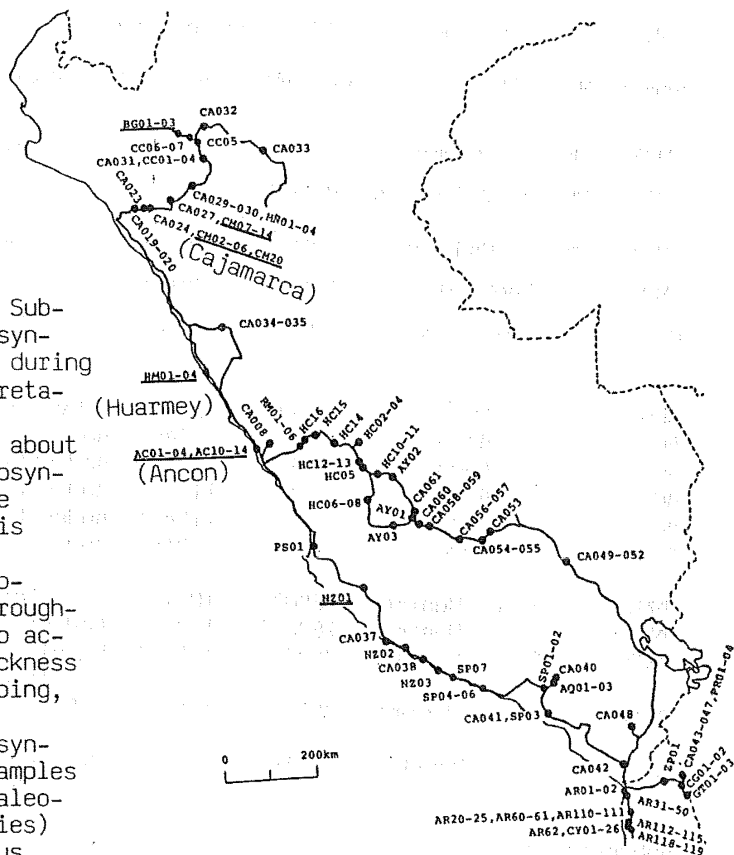


Fig.2 Localities of the sampling sites. Site numbers reported in this article are underlined.

Table 1. Sampling localities and rock types.

Sample No.	Place	Long.(°W)	Lat.(°S)	Rock name	Formation(Age)
CM08	W. of Cajamarca	78°26'	7°09'	Limestone	Chulec Fm.(Al.)
CM10	NW. of Cajamarca	78°20'	7°05'	Limestone	Pariatambo Fm. (Al.)
CM13	NW. of Cajamarca	78°16'	7°03'	Limestone	Chulec Fm.(Al.)
CM20	Tembladera	79°07'	7°15'	Andesitic dike	Cretaceous?
BG01	Bagua Grande	78°09'	5°54'	Limestone	Cajamarca Fm. (Tur.)
AC02	Ancon	77°11'	11°46'	Pyx. Andesite	Cretaceous
AC10	Ancon	77°11'	11°46'	Andesitic dike	Cretaceous
AC11	Ancon	77°11'	11°46'	Andesitic dike	Cretaceous
AC12	Ancon	77°11'	11°46'	Andesitic dike	Cretaceous
AC13	Ancon	77°11'	11°46'	Andesitic dike	Cretaceous
AC14	Ancon	77°11'	11°46'	Andesitic dike	Cretaceous
HMO1	S. of Huarney	78°03'	10°19'	Andesite	Cretaceous
HMO2	S. of Huarney	78°03'	10°19'	Andesitic dike	Cretaceous
HMO3	S. of Huarney	78°01'	10°21'	Basalt pillow lava	Cretaceous
HMO4	S. of Huarney	78°01'	10°21'	Basaltic dike	Cretaceous
NZ01	Rio Grande	75°14'	14°31'	Pyx. Andesite dike	Cretaceous

Abbreviations

W.:west, NW.:northwest, S.:south, Pyx.:pyroxene, Al.:Albian, Tur.:Turo-
nian.

of these sedimentary rocks. Some number of the samples had natural remanent magnetization (NRM) of the order of 10^{-7} Am²/kg, but typical NRM intensity was of the order of 10^{-8} Am²/kg, which is the weakest possible intensity to measure even with a cliogenic magnetometer. Step-wise alternating field (AF) demagnetization was performed up to 80mT in peak intensity on each specimen.

Rock magnetic study of marine limestone have been very difficult owing to the low concentration of magnetic minerals, but current knowledge was recently summerized in Lowrie and Heller (1982). According to them, both magnetite and hematite are thought to be the most popular carrier of the NRM of marine limestone, in which magnetite is generally of depositional origin while hematite is thought to grow during diagenesis (see also Channel et al., 1982). Dominance of these two magnetic component is determined by their relative percentage of contribution to the total NRM. Limestone whose NRM is carried mainly by hematite can be, in general, characterized with its pinkish color and shows higher coercivity and blocking temperature than the limestone with magnetite-carried NRM. Peruvian limestone studied here ranges in its color from gray to pinkish gray and purely gray limestone specimens were found to be demagnetized considerably during stepwise AF demagnetization as far as 80mT while ones with pinkish color hardly change their direction nor intensity throughout the AF demagnetization. It suggests bimodal remanence carried by magnetite and hematite. In this study, we preferred magnetization component carried by magnetite because hematite of

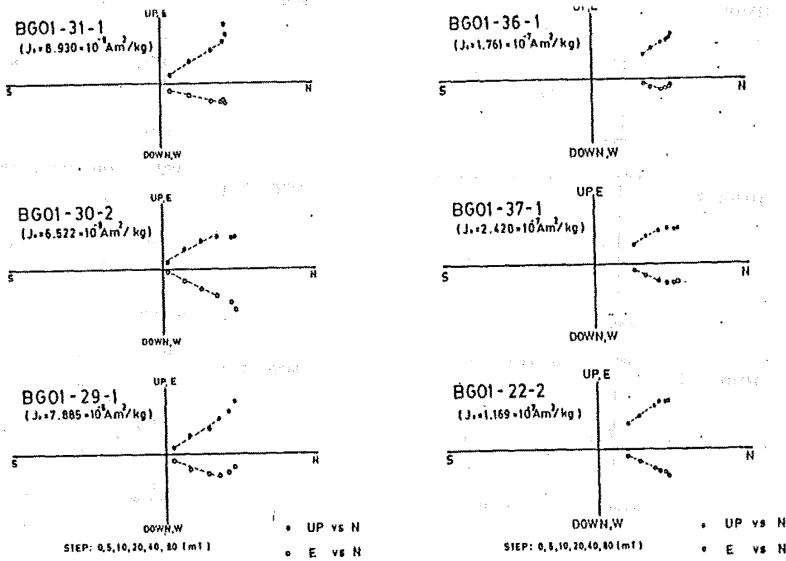


Fig.3 Zijderveld diagram plot (Zijderveld, 1967) of the AF demagnetization of Peruvian limestones. Characteristic remanence direction was determined from the gradient of the linear portion (dashed line) of the diagram.

the degree of the dominance of the magnetite in the total NRM. Paleomagnetic direction was determined by the gradient of the linear portion of the diagram as far as 80mT irrespective of the proportion of the destroyed remanence (Fig.3). Obtained field directions are structurally corrected and plotted on equal area projections in Fig.4. Only CM20 is of reversed polarity and the others are normal and no field directions showed the coincidence with the present axial dipole field direction but deviates by 20°-50° in their declination counterclockwisely. Statistical parameters and mean field directions by Fisher's (1953) method are given in Table 2.

Volcanic rocks

NRM of the volcanic rock was measured using a Schonstedt spinner magnetometer of University of Tokyo. Stepwise AF demagnetization was also performed and most samples showed relatively hard remanent magnetization with their median destructive field (MDF) of more than 30mT. Their Zijderveld diagrams indicate univectorial

of diagenetic growth might delay in its acquisition of the remanence. As a practical method, Zijderveld diagram (Zijderveld, 1967) was used because it is convenient to isolate the direction of the remanence from multi-component magnetized specimen by the application of linear regression to the linear portion of the diagram (Dunlop, 1979). The "demagnetizability" of the remanence as far as 80mT was not uniform even within a single outcrop reflecting

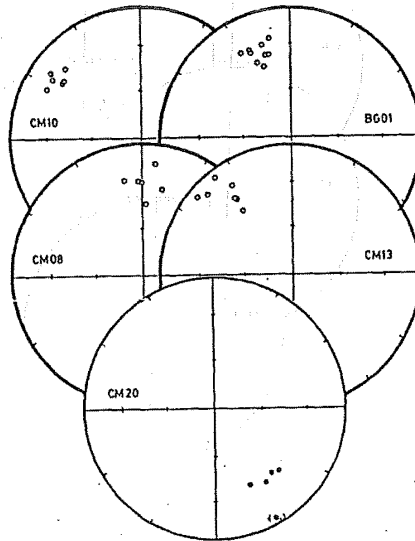


Fig.4 Equal area projection of characteristic remanence direction of sedimentary rocks. Open circle: upward, solid circle: downward.

nature of the remanence (Fig.5) and paleomagnetic field direction was also obtained from the gradient of the diagram. Equal area projection of the field directions are given in Fig. 6. Paleomagnetic results are tabulated in Table 2. Paleohorizons were not observable at the outcrops in many cases, although for HMO3 bedding plane was found to be nearly parallel to the present horizontal plane from

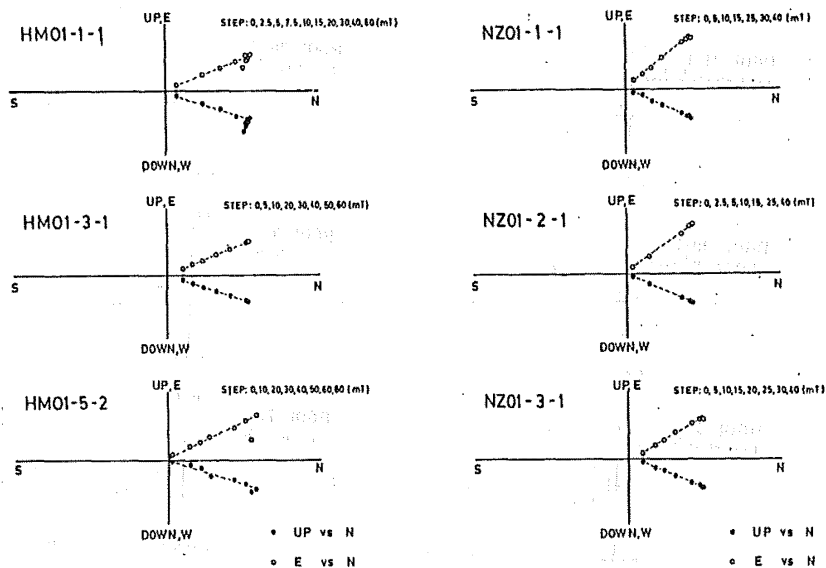


Fig.5 Zijderveld diagram plot of the AF demagnetization of Peruvian coastal volcanic rocks.

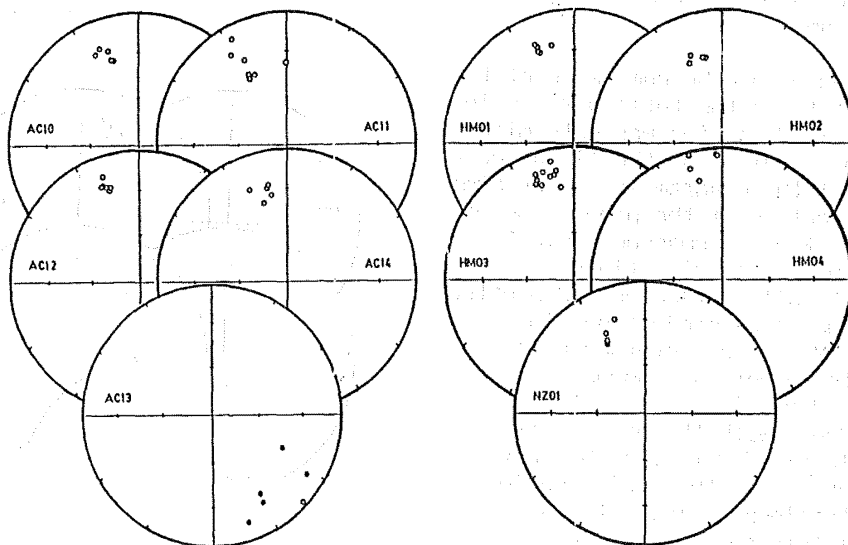


Fig.6 Equal area projection of remanent magnetization of Peruvian coastal volcanic rocks. Open circle: upward, solid circle: downward.

the shape of the pillow structures. In this report, no structural corrections are made on the paleomagnetic field directions of volcanic rocks.

Paleomagnetic field directions were almost of normal polarity with only one exception of AC13 which is of reversed polarity and showed 20°-30° counter clockwise deviation of the declination from axial dipole field direction, which is concordant with the results from sedimentary rocks but

Table 2. Paleomagnetic results of the sedimentary rocks and volcanic rock of the Andean Peru.

Site No.	N	Incl.	Decl.	R	k	Alpha 95	Bedding collection
CM08	7	-31.8	4.7	6.7824	27.6	11.7	o
CM10	6	-24.7	-54.7	5.9676	154.4	5.4	o
CM13	7	-22.6	-38.3	6.8328	35.9	10.2	o
CM20	4	34.6	145.0	3.9776	134.1	8.0	o*
BG01 (30-42)	9	-32.3	-20.6	8.9220	102.6	5.1	o
AC02	6	-38.8	-26.8	5.8504	33.4	11.8	x
AC10	5	-28.4	-20.4	4.9729	147.3	6.3	x
AC11	7	-33.1	-23.8	6.8011	30.2	11.2	x
AC12	6	-24.4	-19.2	5.9867	375.7	3.5	x
AC13	6	21.9	140.0	5.6136	12.9	19.3	x
AC14	5	-31.1	-14.4	4.9715	140.3	6.5	x
HMO1	5	-26.2	-20.0	4.9892	370.6	4.0	x
HMO2	4	-34.2	-16.7	3.9886	262.2	5.7	x
HMO3	10	-20.5	-14.7	9.9014	114.5	4.5	x
HMO4	5	-8.9	-9.8	4.8854	34.9	13.1	x
NZ01	5	-33.0	-26.4	4.9600	100.1	7.7	o*

N: number of samples, Incl.: inclination (degree), Decl.: declination (degree)
 R: length of the resultant vector, k: precision parameter, Alpha 95: diameter
 of 95% confidence circle, *Bedding plane of the country rock was used.
 (in degrees)

the amount of the deviation seems a little smaller than that derived from
 the sedimentary rocks.

4. Discussion

Phanerozoic polar wander path of South American Plate was established
 by Creer (1970), which demonstrates that paleomagnetic pole during Mesozoic
 time should approximately coincide with the present geographic pole, in
 other words, Mesozoic paleomagnetic field direction should not present
 serious deviation from today's axial dipole field direction. Paleomagne-
 tic results of Cretaceous sediments and volcanics in Peruvian Andes yield,
 however, several tens of degrees of counterclockwise declination shift
 (paleomagnetic declination is almost parallel to the Peruvian coastline,
 see Fig. 7), which significantly differ from axial dipole field.

Cretaceous paleomagnetic data of South America is plainly reviewed
 in Palmer et al. (1980b), where Cretaceous poles were divided into two
 groups, that is, poles from stable platform and those from Andean orogenic
 belts. Note that Palmer et al.'s (1980b) paleomagnetic pole from Chilean
 Andes at the latitude of about 30°S is almost consistent with that of
 stable area and does not indicate any rotational movement of that region,
 which is also true for the pole of Colombian Andes (Creer, 1970). If

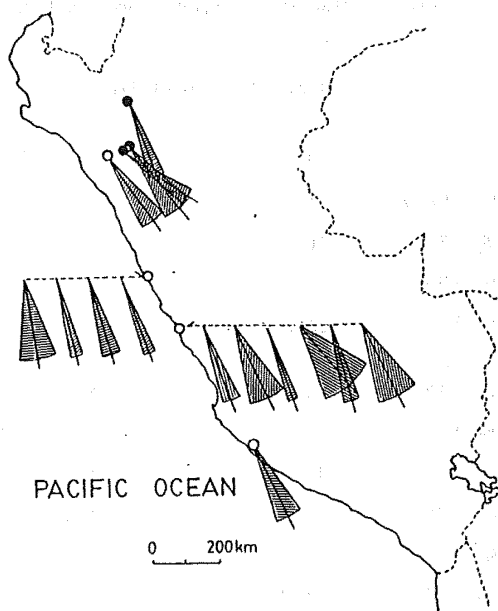


Fig.7 Paleomagnetic declination with their 95% confidence intervals of Cretaceous rock formations of Andean Peru. All the declinations are converted to "reversed" directions for the sake of visual simplicity. Open circle indicates volcanic rock, solid circle indicates sedimentary rock.

in the pre-folding stage of the sedimentary troughs, in the early stage of the compressional deformation, or longer-term phenomenon covering the whole history of the orogeny. Further paleomagnetic study, especially of Paleogene rocks, would be necessary to reduce the ambiguity of the timing of the bending.

References

Bellido, B. E. (1979) Sinopsis de la geologia del Peru, Instituto Geologico Minero y Metalurgico Boletin, 22, 54pp.
 Burns, K. L., M. J. Rickard, L. Belbia and F. Chamalaun (1980) Tectonophysics, 63, 75-90.
 Channell, J. E. T., R. Freeman, F. Heller and W. Lowrie (1982) Earth Planet. Sci. Lett., 58, 189-201.

such declination anomaly are confined between Huancabamba deflection and Santa Cruz deflection (Fig.1), this can be explained with counter-clockwise rotation of Peruvian region as the origin of these two deflections (Fig.8). Paleomagnetic study of younger Neogene and Quaternary volcanic rocks is in progress by the authors but no anomalous paleomagnetic declination have been coming out, which gives younger limit of the timing of the bending. It suggests that the bending occurred between Middle Cretaceous and Neogene times. Palmer et al.'s (1980a) report of 30°-40° counter-clockwise rotation of Arica region after Jurassic time does not conflict with our results if Arica region is assumed to be just on the hinge of Santa Cruz deflection.

The mechanism of the bending process of the Andean mountain chain is still unclear due to its ambiguity of the timing. Tectonic evolution history of the Andes suggests major folding began in Late Eocene (Noble et al., 1979). It is important to know at what stage of the evolution history of the Andes the bending actually occurred;

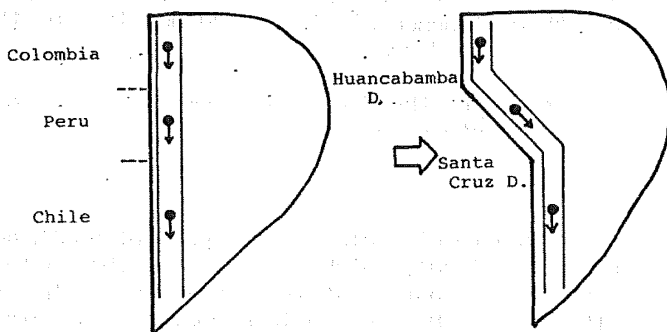


Fig.8 A cartoon illustrating the bending of the Andes and anomalous declination of the Peruvian Andes. D.: deflection.

- Cobbing, E. J. (1976) *Tectonophysics*, 36, 157-165.
- Creer, K. M. (1970) *Phil. Trans. R. Soc.* 267, 457-555.
- Dunlop, D. J. (1979) *Phys. Earth Planet. Inter.*, 20, 12-24.
- Fisher, R. A. (1953) *Proc. Roy. Soc. ser. A.*, 217, 295-305.
- Lowrie, W. and F. Heller (1982) *Rev. Geophys. Space Phys.*, 20, 171-192.
- MacDonald, W. D. and N. D. Opdyke (1972) *J. Geophys. Res.*, 77, 5720-5730.
- Myers, J. S. (1974) *Am. Ass. Petrol. Geol. Bull.*, 58, 474-487.
- Noble, D. C., E. H. McKee and F. Megard (1979) *Geol. Soc. Am. Bull.*, 90, 903-907.
- Palmer, H. C., A. Hayatsu and W. D. MacDonald (1980a) *Geophys. J. R. astr. Soc.*, 62, 155-172.
- Palmer, H. C., A. Hayatsu and W. D. MacDonald (1980b) *Geophys. J. R. astr. Soc.*, 62, 133-153.
- Reyes, R. L. (1980) *Geologia de los Cuadrangulos de Cajamarca, San Marcos y Cajabamba*, Instituto Geologico Minero y Metalurgico, 67pp.
- Webb, S. E. (1976) *The Volcanic Envelope of the Coastal Batholith in Lima and Ancash, Peru*. Ph.D. Thesis University of Liverpool, 202pp.
- Zijderveld, J. D. A. (1967) in: D. W. Collinson, K. M. Creer and S. K. Runcorn (Editors), *Methods in Paleomagnetism*, Elsevier, Amsterdam, pp. 254-286.

NATURAL REMANENT MAGNETIZATIONS OF BEACON GROUP
IN MCMURDO SOUND, ANTARCTICA.

Minoru FUNAKI

National Institute of Polar Research
9-10, Kaga 1-chome, Itabashi-Ku
Tokyo 173, Japan

1. Introduction

Paleomagnetic investigations of the Beacon Group were carried out for the samples collected from Ferrar Glacier (78°S, 161°E) by TURNBULL (1959), and for the Wright and Victoria Valleys (77.5°S, 161.0°E) by BULL et al. (1962). They reached the general conclusion that NRM at these sites is parallel to that of indubitably younger dolerite sills (Ferrar dolerite). That is, a large intrusive mass of Ferrar dolerite nearby caused sufficient heating to raise the Beacon Group to the Curie point and must have been remagnetized in alignment with the ambient geomagnetic field in the Jurassic Age.

According to the geological evidence, the formations from the middle Paleozoic to the Mesozoic Age in East Antarctica consist of only the Beacon Group in the Transantarctic Mountains and Prince Charles Mountains of the Lambert Glacier (i.g. RAVICH and FEDOROV, 1977). Therefore it is very important to carry out an investigation of the Beacon Group paleomagnetically in order to solve the history of Gondwanaland, as the East Antarctic plate is probably situated in the center of that region.

2. Geology of Beacon Group and sampling sites.

In the McMurdo Sound more than 2100m of sedimentary sequence, is found, overlying unconformably the igneous and metamorphic rocks of the basement complex. These sequences, were provisionally brought together under the same Beacon System, with the Beacon Sandstone (Group) of the McMurdo Sound area, as the type rock (HARRINGTON, 1958). The inferred sedimentation ages of these Beacon Group are from Devonian to Jurassic (MCKELVEY and WEBB, 1961; WEBB, 1963). In almost every section where an appreciable thickness of Beacon Group is exposed, one or more horizontal sills of dolerite are present. These sills are from a few meters to more than 300m thick and most of the sills are of uniform thickness (GUNN and WARREN, 1962). The geology of the Beacon Group in the Dry Valley region was described by WEBB (1963); from the oldest to the youngest, Boreas Subgreywacke Member, Odin Arkose, Beacon Height Orthoquartzite, Aztec Siltstone and Weller Sandstone. This geological evidence expands into the Beacon Heights and Mt. Knobhead regions.

Exposed formations at Mt. Circe, located in the upper Olympus Range, consist of Odin Arkose and Beacon Heights Orthoquartzite from the early pre- Devonian to middle- Devonian period. Their lower boundary is dolerite sill "c" 180m thick, as described by MCKELVEY and WEBB (1961). Formations of Beacon Heights Orthoquartzite and Aztec Siltstone of the Devonian

period are exposed at Mt. Knobhead. Intrusions of two dolerite sills, one on the top of the mountain and one about 470m below the top, can be observed on that mountain (WEBB, 1963). A thick sequence of Beacon Group with lower or middle Triassic Age plant fossils is found at Mt. Fleming, on the upper Wright Glacier (GUNN and WARREN, 1962). A synthesized geology of Allan Hills According to BALLANCE and WATTERS (1971), sedimentary rocks referred to the Beacon Group, having a coal bed and fossil plants, which dominated Glossopteris from Permian to Triassic, are exposed at Allan Hills.

A total of 216 paleomagnetic samples were collected from the Beacon Group at Mt. Circe, Mt. Knobhead, Allan Hills and Mt. Fleming. The sampling sites at Mt. Circe, from lower to higher, are sites A, B, C and D, and the mutual vertical distances are about 10, 30 and 20 m respectively. Site A is situated 40 m above the upper boundary of a Ferrar dolerite sill of 180 m in thickness. The formation of these sites is identified as Beacon Heights Orthoquartzite (WEBB, 1962). Sampling sites A, B, C and D at Mt. Knobhead, with mutual vertical distances of 50, 20, and 20 m respectively from lower to higher, are situated on the north side of that mountain. Site A is located at about 2000 m in altitude and probably separated of 140 m above the upper boundary of a dolerite sill. Sampling sites A, B, C and D at Allan Hills should be included in the same formation. At Mt. Fleming, site A is located on the west ridge and sites B and C on the east ridge of the mountain. A dyke of 50 - 200 cm in thickness, resulting from the Ferrar dolerite sills, invades the Beacon Group at site C, and the samples were collected within 20 m from the dyke. However there is no intrusion of the dyke at sites A and B.

3. Theory of experiments

In general, TRM and DRM are very stable (hard) as compared to IRM and VRM (soft). It is possible that the Beacon Group in McMurdo Sound has TRM and the magnetic soft component, besides DRM. We have therefore defined these magnetizations as follows. The soft component is removed from the samples by AF demagnetization in a relatively weak alternating field. The NRM intensity of sediment is considerably weaker as compared to that of igneous rock, ranging from 10^{-7} to 10^{-4} emu/g (i.e. NAGATA, 1961). Consequent comparison of the intensities of the stable component of NRM and acquired TRM in the laboratory would suggest the NRM magnetization method. However, this method may result in chemical alteration during heating. Therefore anhysteresis remanent magnetization (ARM) was adopted as a substitute for TRM in this study. ARM has characteristics quite similar to those of TRM (PATTON and FITCH, 1962), however the low field susceptibility of ARM has a magnetic grain size dependence as suggested by LEVI and MERRILL (1976). Thus, it may be possible to determine the origin of NRM by means of synthesized results from ARM acquisition, AF demagnetization of NRM and ARM, thermal demagnetization of NRM and TRM acquisition properties.

4. Experimental results

The curves obtained for AF demagnetization of NRM and ARM and ARM acquisition for the 3 representative samples from each respective site were divided into the following categories. Type 1: NRM intensity and direction is fairly stable against AF demagnetization up to 1000 Oe. The ARM acquisition curve shows a smooth increase and no saturation up to the maximum field. AF demagnetization of ARM is fairly similar to that of NRM. Thus, the inferred magnetic grains probably have a single domain structure. Type 2: Stable NRM is observed up to approximately 500 Oe but is destroyed in higher fields, ARM acquisition is smooth up to approximately 500 Oe but increases in a zigzag above that field. The AF demagnetization curves of ARM are essentially the same as that of NRM. Type 3: The direction and inclination of NRM are quite unstable against AF demagnetization. However ARM acquisition and AF demagnetization of ARM are fairly stable up to at least 500 Oe. That is, samples of this type are able to have a stable ARM, but the NRM is unstable. Type 4: Both NRM and ARM are fairly unstable up to 1000 Oe against AF demagnetization except when in a weak field. The ARM acquisition curve is also a zigzag on the whole. That is, stable remanent magnetization is impossible. A multi-domain structure for the magnetic grains is inferred. Three representative samples collected from the same site were classified as essentially of the same type, although some may be included in the neighboring type. The types for each site are listed in Table 1 together with the mean NRM and ARM intensities and the NRM/ARM ratios.

	NRM emu/g	ARM h/\tilde{H} emu/g	ARM/NRM	Type		
				AF demag. group	Thermal demag. group	
Mt. Circe	A	3.28×10^{-6}	9.50×10^{-6}	2.89	1	1
	B	9.03×10^{-7}	1.37×10^{-6}	1.52	1	1
	C	9.41×10^{-6}	9.12×10^{-6}	0.97	1	1
	D	1.42×10^{-6}	3.29×10^{-6}	2.31	1	1
Mt. Knobhead	A	1.05×10^{-6}	1.57×10^{-6}	1.50	1	1
	B	3.568×10^{-7}	1.25×10^{-6}	3.51	2	2
	C	7.07×10^{-8}	3.51×10^{-7}	4.96	3, 4	3
	D	1.63×10^{-7}	4.54×10^{-7}	2.78	2, 3	2, 3
Allan Hills	A	6.71×10^{-8}	1.26×10^{-7}	1.88	3	3
	B	9.84×10^{-8}	1.64×10^{-7}	1.67	3, 4	3
	C	3.48×10^{-7}	2.82×10^{-6}	8.11	1, 2	2
	D	3.66×10^{-8}	4.10×10^{-7}	10.97	3	3
Mt. Fleming	A	1.64×10^{-7}	2.75×10^{-7}	1.67	3, 4	3
	B	3.56×10^{-8}	1.85×10^{-7}	5.21	3	3
	C	1.071×10^{-7}	1.49×10^{-7}	1.40	2	2, 3

Table 1. Mean intensities of NRM and ARM ($\tilde{H}=1000$ Oe, $h=0.42$ Oe, h/\tilde{H}), and classified types at room temperature of Beacon Group in McMurdo Sound. AF demag. group: AF demagnetization of NRM and ARM and ARM acquisition. Thermal demag. group: thermal demagnetization of NRM and TRM acquisition.

Three samples were also selected from each site for step-by-step thermal demagnetization and TRM acquisition testing up to 600°C. The results of these experiments are classified into the following categories. Type 1: The decay

curves of NRM against thermal demagnetization have smooth and clear blocking temperatures of NRM between 550°C and 600°C. The directions are fairly stable up to 550°C and disperse at 600°C. Type 2: The intensities decay gradually from approximately 200°C to 450°C and the directions are stable up to at least 400°C - 500°C against thermal demagnetization. But both intensity and direction are unstable from 450°C - 500°C to 600°C. That is, various kinds of blocking temperature may be observed from 200°C to about 450°C. TRM acquisition increases gradually up to approximately 450°C and then steeply to 600°C. Since no stable NRM were observed at more than 450°C, the increasingly steep magnetization from 450°C to 600°C is probably due to chemical alterations of magnetic grains. Type 3: The intensities and directions of NRM are stable to 300°C; this is the most stable type. TRM acquisition increases gradually to 300°C and then zigzags to 600°C; in many cases it is fairly unstable from 200°C to 600°C. That is, the inferred blocking temperature must be very low or undefined. As the results of these thermal examinations are almost identical in samples collected from the same site, the classified types from each site are listed in Table 1.

NRM's of 216 samples collected from 4 formations of the Beacon Group were measured before and after optimum AF demagnetization. Based on the results of AF demagnetization of representative samples, the samples with an optimum 100 or 150 Oe AF demagnetization field were chosen. Obtained results of the mean value are summarized in Table 2. The NRM's of mean intensities of the samples from Mt. Circe are strong, 8.74×10^{-7} - 8.82×10^{-6} emu/g, as compared to those from Mt. Knobhead, Allan Hills and Mt. Fleming. The samples from Allan Hills and Mt. Fleming are weak, with a magnitude of 10^{-8} - 10^{-7} emu/g. Most of the samples are magnetized to the normal polarity but some samples from Allan Hills D and Mt. Fleming B are magnetized to reverse polarity. Individual NRM directions for all samples from one site formed a cluster in the case of the samples from all sites of Mt. Circe, A and B sites of Mt. Knobhead and site C of Allan Hills and Mt. Fleming, but were scattered for the others. The mean intensities of clustered samples from each site are generally larger than those of scattered ones; and the mean directions are limited from -62.3° to -82.3° inclination and 230.9° to 280.7° declination.

sampling site	demag	N	R emu/g	I	D	K	α_{95}	pLat	pLon
Mt. Circe (total)	150	47	4.00×10^{-6}	-69.9	255.9	118.9	1.9	49.1S	138.0W
Mt. Knobhead (A+B)	150	47	8.39×10^{-7}	-82.4	275.1	159.6	1.7	71.7S	143.6W
Allan Hills (C)	150	12	3.62×10^{-7}	-78.8	253.5	97.2	5.3	62.3S	151.4W
Mt. Fleming (C)	150	10	1.57×10^{-7}	-77.1	244.5	24.5	9.9	58.2S	154.5W

Table 1. Paleomagnetic results of Beacon Group in McMurdo Sound, Antarctica.

5. Paleomagnetic discussion and concluding remarks.

TURNBULL (1959) and BULL et al. (1962) pointed out that the directional NRMs of the Beacon Group from Ferrar Glacier and the Wright and Victoria Valley regions were parallel to that of Ferrar dolerite. Obtained results in this study support not only their results but also expand it to include the region from Mt. Knobhead to Allan Hills. This uniformity of direction for the Beacon Group and Ferrar dolerite may be caused by the geomagnetic field in this region being constant in direction from the Devonian to the Jurassic period, or by the reheating of the Beacon Group during the intrusion of Ferrar dolerite in the Jurassic period. The following analysis is carried out in order to find a solution to this problem by applying the different types of AF and thermal demagnetization groups and the mean directions of NRM for each site. The significance of each type of AF demagnetization group may be estimated as follows: Types 1 and 2: As the AF demagnetization curves of NRM and ARM are similar, the inferred origin of NRM may be DRM when both intensities differ greatly. Type 3: Although NRM is unstable, it has stable ARM. DRM and TRM cannot be acquired, and the ratio ARM/NRM is large. Type 4: As there is no possibility of stable remanence, it cannot be judged whether the samples were heated or not.

The representative samples from Mt. Circe, A, B, C and D, are similar not only in the ratio ARM/NRM but also in their classified type for the AF and thermal demagnetization groups as shown in Table 1: the ratios range from 0.97 to 2.89 and the samples all belong to one type. A dolerite sill 180m thick intruded into the boundary between the basement complex and the Beacon Group (MCKELVEY and WEBB, 1961), and the sampling site at Mt. Circe is within a vertical distance of 50m from the upper boundary of that sill. Taking into account the calculation of temperature in the neighborhood of the intrusive sheet (JAEGER, 1957; 1959), it is possible that the temperature at the sampling site rises to over 570°C. The NRM direction for Ferrar dolerite collected from the Olympus Range is reported by FUNAKI (1982). Since the mutual angular deviation (θ) of NRM direction between the Beacon Group and Ferrar dolerite is 6.4°, their NRM directions should correspond to each other, taking into account the α_{95} values. This suggests that the Beacon Group around the sampling sites at Mt. Circe was heated to over 570°C and remagnetized during cooling down through that temperature during the Jurassic Age.

The samples from Mt. Knobhead are of different kinds of type of AF demagnetization group for each site. The samples from sites 1 and 2 are Type 1 and 2 respectively for both the AF and thermal demagnetization groups, and have small ARM/NRM ratios of 1.50 and 3.15. That is, the inferred origin of NRM at these sites is probably TRM for the same reasons as given for the samples from Mt. Circe. The samples from site C are classified as types 3 or 4 for the AF and thermal demagnetization groups; NRM is generally unstable, but some are capable of stable remanence. Therefore it may be assumed that the samples at site C were not placed under conditions of DRM acquisition, and were not then heated up to Curie temperature. The samples from site D are classified as Types 2 and 3 for both AF and thermal demagnetization groups, having a small

ARM/NRM ratio of 2.78; all samples are capable of stable remanent magnetization, and some of them actually show stable NRM. Therefore the formation at this site was probably heated up to the same temperature, limited from 200° to 450°C. Consequently the samples which have a blocking temperature than below temperature would acquire TRM. Dolerite sills intrude into Mt. Knobhead at the top (2400m) and about 540m below the top (WEBB, 1963). The vertical distance of sampling site A from the lower sill is estimated as about 140m above. The mean NRM direction for whole samples from sites A and B shows an inclination of -82.4° and a declination of 275.1° with a α_{95} value of 1.7°. TURNBULL (1959) obtained the NRM directions for Ferrar dolerite sills from the upper Ferrar Glacier region. As Mt. Knobhead is also situated in the same region, the representative NRM direction for Ferrar dolerite from the upper Ferrar Glacier region, referring to his data, should show an inclination of -76° and a declination of 255° with a α_{95} value of 2.7°. Therefore, since the angular deviation is $\theta = 7.3^\circ$, the directions of both formations are parallel, taking into account the α_{95} values. Therefore these sampling sites may have been heated by a dolerite sill to more than 570°C for site A and less than that temperature for the other sites. Later many samples were remagnetized completely or partially to the geomagnetic field direction during the Jurassic Age.

In the case of Allan Hills, the representative samples from site C have stable NRM; they are classified as types 1 or 2 for the AF and thermal-demagnetization groups. As the ARM/NRM ratio is large, 8.11, it may be estimated that the formation was magnetized by DRM rather than by TRM. The samples from sites A, B and D are of Type 3 or 4 AF demagnetization group.

The results of chemical analysis of coal from near site C in Allan Hills suggest that the coal samples are anthracite. The value of the fuel ratios (volatile matter/fixed carbon), ranging from 16.9 to 20.4, shows that this coal includes a relatively large quantity of volatile matter in the case of anthracite. That is, it may be concluded that these samples were not heated between the Permian Age and the present. Thus, the surface of Allan Hills was probably not heated, and the DRM of the samples from site C survived.

The Earth's geomagnetic field from the late Permian to the middle Triassic period showed alternate changes of normal and reversed polarity, but prior to the Permian age showed only reversed polarity (Kiaman interval) (MCELHINNY and BUREK, 1971). Therefore the magnetization polarity of Allan Hills would suggest the age confirmed by fossil evidence, namely from the late Permian to the early Triassic period.

The NRM direction of Ferrar dolerite in this area has an inclination of -67.6° and a declination of 262.6°, and a α_{95} value of 5.1° (FUNAKI, 1982). An angular deviation between the Beacon formation at site C and Ferrar dolerite is $\theta = 11.5^\circ$. That is, both directions are in mutual agreement taking into account these α_{95} values. Since the inferred age of the Beacon Group at Allan Hills form Permian to Triassic (TOWNROW, 1966; BALLANCE and WATTERS, 1971), it may be concluded that the shift of Antarctica against VGP was small from the Permo-Triassic to the Jurassic Age. This conclusion is consistent with the results of analysis of Mesozoic rocks from Australia (IRVING, 1963; IRVING et al., 1963); directional magnetizations

from Lower Triassic to Lower Cretaceous are approximately uniform for Eastern Australia including Tasmania Island. Hence it seems that Australia separated off from East Antarctica in early Tertiary time.

The representative samples collected from site C at Mt. Fleming are classified as types 2 or 3 for AF and thermal demagnetization groups, and the ARM/NRM ratio is small, 1.40. The NRM direction of the dyke from which Ferrar dolerite originates, showing an inclination of -76° and a declination of 255° with α_{95} of 2.7° , was obtained at a site separated by 30 m from site C⁵ (FUNAKI, 1982). The angular deviation θ between the mean NRM direction of the Beacon Group at site C, as shown in Table 2, and that of the dykes is 6.6° ; they are mutually parallel taking into account the α_{95} values. A total of 10 samples from site C were collected from the area between a dyke 50 to 100 cm in thickness and 20m away from the dyke. It is impossible to determine from the NRM direction whether the formation at site C was heated by the dyke or not, because the inferred ages of the Beacon Group and Ferrar dolerite are Triassic and Jurassic respectively and, as mentioned above, the NRM directional change during Mesozoic time was small. From the ARM/NRM ratio, however the formation must have been heated to above the Curie point. The samples at site A and B, including the same formations as site C, are of Type 3 or 4 of the AF and thermal demagnetization groups; they were not heated up to the Curie point. From this it may be concluded that the samples which were heated by dykes (site C) have a stable NRM, but samples which were not heated (sites A and B) do not have a stable NRM.

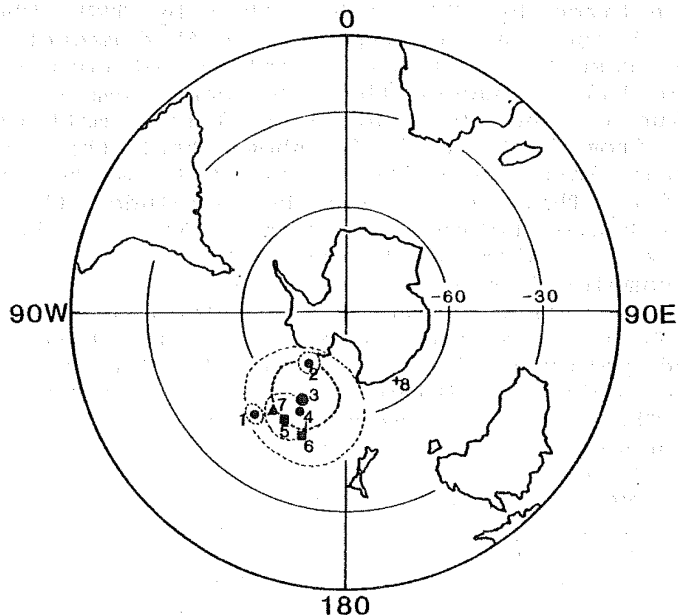


Fig. 1. Obtained VGP positions for Beacon Group, McMurdo Sound, Antarctica. No. 3: Permo-Triassic VGP.

The four obtained VGP positions of the Beacon Group, for (1) Mt. Circe, (2) Mt. Knobhead, (3) Allan Hills and (4) Mt. Fleming, are illustrated in Fig. 1 together with those of

previous data about the Beacon Group ((5) TURNBULL, 1959; (6) BULL et al. 1962), (7) Ferrar dolerite and (8) the present geomagnetic pole. The VGP of Ferrar dolerite is estimated as the average position of 10 independent data from the whole Transantarctic Mountains (FUNAKI, 1982). The VGPs of the Beacon Group from the Wright and Victoria Valley regions (1) and (6) are distributed on the low latitude side. This is consistent with the results of analysis of Ferrar dolerite from the Wright and Victoria Valley regions; the latitude of VGP is the lowest for these 10 data. In general, VGP distribution in Fig. 1 resembles that of Ferrar dolerite in the Jurassic Age fairly closely. VGP (3) shows the location of the geomagnetic pole position for Allan Hills during the Permo - Triassic period. However it is included in the cluster of VGPs from the Beacon Group which were heated by Ferrar dolerite as shown in the figure. Therefore, as mentioned above, Antarctica probably did not shift during the late Permian to Jurassic periods.

References

- BALLANCE, P. F. and WATTERS, W. A. (1971), *N. Z. J. Geol. Geophys.*, 14(3), 512-527.
- BULL, C., IRVING, E. and WILLIS, I. (1962), *Geophys. J. R. astr. soc.*, 6: 320-336.
- FUNAKI, M. (1982), *Antarctic Record*, 77, in press.
- HARRINGTON, H. J. (1958), *Nature*, London, 182, (4631), 290.
- IRVING, E. (1963), *J. Geophys. Res.*, 68, 8, 2283-2287.
- JAEGER, J. C. (1957), *American Journal of Science*, 225, 306-318.
- JAEGER, J. C. (1959), *American Journal of Science*, 257, 44-54.
- LEVI, S. and MERRILL, R. T. (1976), *Earth and planetary sci. Lett.*, 32, 177-184.
- MCELHINNY, M. W. (1973): *Paleomagnetism and plate tectonics*, Cambridge, at the University Press, p358.
- MCELHINNY, M. W. and BUREK, P. J. (1971): *Nature*, London, 232, 98-102.
- MCKELVEY, B. C. and WEBB, P. N. (1961), *N. Z. J. Geophys.* 5, 143-162.
- NAGATA, T. (1961): *Rock magnetism*. Maruzen, Tokyo, p350.
- PATTON, B. J. and FITCH, J. L. (1962), *J. Geophys. Res.*, 67, 1, 307-311.
- RAVICH, M. G. and FEDOROV, L. V. (1977), 3rd symposium on Antarctic geology and geophysics. The University of Wisconsin Press, 499-504.
- TOWNROW, J. A. (1966), *N. Z. J. Geol. Geophys.*, 10, 456-473.
- TURNBULL, G. (1959), *Arctic*, 12, 151-157.
- WEBB, P. N. (1963), *N. Z. J. Geol. Geophys.*, 6, 361-387.

A PRELIMINARY INVESTIGATION OF BASEMENT COMPLEX IN WRIGHT VALLEY, MCMURDO SOUND, ANTARCTICA

Minoru FUNAKI

National Institute of Polar Research
9-10, Kaga 1-chome, Itabashi-Ku, Tokyo 173, Japan.

1. Introduction

There is a wide ice free area called Dry Valley at the west side in McMurdo Sound, South Victoria Land, Antarctica. It has three major valleys from north to south as Victoria Valley, Wright Valley and Taylor Valley. Basement complex (Cambro - Ordovician Age) with several kinds of dyke swarms are observed to the bottom of those excavated valleys, and the sedimentary strata called Beacon Group (Devonian Age) are also observed at top of those valleys. A single sill 240 to 300m in thickness is intruded into the basement complex in most place of Dry Valley region (i.g. MCKELVEY and WEBB, 1961), consequently every rock mass have a possibility of the reheating by dolerite sill's intrusions.

The paleomagnetic investigations were carried out at Wright Valley and Victoria Valley (BULL and IRVING, 1960; BULL et al., 1962) and at Taylor Valley (MANZONY and NANNI, 1977). Obtained main result from those investigations are as follows. The directions of NRM in Wright and Victoria Valley area are parallel in all the units for basement complex and dolerite sills. This uniformity could have resulted the reheating the whole area during the last phase of intrusion in Jurassic time. In the case of Taylor Valley, the mean direction of NRM from four lamprophyric dyke (Cambro-Ordovician Age) yielded of 222.6° in declination and 0.6° in inclination. The corresponding paleomagnetic pole position lay at 9.3°S and 26.7°E and was consistent with the previous results from lower Ordovician rock from distant area of East Antarctica.

Total of 110 block rocks of Cambro - Ordovician with orientation were collected from Olympus granite, Theseus granodiorite, Vanda lamprophyre, Vanda porphyry and red dyke from bottom of Wright Valley. As the inclination of geomagnetic field in this area is -83.5° , the direction of samples were determined by means of Sun compass, but magnetic compass was used when it was cloudy.

2. AF and thermal demagnetizations

The results of AF demagnetization of NRM suggests that all the samples except Theseus granodiorite and red dyke have stable NRM. The median demagnetization field (MDF) of these samples exceeds 500 Oe and their NRM directions change within 12° during AF demagnetization up to a peak of 600 Oe. However the samples of Theseus granodiorite and red dyke do not have such a stable NRM against AF demagnetization. These AF demagnetization curves suggest that an alternating field around peak of 150 Oe removes the unstable component from NRM.

Since the NRM of all samples of granitic rock is distributed along the meridian from middle to low latitude in the southern hemisphere, as described later, each of the three

samples was selected from the middle and low latitude groups. The inclination of these samples ranges from -8.5° to -21.9° for Ath 1, Ath 2 and Ath 3 of the low latitude group, and from -46.7° to -69.0° for Ath 4, Ath 5 and Ath 6 of the middle latitude group. The NRM_6 intensities of the low latitude group ($1.566 - 4.140 \times 10^{-6}$ emu/g) decay steeply from 500° to 600° as shown in Fig. 1. The directions of this group show almost no change up to 500° and then scatter from the cluster at 600° . In the case of the middle latitude group, the NRM_6 changes gradually not only in intensity ($1.034 - 5.797 \times 10^{-6}$ emu/g) but also in its direction against thermal demagnetization up to 500° ; the NRM direction of in the middle latitude systematically shifts to low latitude, synchronizing with the decay of intensity up to 500° , but scatters widely at 600° .

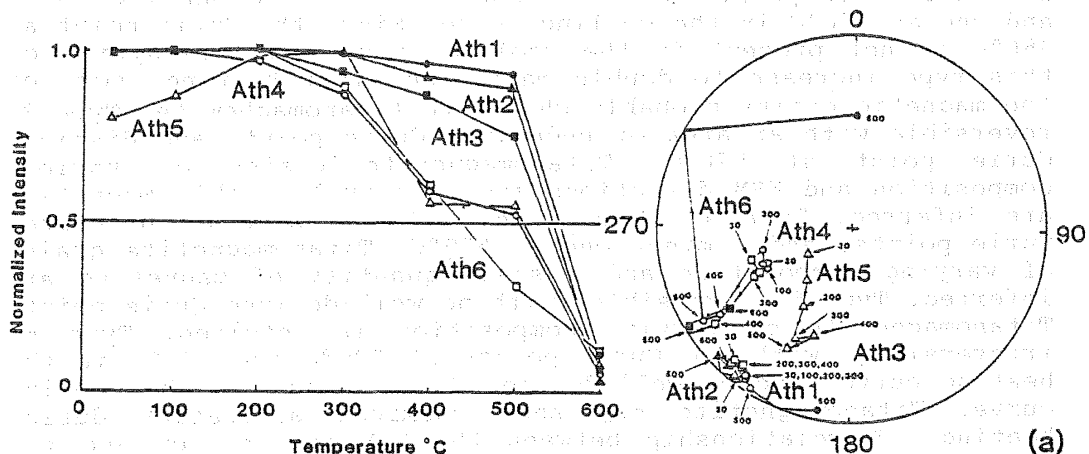


Fig. 1 Thermal demagnetization curves of granitic rocks from Wright Valley in McMurdo Sound.

In case of the samples of Theseus granodiorite, the intensities demagnetize steeply between 300° and 400° . The corresponding directions, distributed in the high latitude, show almost no change up to $300^\circ - 400^\circ$; they then shift systematically to low latitude up to 500° . Since the NRM directions of Vanda lamprophyre are distributed along a meridian from 0° to 90° in latitude in the southern hemisphere. The results of thermal demagnetization analyses are fairly similar to those of the granitic rock.

The thermomagnetic curves of Vanda porphyry are fairly similar to those of the low latitude group of granitic rock.

That is, their original NRM intensity, does not show much decay up to 500° and then decays steeply from 500° to 600° . The NRM direction at low latitude shows almost no change up to 400° and then shifts towards low latitude and scatters at 600° .

The NRM s of Vanda red dyke are unstable against thermal demagnetization as a whole as compared with other formations.

Their NRM intensities decay smoothly from 200° to 600° . The NRM directions are relatively stable from 100° to 450° .

3. Thermomagnetic curves.

Thermomagnetic curves (I_s -T curve) were obtained under 1×10^{-4} torr in atmospheric pressure, from room temperature up to 650°C . The applied field intensity was 5k Gauss, and the heating and cooling rate was $200^\circ\text{C}/\text{hour}$. I_s -T curves for granitic rock, Theseus granodiorite and Vanda porphyry could not be obtained because of instrumental noise. The obtained I_s -T curves of typical samples of Vanda lamprophyre and red dyke are classified into six types. Type 1; irreversible, with a single Curie point at 570°C ; the ferromagnetic minerals are probably magnetite of constant composition, but may show low temperature oxidation (titanomaghemite) due to increasing magnetization during heating. Type 2; irreversible, with two distinct Curie points at 350°C and 570°C in the heating curve and one at 570°C in the cooling curve. Since the Curie point at 350°C is not present in the cooling curve and intensities of this type increase to double magnitude after heating, some of the magnetic grains probably change to titanomaghemite. Type 3; reversible with an area of undefined Curie points and distinct Curie point at 570°C . Titanomagnetite grains of various composition and NRM directions are relatively stable magnetite are inferred. Type 4; reversible, with an area of undefined Curie points, and a minor one at 570°C . Titanomagnetite grains of varying composition and a small quantity of magnetite are inferred. Type 5; reversible, with no well-defined Curie point. Titanomagnetite of varying composition is inferred. Type 6; irreversible, with two Curie points at 220°C and 330°C in the heating curve, and no well-defined Curie points in the cooling curve. Titanomagnetite may show chemical alteration during heating. A relationship between the NRM inclination and the Curie point of these representative samples can be identified in the case of the samples of Vanda lamprophyre. That is, the samples of Type 1 and 3 have clearly distinct Curie points for magnetite, and have a low inclination of about -20° ; those of Type 5 and 6 have a lower Curie point at more than 500°C and have high inclinations of $70^\circ - 80^\circ$; that of Type 4 is midway between these two cases. However there is no correlation between the Curie points and the inclinations in the case of the red dyke. Pilot samples from red dyke, with all samples showing a Type 2 I_s -T curve, magnetized at an inclination of about $-32^\circ - -65^\circ$.

4. Directional NRM against demagnetization.

The NRM of every sample before and after AF demagnetization up to 140 Oe was measured, and the samples were then thermal demagnetized in air at 300° , 400° , 500° and 550°C . The individual NRM directions of granitic rock are plotted by demagnetization step in Fig. 2. The NRM directions for a major part of the specimens are found in low to middle latitudes in the southern hemisphere. This distribution tendency is not changed by AF demagnetization up to 140 Oe. However the NRM directions distributed from middle to high latitude have a tendency to shift towards low latitude through thermal demagnetization. The individual directions at 500°C lie along a great circle of low inclinations quite close to the horizontal plane.

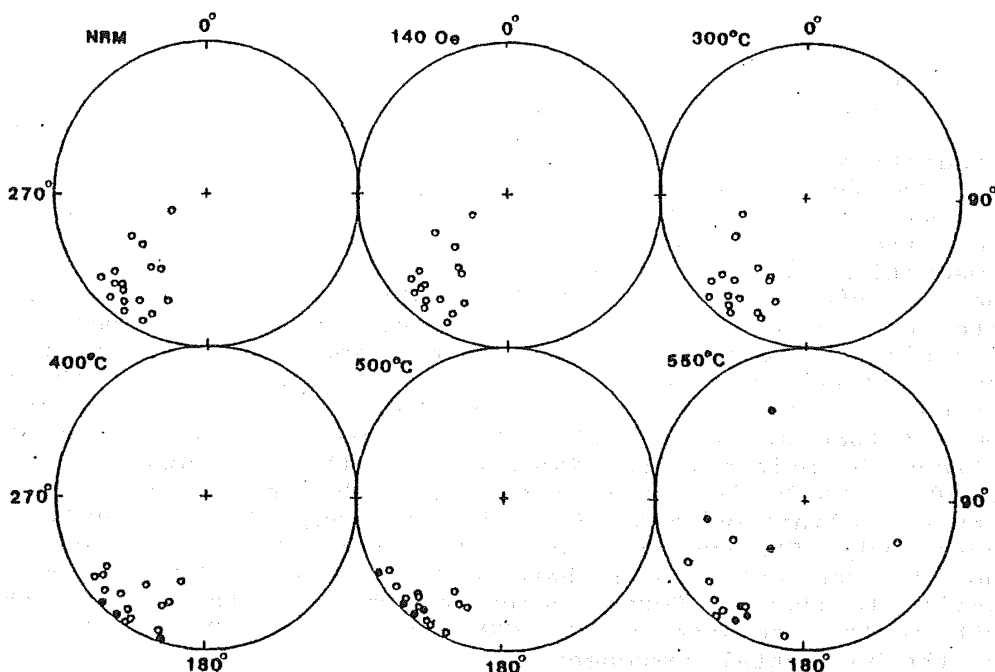


Fig. 2. Directional changes of NRM against AF and thermal demagnetizations for granitic rocks from Wright Valley in McMurdo Sound.

The individual NRM directions of specimens from Theseus granodiorite make a cluster around -75.5° inclination, 255.3° declination, with a confidence of $\alpha_{95} = 5.3$. These original directions are scattered by thermal demagnetization at 400°C and 500°C . The original NRM directions of specimens from Vanda lamprophyre are distributed around high to low latitude along 228.1° of the meridian. The patterns of direction changes and intensity variations are quite different from dyke to dyke. This tendency is not greatly affected by AF demagnetization at 140 Oe . However, these directions are changed by thermal demagnetization at 400°C and 500°C . This characteristic behavior under thermal demagnetization is essentially similar to that of granitic rock. Since the clearest precision and confidence, $K = 15.0$ and $\alpha_{95} = 6.9$, are obtained by thermal demagnetization at 500°C , the inclination of -20.3° and the declination of 219.8° at that temperature are the most significant directions paleomagnetically for Vanda lamprophyre.

The distribution of NRM directions collected from Vanda porphyry have middle to low inclination of normal magnetization, and they are clustered with a precision of $K = 39.1$ and a confidence of $\alpha_{95} = 4.4$. This distribution characteristic is not changed by AF demagnetization at 140 Oe . However it is changed by thermal demagnetization from 300°C to 500°C . That is, the original mean NRM direction with an inclination of -25.1° and a direction of 227.8° is settled at -6.6° and 223.0° respectively by thermal demagnetization up to 500°C .

In the case of the red dyke rocks, the individual

directions of NRM, magnetized at normal polarity, do not make such a clear pattern. However NRMs after AF demagnetization at 140 Oe make a cluster around an inclination of -61.7° and a declination of 238.4° , with α_{95} of 8.1. This cluster formation tendency is not changed by thermal demagnetization at 300°C and 400°C , but these directions are dispersed by thermal demagnetization at more than 500°C .

The results of these demagnetizations are summarized as follows. The mean NRM direction of each formation, except for the red dyke rocks, is not effectively changed by AF demagnetization at 140 Oe. In the case of the specimens from the red dyke rocks, the individual NRM directions are gathered into one direction by AF demagnetization. The mean NRM directions of granitic rocks, Vanda lamprophyre and porphyry are shifted gradually to low inclination by thermal demagnetization, and settled along the $210 - 230^\circ$ meridian of low latitude at $500^\circ - 550^\circ\text{C}$. The differential directional NRM between the original mean NRM and after thermal demagnetization at $500 - 550^\circ\text{C}$ is fairly similar to that of Ferrar dolerite (-69.4 inclination and 237.6 declination, FUNAKI, 1982) for these rocks. The specimens collected from Theseus granodiorite and the red dyke rocks have only a stable NRM direction, similar to that of Ferrar dolerite. That is, they show either both or the opposite of the NRM direction of Ferrar dolerite and the horizontal component.

From the thermal demagnetizations of all specimens and their basic magnetic properties, the magnetization mechanism for the rock formations of the basement complex in Wright Valley can be explained as follows. The ambient geomagnetic field when the basement complex was formed in 480 - 500 m.y. (lower Ordovician to early Cambrian) was almost horizontal in McMurdo Sound. This region was then heated up to 500°C by the intrusion of dolerite sills in 160 m.y. (Jurassic Age) at the bottom of Wright Valley. Consequently the NRM directions of specimens magnetized in the Cambro - Ordovician Age, which have a high blocking temperature of more than 500°C , survived (primary magnetization). However, the primary magnetizations of the specimens which have a low blocking temperature of less than 500°C have completely disappeared, and the specimens were remagnetized (secondary magnetization) to the direction of the geomagnetic field when dolerite sills intruded into the Dry Valley area in the Jurassic Age. On the other hand, the specimens included in both magnetite and various compositions of titanomagnetite have a superposed magnetization of primary and secondary magnetization at room temperature.

5. Paleomagnetic discussion

The VGP positions obtained from the mean NRM direction of each formation by thermal demagnetization at 500°C and sampling site are illustrated in Fig. 3. Since Vanda lamprophyre and porphyry are included in the same age, these two data are combined in Fig. 3. MANZONI and NANNI (1977) obtained a VGP position of 470 m.y. ago from lamprophyre dykes (maybe the same sequence as Vanda lamprophyre) in Taylor Valley (77.64°S , 163.35°E) which is 20 km south of Wright Valley. Their VGP position is located in almost the same area as our positions.

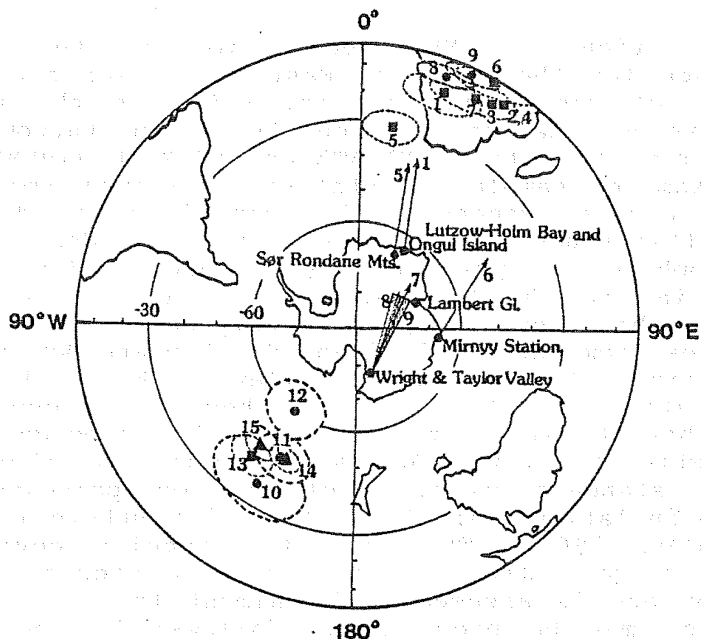


Fig. 3. Positions of VGP in Cambro - Ordovician Age for Antarctica and the declinations of NRM. 1: Ongul Island (NAGATA & SHIMIZU, 1959), 2 and 3: Ongul Island (NAGATA & YAMA-AI, 1961), 4: Lutzow-Holm Bay (KANEOKA et al., 1968), 5: Sor Rondane Mts. (ZIJDERVELD., 1968), 6: Mirnyy Station (MCQUEEN et al., 1972), 7: Taylor Valley (MANZONI & NANNI, 1977), 8 - 12: this study, 13: Wright & Victoria Valley (BULL et al., 1962), 14: Wright Valley (Ferrara dolerite): this study, 15: Wright & Victoria Valley (Ferrara dolerite) (BULL et al., 1962). equal-area projection.

MCQUEEN et al. (1972) reported a VGP position of the Cambro-Ordovician Age at Mirnyy Station ($66^{\circ} 33'S$, $93^{\circ} 01'E$). This value is located in almost the same position as the data from the Wright and Taylor Valleys. High - grade metamorphic rocks of Cambro - Ordovician Age are distributed along most parts of the coast line of Lutzow-Holm Bay (e.g. TATSUMI and KIKUCHI, 1959). Paleomagnetic investigations for these formations were carried out by NAGATA and SHIMIZU (1959, 1960), NAGATA and YAMA-AI (1961) and KANEOKA et al. (1961). They reached the general conclusion that the VGP was situated near the equator in the Cambro-Ordovician Age as shown in Fig. 3; VGPs from the Wright and Taylor, Valleys, Mirnyy Station and Lutzow-Holm Bay were located around $0.9^{\circ}N - 21^{\circ}S$ in the latitude of Africa. However a VGP position of the same age from the Sor Rondane Mountains ($72^{\circ}S$, $24^{\circ}E$) was isolated from the other data in East Antarctica as shown in Fig. 3. Taking into account these VGP distributions, paleomagnetic results may be concluded as follows; VGP was located in approximately the position below the equator in the Cambro-Ordovician Age; the Transantarctic Mountains should be included in East Antarctica.

The directions of MRM declination in the Cambro - Ordovician Age for the whole of East Antarctica are shown to the location of respective sampling sites in the figure. A representative declination for Ongul Island and Lutzow Holm Bay is adopted from the data of NAGATA and SHIMIZU (1959), as the number of examined samples is statistically very small in the case of the others. Ranges of 95% confidence of declination obtained in this study for granitic rock ($\alpha_{95}(\text{dec}) = 4.7$) and Vanda lamprophyre and porphyry ($\alpha_{95}(\text{dec}) = 3.5$) are also illustrated in Fig. 3. A remarkable characteristic of these directions is that they are approximately parallel in the case of the samples from Ongul Island and Sor Rondane Mountains, and those from Mirnyy Station, Taylor Valley and Wright Valley. The angular deviation is $15^\circ - 20^\circ$ for these two groups. On the assumption that the structure of the Earth's geomagnetic field in the Cambro-Ordovician Age was similar to that of the present, the standard precision of the nondipole geomagnetic field at low latitude in the southern hemisphere is probably $8 - 10^\circ$ (COX, 1962). That is, the angular deviation of declination is twice that of the nondipole precision. If the magnetization age is assumed to be almost the same, a simple interpretation may be proposed as follows: In the Cambro - Ordovician Age rock formations were magnetized in the same direction at these locations, and a rift later formed in East Antarctica between Queen Maud Land and Wilkes land. The most reliable possibility for the location of the boundary of the rifting zone may be along the Amery Ice Shelf to the Lambert Glacier. According to deep seismic soundings and aeromagnetic data by the Soviet Antarctic Expedition in 1973, a crustal feature of the MacRobertson - Princess Elizabeth Land through the Lambert Glacier is large - scale normal faulting and the resulting development of a deep graben filled with low - density rocks; the density is 2.3 and the density of country rock is 2.8. Beneath the graben, the crustal thickness is as low as 22 - 24 km, while on both sides of the graben, the crust is 30 - 34 Km thick (KURININ and GRIKUROV, 1982; FEDOROV et al., 1982). They suggested that the beginning of rifting was in the late Mesozoic period according to geological evidence. The features of topography under the ice sheet in these areas suggest that a large valley extends to the south from the Amery Ice Shelf (i.e., Atlas Antarktiki, 1966). The magnetization directions of Cambro - Ordovician rocks in East Antarctica support their results completely and suggest that the rifting angle is about $15 - 20^\circ$.

References

- BULL, C. and IRVING, E. (1960): J. R. aster. soc., 3, 211-224.
- BULL, C., IRVING, E. and WILLIS, I. (1962): Geophy. J. R. aster. soc., 6, 320-336.
- FEDOROV, L. V., GRIKUROV, G. E., KURININ, R. G. and MASOLOV, V. N. (1982): 3rd Symposium on Antarctic Geoscience, the University of Wisconsin Press, 931-936.
- FUNAKI, M. (1982): Antarctic Record, 77, in press.
- KANEOKA, I., OZIMA, M., OZIMA, M., AYUKAWA, M. and NAGATA, T. (1968): Antarctic Record, 31: 12-20.
- KURININ, R. G. and GRIKUROV, G. E. (1982): 3rd symposium on Antarctic Geoscience, the University of Wisconsin Press, 895-901.
- MANZONY, M. and NANNI, T. (1977): Pageoph. 115:961-977.
- MCKELVEY, B. C. and WEBB, P. N. (1961): N. Z. J. Geophys. 5, 143-62.
- MCQUEN, D. M., SCHARNBERGER, C. K., SCHARON, L and HALPERN, M. (1972): Earth and Planet. Sci. Let., 16, 433-438.
- NAGATA, T. and SHIMIZU, Y. (1959): Nature, 184, 1472-1473.
- NAGATA, T. and SHIMIZU, Y. (1960): Antarctic Record, 10, 661-668.
- NAGATA, T. and YAMA-AI, M. (1961): Antarctic Record. 11, 945-947.
- TATSUMI, T. and KIKUCHI, T. (1959): Antarctic Record, 8, 1-21.

ON THERMO MAGNETIC PROPERTY OF SO-CALLED "MAGNETIC STONE"
COME FORM II-NO-URA DISTRICT, MASUDA CITY,
WEST JAPAN

Haruo DOMEN

Institute of Physical Sciences, Faculty of
Education, Yamaguchi University, 753 Japan

At the sea side of the Japan sea, Ii-no-Ura district, Masuda City, Shimane Prefecture, west Japan (Fig. 1); near by the border to Yamaguchi Prefecture, there is a small hill (ca. 30m in height and 150m in circumference) of quartzdiorite, top of which having strong magnetism had been known from older time, then been called "magnetic stone", something like the gabbro of Ko-Yama, Susa district in Yamaguchi Prefecture, only few kilometers apart from each other (Domen 1958).

The rock sample of this massive hill is being examined from rock magnetic view point. In this report, some Js-T curves due to thermomagnetic analysis by means of an automatic thermomagnetic balance (Naruse Kagaku Co. Ltd., Sendai; MB-2) obtained up to this date, are shown. Few samples had been taken at the top of the hill, the bottom part and also a half way up respectively. Thermomagnetic analysis are carried out about the bulk flakes of specimens in the open air, 10^{-5} Torr and also 10^{-6} T. Some typical examples of such Js-T curves are seen in Fig. 2.

Top and bottom specimens have similar size of magnetic susceptibility. The half-way sample are highly altered and show rather weak susceptibility.



Fig. 1. Map showing the sampling site.
Star is for Ii-no-Ura, Masuda,
Shimane Prefecture, Japan.

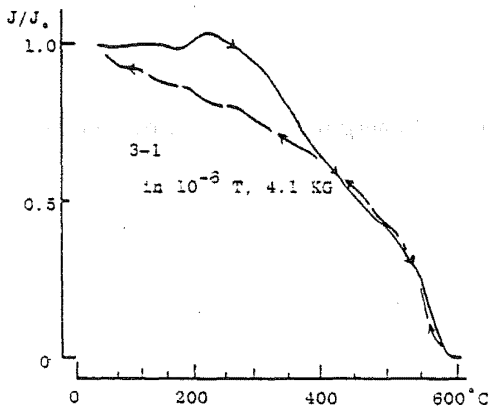
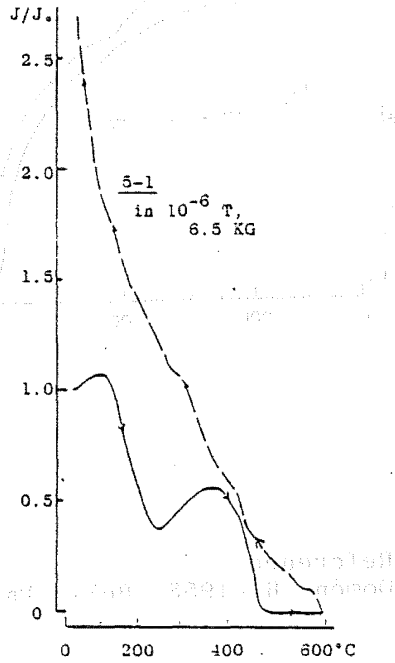
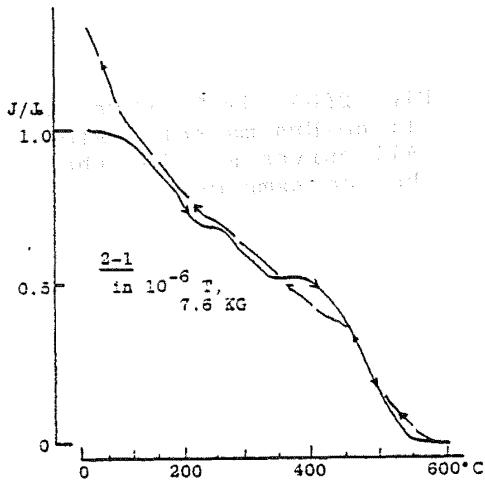
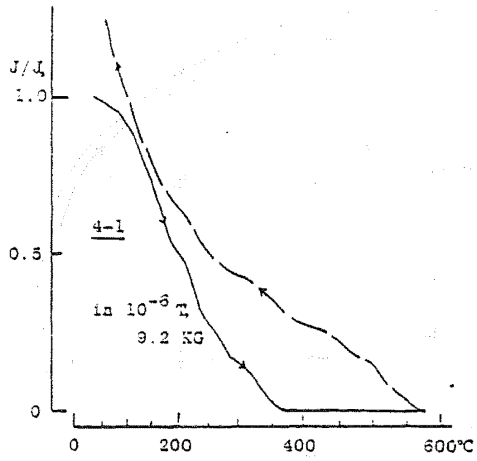
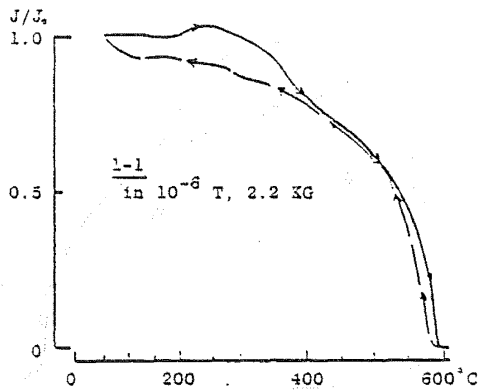


Fig. 2(a). J_s - T curves for Ii-no-Ura magnetic stone. 1-1 and 2-1 are for the Top samples and others for the half-way samples.

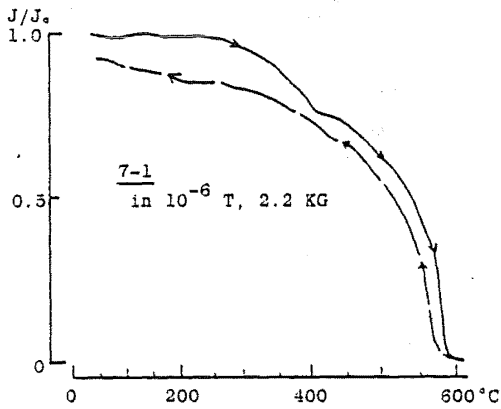
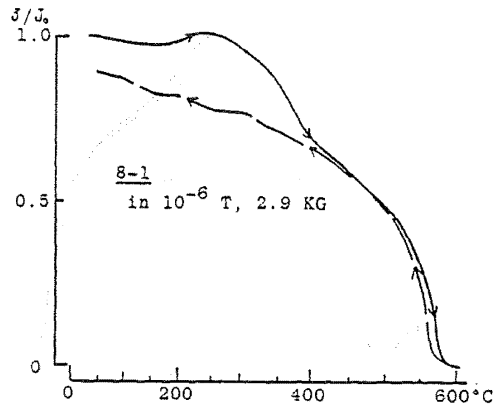
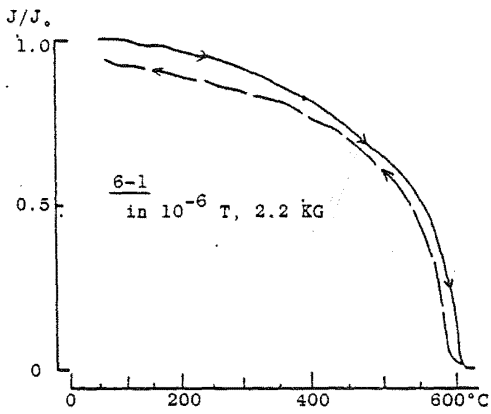


Fig. 2(b). J_s -T curves for Ii-no-Ura magnetic stone. All curves are for the bottom samples.

Reference

Domen, H. (1958) Bull. Fa. Educ., Yamaguchi U., 7(Pt.2), 35.

ERRORS IN ANALYSES OF NRM USING MAGNETIC DIPOLE MODELS

Hiroshi MUNEOKA* and Haruo DOMEN**

* Ozuki Air Base, M.S.D.F. Shimonoseki, 750-11, Japan.

** Institute of physical Sciences, Faculty of Education, Yamaguchi University, 753, Japan.

1. Introduction

When magnetic sources are contained in the closed surface, the magnetic potential of outer space due to these sources is expressed by the perfect orthogonal functions. If the magnetic potential may be developed by the finite terms of the spherical functions which have the spherical boundary, every coefficient of these functions is determined independently from the maximum degrees of terms.

In this report, we are going to discuss the errors in analyses of NRM of rock specimens using magnetic dipole models at the center of a sphere. Especially, some mathematical dipole models are prepared as the data of NRM of vertical magnetic fields on the sphere. Therefore errors of measurements are negligible in comparison with those of processes in spherical harmonic analyses of the fields. If we could make clear the limit of errors concerning to the analyses of the fields, we are able to presume the smallest numbers of measuring points on the sphere and their suitable distributions without preceding the performance of any measurements.

2. Magnetic dipole models

Assuming that the spherical surfaces which have a radius are covered with the charge density $f(\theta, \varphi)$. This is expanded by the spherical harmonics $Y_n(\theta, \varphi)$, and the magnetic potential $\Psi(P)$ of free space, outside of the sphere is expressed by the orthogonal system (Smirnov, 1959).

$$\Psi(P) = a \sum_{n=0}^{\infty} \frac{Y_n(\theta, \varphi)}{2n+1} \left(\frac{a}{r}\right)^{n+1} \quad (r > a) \quad (1)$$

$$f(\theta, \varphi) = \sum_{n=0}^{\infty} Y_n(\theta, \varphi) \quad (2)$$

$$Y_n(\theta, \varphi) = \sum_{m=0}^n P_n^m(\cos \theta) (A_n^m \cos m\varphi + B_n^m \sin m\varphi) \quad (3)$$

$$\begin{pmatrix} A_n^m \\ B_n^m \end{pmatrix} = \frac{2n+1}{2\pi \epsilon_m} \frac{(n-m)!}{(n+m)!} \int_0^{2\pi} \int_0^\pi f(\theta, \varphi) \begin{pmatrix} \cos m\varphi \\ \sin m\varphi \end{pmatrix} P_n^m(\cos \theta) \sin \theta \, d\theta \, d\varphi \quad (4)$$

$$\epsilon_m = \begin{cases} 2 & (m=0) \\ 1 & (m=1, 2, \dots) \end{cases}$$

That is, when the magnetic charge density on the sphere is equivalent to the field produced by the magnetic source of dipole put at the center of the sphere, it is developed into spherical harmonic functions. The magnetic dipole moment of which direction is (θ_0, φ_0) and the moment is M_1 , will be expressed simply by their coefficients.

$$\tan \theta_0 = \sqrt{(A_1')^2 + (B_1')^2} / A_1' \quad (5)$$

$$\tan \varphi_0 = B_1' / A_1' \quad (6)$$

$$M_1 = a^3 \sum Y_1(\theta_0, \varphi_0) \quad (7)$$

On the contrary, if we choose optional numbers as the radius a and coefficients A_1, A_1', B_1' of magnetic dipole component respectively, we can establish the magnetic dipole models at the center of sphere. Then the vertical magnetic fields on the sphere are selected as data of NRM of specimens.

$$H_r = -\left(\frac{\partial \mathcal{F}}{\partial r}\right)_{r=a} = 2/3 \cdot \gamma_1(\theta, \varphi) \quad (8)$$

3. Errors derived from numerical integration around the spherical surface

Concretely, as data have been given in the form of dispersional density, we have to integrate numerically to expand H_r to spherical harmonic functions. When $f(\theta, \varphi) = H_r$, coefficients of spherical functions corresponding to the dipole are

$$\begin{pmatrix} A_1 \\ A_1' \\ B_1' \end{pmatrix} = \frac{3}{4\pi} \int_0^\pi \int_0^{2\pi} f(\theta, \varphi) \begin{pmatrix} \cos \theta \\ \sin \theta \cdot \cos \varphi \\ \sin \theta \cdot \sin \varphi \end{pmatrix} \sin \theta \cdot d\varphi d\theta \quad (9)$$

To execute this double integration, two steps are adopted for a numerical one by a trapezoidal formula. In first step, Fourier coefficients are deduced from the integration according to φ fixing θ . In second, these coefficients are integrated according to θ by Legendre functions (Takeuchi, 1972). The partitioning along the great circles and the small circles are M and N respectively. Incidentally, the numbers of measuring points are $[M(N-1)+2]$.

$$\begin{pmatrix} Q^*(\theta_i) \\ Q^*(\theta_j) \\ b^*(\theta_j) \end{pmatrix} = \frac{2}{M} \sum_{k=1}^M \begin{pmatrix} f(\varphi_k) \\ f(\varphi_k) \cdot \cos \varphi_k \\ f(\varphi_k) \cdot \sin \varphi_k \end{pmatrix} \quad (10)$$

$$\begin{pmatrix} A_1 \\ A_1' \\ E_1 \end{pmatrix} = \frac{3\pi}{4N} \sum_{j=1}^N \begin{pmatrix} Q^*(\theta_j) \cos \theta_j \cdot \sin \theta_j \\ Q^*(\theta_j) \sin^2 \theta_j \\ b^*(\theta_j) \sin^2 \theta_j \end{pmatrix} \quad (11)$$

If the direction and moment of the original dipole model are (θ_1, φ_1) and M_1 , and those of the dipole model reconstructed by the magnetic field analyses are (θ_1', φ_1') and M_1' respectively, then the errors of latter against the former are

$$\cos \delta = \cos \theta_1 \cos \theta_1' + \sin \theta_1 \sin \theta_1' \cos (\varphi_1 - \varphi_1') \quad (12)$$

$$\Delta M = \frac{|M_1 - M_1'|}{M_1} \times 100 \quad (\%) \quad (13)$$

The causes of errors in field analyses from magnetic dipole model result mainly from the numbers of measuring points. Because, as for the simple magnetic dipole model, the errors caused by irregular distribution of the points on a sphere will be strained small compared with those caused by the number of measuring points. Concerning to some magnetic dipole models, we show the influences to the numbers of points affecting the errors of analyses in fig.1 and fig.2.

4. Discussion

We could make clear the influences of errors caused by measuring point numbers as a result of the magnetic dipole field analyses. As the numbers of points are increased, the errors of direction and moment of the dipole are decreased. Particularly, the error of direction is decreased more smoothly than that of moment. As the results of these analyses, we

are able to presume the number of measuring points and their suitable distributions on a sphere.

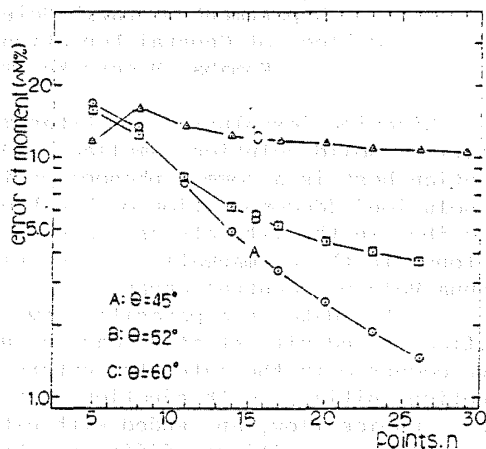
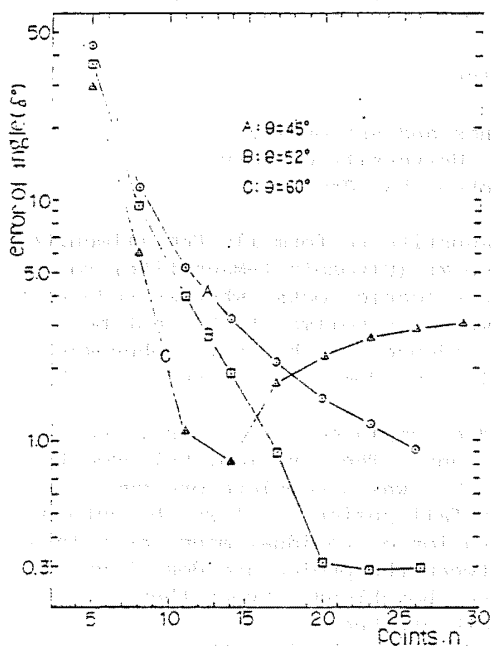


Fig. 2. Error of magnetic dipole moment M relation to the measuring points on a sphere.

Fig. 1. Relations in measuring points on a sphere to the error of angle δ° between the true dipole direction and that from numerical analyses.

There are some kinds of papers (Matuyama, 1930) using spherical harmonic functions to analyze NRM of the specimen. But this method of analysis holds both of a merit and a demerit. Magnetic potential is expanded from lower harmonics to higher ones, and then the complicated magnetization is converted into the magnetic dipole and other multipoles independently. So that, data collected under the earth field don't affect the dipole components. On the other hand, as has been showing in fig. 1 and 2, the numbers of measuring points are needed some times as large as that of coefficients of functions to reach the stable precision.

If the earth field is cut off perfectly, magnetic analysis of NRM using vector components of orthogonal system is more convenient and excellent than that of spherical harmonic functional system. We should choose the most efficient method of magnetic analysis according to the purpose of experiments and to the device restrictions.

References

- Matuyama, M. (1930) Collected papers on earth sciences dedicated to Dr. T. Ogawa on the occasion of his sixtieth birthday, Part 2, 205-220, (in Japanese).
- Smirnov, N. V. (1959) Senior Mathematical Course (Kyoritsu, Tokyo) (in Japanese) P. 463.
- Takeuchi, H. (1972) Some Problems on Earth Sciences (Shokabo, Tokyo) (in Japanese) P5.

REDUCTION DECOMPOSITION OF HEMOILMENITE IN A COOLING MAGMA
AND
ITS RELATION TO THE CHANGES OF MAGNETIZATION OF ROCKS

Osamu OSHIMA

Department of Earth Science and Astronomy,
College of General Education, University of Tokyo,
Komaba, Meguro-ku, Tokyo 153, Japan

Oxidation "exsolution" of titanomagnetite to form Ilm-Hem (Ilmenite-Hematite) solid solution lamellae in Usp-Mt (Ulvospinel-Magnetite) solid solution host is a common phenomenon in volcanic rocks, whereas reduction "exsolution" (decomposition or breakdown) of hemoilmenite has not been described in the literatures. A good evidence for the latter phenomenon is found in the co-magmatic dacite pumice and dome lava of Futatsu-dake, Haruna Volcano, Central Japan.

Futatsu-dake is a parasitic lava dome emplaced on the dissected edifice of andesite stratovolcano of Haruna. The eruption, believed to have occurred in the late 6th century A.D., was a complete one-cycle eruption initiated with ejection of air-fall pumice, followed by outpouring of pumice flow, and ended with extrusion of residual magma as a lava dome. The compositional difference between the pumice and dome lava is very small. Phenocrysts are plagioclase, hornblende, hypersthene, titanomagnetite, and hemoilmenite in both of them.

The hemoilmenite phenocryst is by far less abundant than titanomagnetite phenocryst. It is a euhedral crystal with hexagonal tabular form up to 1mm across, and has no significant compositional zoning in the pumice. Similar hexagonal phenocryst is found in the dome lava; however, it consists of parallel lamellae of titanomagnetite and ilmenite (Fig. 1). The lamellae are nearly parallel to the (0001) basal

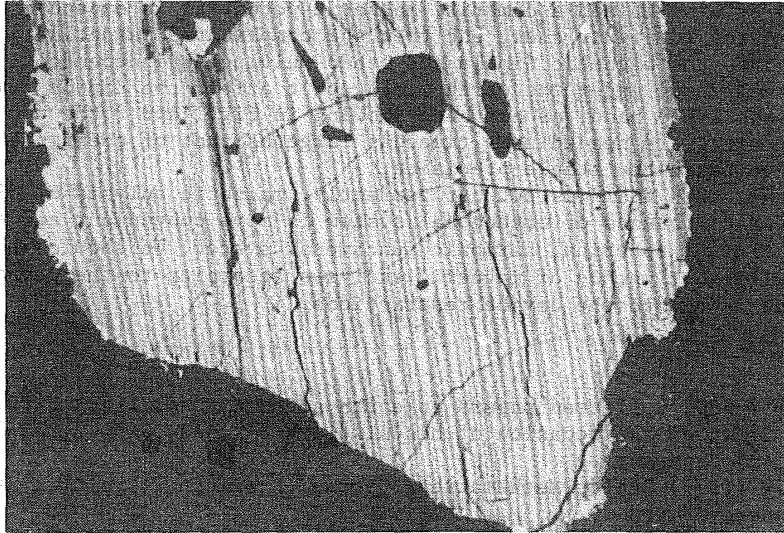


Fig. 1 Backscattered electron image of a reduced (decomposed) hemoilmenite phenocryst in the dome lava, showing lamellae of ilmenite (dark streaks) and titanomagnetite (light streaks).

Table 1. Microprobe analyses of hemoilmenite phenocryst in pumice, and lamellae of decomposed hemoilmenite phenocryst in dome lava.

No.	1	2	3	4
SiO ₂	0.03	---	---	---
TiO ₂	30.16	46.75	17.00	30.75
Al ₂ O ₃	0.44	0.09	0.74	0.45
V ₂ O ₃	0.46	0.40	0.51	0.46
Cr ₂ O ₃	0.04	---	---	---
FeO*	63.06	49.50	76.25	62.88
MnO	0.29	0.71	0.61	0.65
MgO	1.25	1.97	1.06	1.47
CaO	0.00	---	---	---
Sum	95.73	99.42	96.17	96.66
Fe ₂ O ₃	42.70	12.99	35.13	41.77
FeO	24.63	37.81	44.64	25.29
Total	100.01	100.72	99.69	100.84
Mol.% "Usp"			48.0	
Mol.% "R ₂ O ₃ "	42.1	12.7		42.5

- No.1 : Discrete hemoilmenite phenocryst in the pumice (average of 5 analyses).
 No.2 : Ilmenite lamellae of decomposed phenocryst in the dome lava (average of 4 analyses).
 No.3 : Titanomagnetite lamellae of decomposed phenocryst in the dome lava (average of 4 analyses).
 No.4 : Bulk composition of decomposed phenocryst in the dome lava (average of 4 analyses).

* The amounts of Fe₂O₃ and FeO were calculated from FeO* (total Fe as FeO) assuming that the compositions of cubic and rhombohedral phases are on the RO₂·2RO-R₂O₃·RO (metal(R):oxygen(O)=3:4) join and RO₂·RO-R₂O₃ (R:O=2:3) join, respectively. This procedure of calculation is basically the same as that of Carmichael(1967)'s.

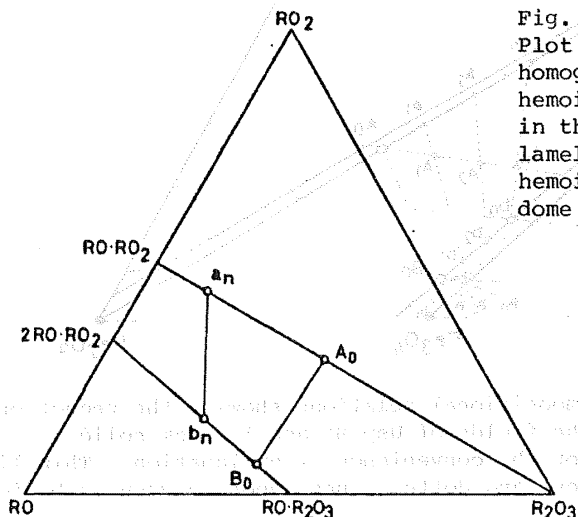


Fig. 2 Plot of chemical compositions of homogeneous phenocrysts of hemoilmenite and titanomagnetite in the pumice (A₀, B₀) and lamellae of decomposed hemoilmenite phenocrysts in the dome lava (a_n, b_n).

plane of the hexagonal tabular crystal form. The chemical compositions of homogenous phenocrysts in the pumice and phenocrysts with two-phase lamellae in the dome lava are given in Table 1. The bulk composition of the latter phenocryst, estimated by the compositions and ratio (~1:1) of the lamellae, is close to that of the former phenocryst.

It is most probable that the two-phase phenocryst was originally a single phase hemoilmenite similar to that found in the pumice, and "exsolution" or decomposition would have occurred after the eruption of pumice in the dome lava which must have cooled slowly.

The compositional relation between the single-phase phenocryst in the pumice and the two-phase phenocryst with titanomagnetite and ilmenite lamellae in the dome lava (Fig. 2), clearly indicates that the "exsolution" occurred due to reduction of the single-phase phenocryst. This "exsolution" is not a real exsolution but is a decomposition due to reduction, and may be called "reduction decomposition".

The process of this "reduction decomposition" of hemoilmenite is illustrated schematically in Fig. 3. The compositions of hemoilmenite and titanomagnetite phenocrysts which were crystallizing in a cotectic relation before eruption were at A_0 and B_0 respectively. Upon eruption, these compositions were frozen in the pumice. After the eruption of pumice, the residual magma was reduced. (Reduction of the residual magma might have occurred due to the loss of volatiles upon pumice eruption. If so, reduction might be a common phenomenon associated with eruption.) The bulk composition of hemoilmenite shifted from A_0 toward more reduced compositions (e.g., A_1 and A_2) along the oxidation-reduction line. At the same time "reduction decomposition" occurred to form the two phase

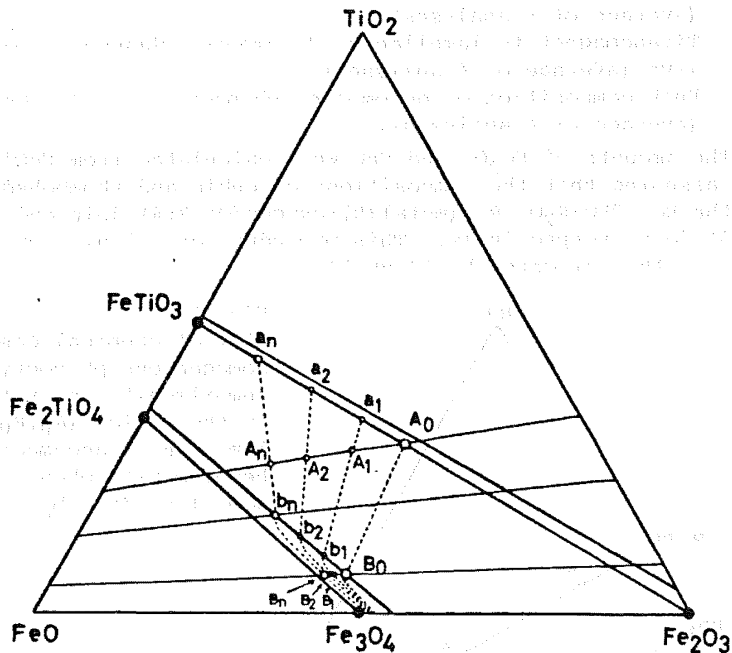


Fig. 3 Schematic compositional relations showing the reduction process of hemoilmenite. The fields of Usp-Mt and Ilm-Hem solid solutions are exaggerated for the convenience of explanation. Thin lines are oxidation-reduction lines, and dotted lines denote oxygen isobaric lines.

lamellae, whose compositions shifted from A_0 to a_1, a_2, \dots , and from B_0 to b_1, b_2, \dots , respectively, with changes of oxygen fugacities and temperatures during cooling. When the bulk composition shifted to A_n , the reduction stopped and the lamellae consisted of ilmenite a_n and titanomagnetite b_n .

The composition of titanomagnetite phenocryst, which was crystallizing with hemoilmenite before the pumice eruption was at B_0 . After the pumice eruption, the composition of titanomagnetite phenocryst shifted from B_0 to more reduced compositions (e.g., B_1, B_2 , and B_n), along the oxidation-reduction line within the field of Usp-Mt solid solution. Thus, titanomagnetite remained stable and continued further to crystallize in the dome lava with the compositional variation as described in Oshima (1971).

Hemoilmenite phenocryst (about $Ilm_{58}Hem_{42}$) in Futatsu-dake pumice is well known for the self-reversal magnetization (Nagata et al., 1952). Yokoyama (1953) found a magnetic anomaly in the eastern area of Haruna where the Futatsu-dake pumice covered, but not in the Futatsu-dake lava dome. This difference is well explained by the fact that hemoilmenite phenocryst is stable in the pumice whereas it is decomposed in the dome lava.

References

- Carmichael, I.S.E. (1967) *Contr. Mineral. and Petrol.*, **14**, 36.
Nagata et al. (1952) *Jour. Geomag. Geoelectr.*, **4**, 22.
Oshima, O. (1971) *Mineral. Jour.*, **6**, 249.
Yokoyama, I. (1953) *Bull. Earthq. Res. Inst.*, **31**, 33.

(To be submitted to Nature)

Reconnaissance Paleomagnetic and Rock Magnetic Investigation
of Basaltic Rocks from Ponape Island, East Carolines

Kazuo KOBAYASHI, Toshio FURUTA and Teruaki ISHII
Ocean Research Institute, University of Tokyo

Abstract

Paleomagnetic measurement of volcanic rocks collected from Ponape Island in the Caroline chain has revealed that both the normal and reversed polarities occur in the island, although direction of the natural remanent magnetization is roughly parallel to that of the present field. Thermomagnetic analyses have indicated that titanomagnetite contained in these rocks is oxidized at low-temperature, particularly highly in fine-grained basalts.

1. Introduction

A chain of the Caroline islands and seamounts including islands of Truk, Ponape and Kusaie in the equatorial western Pacific Ocean (Fig. 1) is supposed to be a trace of a hot spot at which a fixed mantle plume holds an upper outlet through the moving Pacific floor. Keating et al (1981) reported that the K-Ar ages of volcanic rocks from Kusaie and Truk Islands are 4 and 12 MaBP, respectively. They showed that trend of the Caroline Islands is parallel with the 1 to 14 Ma old segment of the Hawaiian ridge.

During a port of call at Ponape island (August 23-27, 1980) in the research cruise KH80-3 of the R.V. Hakuho-maru of Ocean Research Institute, University of Tokyo we collected 12 oriented rock samples at 3 sites for paleomagnetic purpose and more than 50 unoriented rocks at about 10 sites for petrographic investigation. In this paper the results of paleomagnetic and rock magnetic measurement are described.

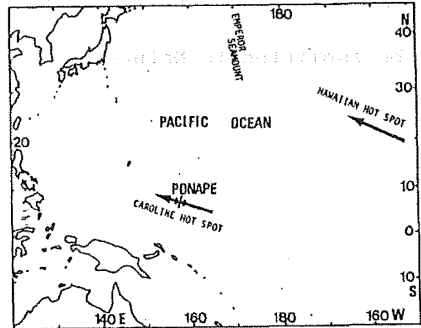


Fig.1 Hawaiian and Caroline Chains

2. Paleomagnetic Measurement

Paleomagnetic samples were collected at 3 sites; 2 in the northern part and 1 in the eastern part of the Ponape Island (Fig. 2). Hand-samples were oriented by a field compass with a level. Direction and intensity of the natural remanent magnetization were measured with cylinders with 2.54cm in diameter and height cut from these hand samples. Magnetic susceptibility k of these samples was also measured in a weak field of 1 oersted. Results of these measurements are summarized in Table 1. As the total force of the present geomagnetic field at Ponape is 0.35 oersted, the Königsberger ratio $Q_n = J_n / 0.35k$ is calculated and shown in Table 1. Q_n is generally larger than unity except for one sample from Japtik Island (2501-2).

Stability of natural remanent magnetization was tested by alternating field demagnetization (Fig. 3(a)-(c)). Median destructive field (MDF) amounts to 44~340 oersted.

Directions of natural remanent magnetization are well concentrated within sites 2502 (Param Island) and 2504 (water fall), while those at site 2501 (Japtik Island) are quite scattered (Fig. 4). The averaged direction of Param Island ($D=3^\circ$, $I=12^\circ$) is nearly concordant to that of the present field ($D=7^\circ$, $I=8^\circ$). In contrast the averaged direction of the water-fall site ($D=194^\circ$, $I=-13^\circ$) is reversed to that of the present.

Although the K-Ar ages of rocks in Ponape Island have not been determined, geographical position of the Ponape island between Truk and Kusaie Islands implies that the age of Ponape Island is around 8 MaBP, so long as velocity of the Pacific plate motion is constant. According to LaBreque et al (1977) the polarity of the earth's magnetic field at a period around 8 MaBP was alternating with cycles shorter than 0.2 Ma. It is, therefore, likely that both the normal and reversed polarities of magnetization coexist in one island, since a period of active volcanism in an island seems to exceed 0.5 Ma, as shown in the Hawaiian volcanoes.

Deviation of the paleomagnetic directions from that of the present field seems to be insignificant, as circles of 95% confidence are about 7° with both Param Island and wall-fall sites. As the effect of non-dipole field is particularly large in the equatorial region at which intensity of the dipole component is smaller than at high latitudes, change in latitude due to the plate motion may not be detectable.

Scatter in direction of natural remanent magnetization at Japtik Island may probably be due to secondary rotation of small blocks of rocks.

3. Rock-magnetic Properties

Thermomagnetic curves were measured by an automatic magnetic torque balance in a field of 4300 oe in vacuum of 10^{-5} torr (Fig. 5). The initial Curie temperature, T_{c1} of Param Island dolerite and water-fall basalt is 160°C and 200°C , indicating that titanomagnetite contained in these rocks are Ti-rich (the x value in $x\text{FeTi}_2\text{O}_3 \cdot (1-x)\text{Fe}_3\text{O}_4$ exceeds 0.6). Thermomagnetic curves of these samples are irreversible and the after-heating Curie temperature T_{ch} is 525°C and 530°C . Such an irreversible thermal behavior is owing to oxidation of titanomagnetite at a low temperature. The higher initial Curie temperature (200°C) with water-fall basalt than that (160°C) with Param Island dolerite may be caused by higher degree of oxidation in fine-grained basalt than in coarse dolerite.

Japtik Island rock has the initial and after-heating Curie temperatures of 420°C and 525°C , respectively. These values seem to imply that titanomagnetite contained in this sample is poorer in Ti than that in the other two samples.

These rock-magnetic properties show that these rocks are good for paleomagnetic tools so far as their magnetic constituents are concerned. Scattered directions of NRM in Japtik Island basalts may be due to a tectonic disturbance.

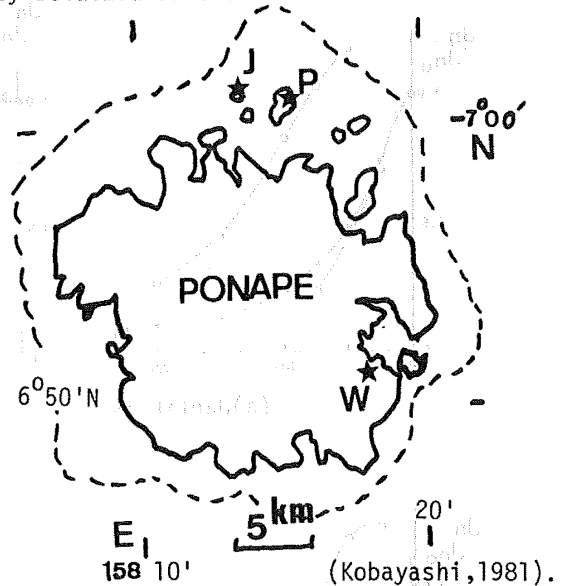
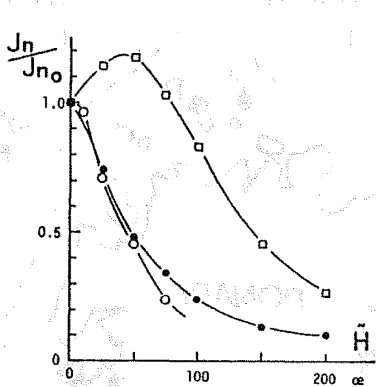


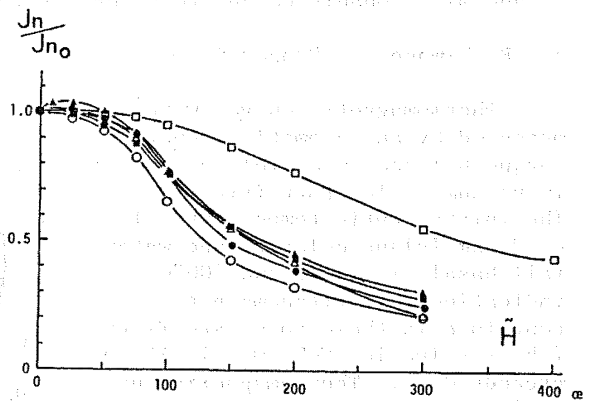
Fig.2 Sampling Sites in Ponape Island

Table Summary of Paleomagnetic and Rock-magnetic Properties of Ponape Rocks

Sampling Site	Petrography	J_n emu/gr $\times 10^{-3}$	NRM D	NRM I	α (95%)	MDF (\AA)	k emu/cc $\times 10^{-3}$	Q_n	J_s emu/gr	T_c ($^{\circ}\text{C}$)	T_{c2}	T_{ch}
2501 Japtik Island	Alkali- olivine Basalt	0.7	93 $^{\circ}$	7 $^{\circ}$		44	81.1	0.7	2.25	420	525	525
		8.5	259	42		140	16.5	43				
		1.1	175	16		48	24.5	4				
		3.4	scattered		74.8							
2502 Param Island	Alkali- olivine Dolerite	6.5	11	17		160	3.2	168				
		8.3	6	14		130	4.3	160				
		8.2	-5	10		170	5.5	124	0.36	160	530	530
		8.4	-1	4		140	5.0	139				
		7.8	-4	16		170	5.4	120				
		7.2	11	9		340	5.4	110				
		7.7	3	12 $^{\circ}$	6.8							
2504 Water- fall (SE Ponape)	Alkali- olivine Basalt	1.4	197	-10		45	30.7	4				
		0.4	198	-12		100	34.4	1				
		0.5	186	-15		100	17.4	2	0.66	200	-	425
		0.8	194	-12	6.8							



(a) Japtik Is.



(b) Param Is.

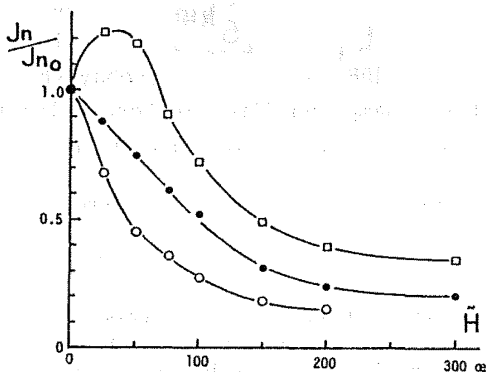


Fig.3 A.f. demagnetization of NRM

left (c) Water-fall

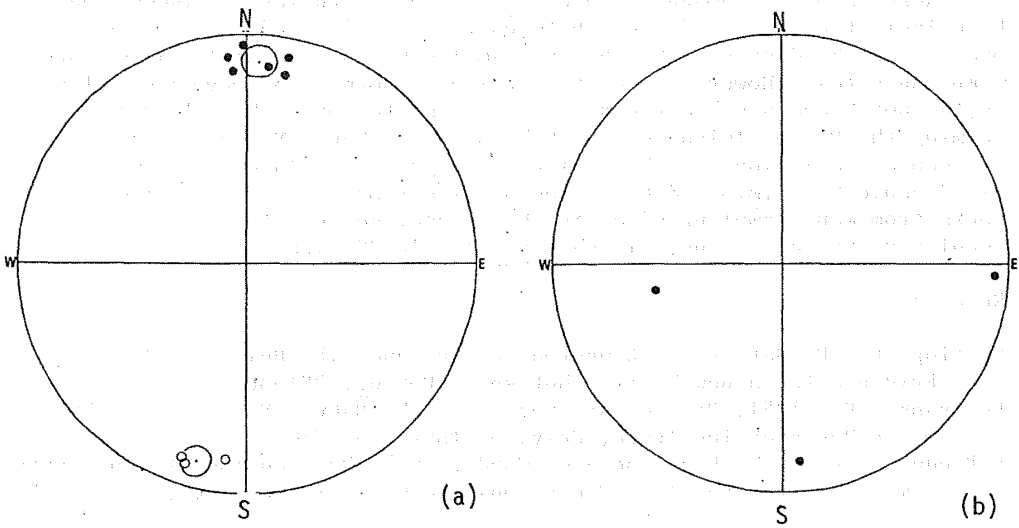


Fig.4 Directions of NRM projected on the Schmidt equal-area projection net with oval of confidence

- (a)Param Is.(normal) and Water-fall site(reverse)
- (b)Japtik Is. site (scattered)

Solid and hollow circles denote down and up dip, respectively.

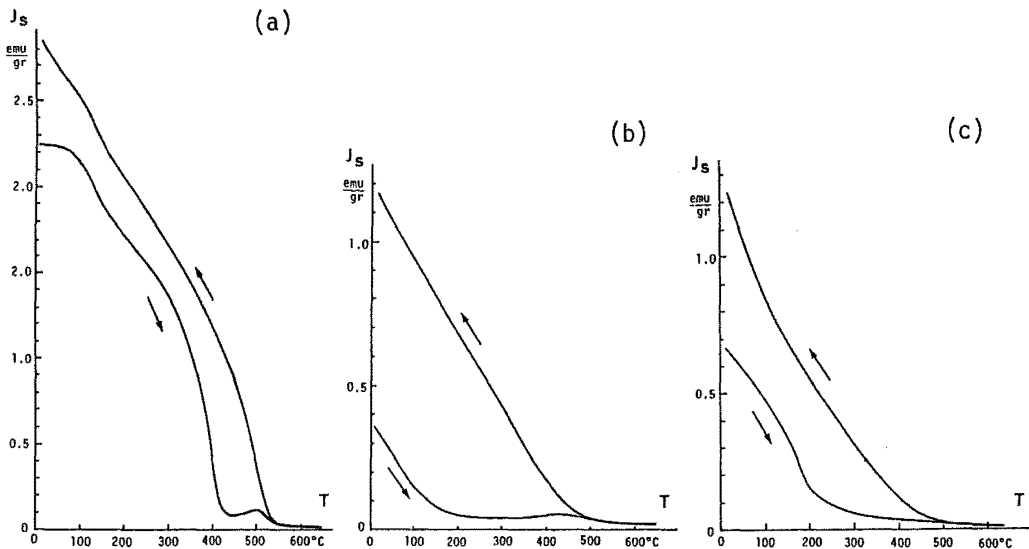


Fig.5 Thermomagnetic curves of Ponape rocks

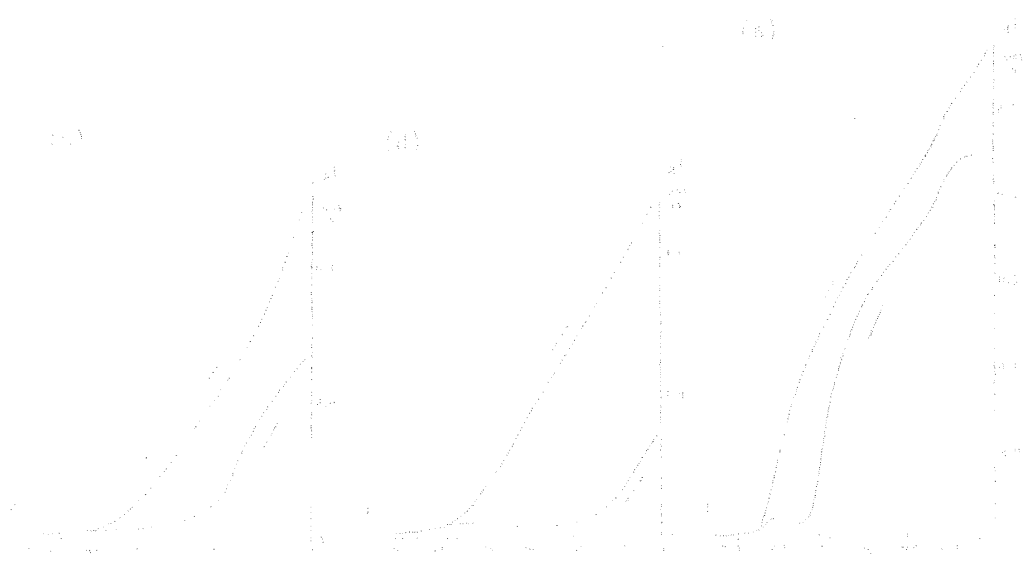
- (a) Japtik Is. (b) Param Is.(c) Water-fall site

4. Discussion

Results of paleomagnetic and rock-magnetic studies of Ponape rocks have indicated that difference between the paleolatitude and the present one can not be distinguished by our samples because of small number of sampling sites. However, occurrence of both normal and reversed polarities in the north and southeast coast sites seems to imply that the time span forming the Ponape Island was probably longer than 1 Ma and so the effect of secular variations of the ancient geomagnetic field due to non-dipole field could be eliminated by averaging directions of greater number of rocks from many sampling sites in the island, because the period of secular variations is usually shorter than 10,000 years.

References

- Keating, B., D. Matthey, J. Naughton, D. Epp and C.E. Helsley, 1981, Evidence for a new Pacific hot spot, *EOS* 62, 381-382.
Kobayashi, K., 1981, Preliminary report of the Hakuho Maru cruise KH80-3, Ocean Research Institute, Univ. of Tokyo, pp.210.
LaBreque, J.L., D.V. Kent and S.C. Cande, 1977, Revised magnetic polarity time scale for the late Cretaceous and Cenozoic, *Geology*, 5, 330-335.



K-Ar AGE DETERMINATION OF THE LATE TERTIARY AND QUATERNARY ANDEAN VOLCANIC ROCKS, SOUTHERN PERU

Ichiro KANEOKA

Geophysical Institute, University of Tokyo
Bunkyo-ku, Tokyo 113, Japan

Introduction

In order to clarify the geochemical and petrographical characteristics of the Andean volcanic rocks, it is essential to examine the rocks of the same period. In this context, it is indispensable to know the age of volcanic activity.

Concerning the period of volcanic activity in the Andean volcanic zone, some investigators have studied it by radiometric dating (e.g., Bellon and Lefèvre, 1976; Weibel et al., 1978). Drake (1976) have revealed that there are systematic differences in the period of volcanic activity along the latitudes as shown in Fig. 1. Furthermore, Baker and Francis (1978) summarized the data on the dating results of volcanic rocks from the central Andes by comparing them to those of samples from the central Oregon and assigned the main volcanic activities to around 20-25 Ma, 10 Ma and 5 Ma ago. Noble et al. (1974) demonstrated a possibility of the correlation between the Andean volcanic and tectonic activities since Tertiary. Although they determined only seven samples by themselves, they also identified the relatively intense volcanic activity in the southern Peru area about 12 Ma ago together with that of about 40-50 Ma ago based on the compilation of the radiometric age data. Although Stewart et al. (1974) reported more than 60 K-Ar ages on the Andean igneous rocks from Peru, which ranged from 27 to 679 Ma, those rocks were mostly plutonic and metamorphic rocks. Hence, we cannot use the data to infer the Andean volcanic activity directly.

On the other hand, Baker (1977) pointed out a possible migration of volcanic activity in the central Andes from west to east and Farrar et al. (1970) also identified a similar migration for the age of igneous rocks. However, such tendency has been revealed to be a reverse trend for recent volcanic activity (Thorpe and Francis, 1979). In effect, the youngest volcanic activity occurs along the western edge of the Cordillera Occidental. Furthermore, Schwab and Lippolt (1976) reported that the andesitic volcanic activity became remarkable about 10 Ma ago. In the southern Peru area, the activity of ignimbrite were identified to have occurred about 25 Ma ago (Tosdal et al., 1979).

As shown above, most dated rocks were of Tertiary in age. However, some radiometric age data have revealed that even the volcanic rocks which were assumed to be of Quaternary show the age of Tertiary (e.g., Bellon and Lefèvre, 1976). This demonstrates an example for the importance of radiometric dating. In the present study, K-Ar age determinations were made for 30 volcanic rocks, which were collected during the summer of 1980 by the scientific team on "Geochemical Investigation of the Central Andes Volcanic Zone" (Leader : Naoki ONUMA) sponsored by the Ministry of Education under contract No. 504112. These rocks have been regarded to belong to the Barroso Group of Quaternary in southern Peru. The main objectives in this study are to examine the lateral variations of young volcanic activity in southern Peru and to check the stratigraphically assigned ages based on the K-Ar dating.

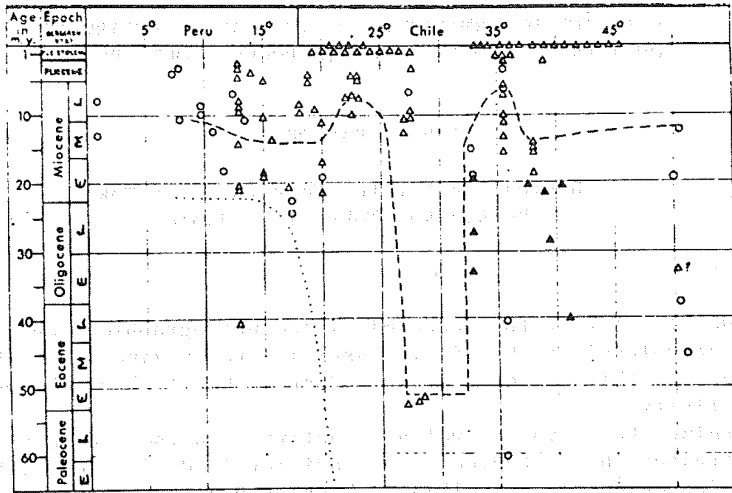


Fig. 1. Cenozoic igneous and tectonic events plotted against latitude in the central and southern Andes. \circ , intrusive event; Δ , volcanic event. Solid triangles indicate locations west of the present Cordillera. Dotted line shows approximate limit of last marine transgression. Dashed line separates deformed and undeformed volcanic strata. (After Drake, 1976)

STAGE		FORMATION	
CENOZOIC	QUATERNARY	RECENT	Alluvial deposits Pyroclastic deposits
		PLEISTOCENE	Morrains and fluvial glaciers Mud flows
	<u>BARROSO GROUP</u>		
	Conglomerates		
	TERTIARY	UPPER	<u>SENCCA GROUP</u>
			Millo Formation
		MIDDLE	<u>TACAZA GROUP</u>
		LOWER	Sotillo Formation Huanca Formation

VOLCANIC

Fig. 2. Schematic stratigraphic sequence in southern Peru, central Andes. The underlined groups indicate those composed of volcanic materials.

Stratigraphy and samples

In southern Peru, geological periods are classified as shown in Fig. 2, where Barroso Group, Sencca Group and Tacaza Group are belonging to the volcanic series since Tertiary. Among them, only Barroso Group is regarded to be of Quaternary. Although pyroclastic deposits are found in recent years, there are not so many examples to show the extruded volcanic rocks.

As recent volcanic activities in this area, there are several examples. For example, Ubinus volcano, located to the east of Arequipa, is showing fumes or smokes since 1974 and recorded a great eruption in 1622. Huainaputina volcano also has a record of great eruption around 1600 (Weibel et al., 1978).

In the present study, most samples used for K-Ar dating are regarded to belong to the Barroso Group except for one sample (A-166) which is regarded to belong to the Sencca Group. Hence they were expected to show the ages of less than 2 Ma in most cases. However, their appearances of the exposure state were so different for each sample and we had no guarantee that they were surely extruded less than 2 Ma ago. Hence in the present study, we have selected samples in order to cover the wide area in southern Peru as much as possible. Samples were selected by the following criteria.

- (1) The sample should be fresh as much as possible, showing no effects of secondary alteration or oxidation.
- (2) Such a sample as contains large phenocrysts of more than a few mm in size should be discarded to prevent from the possible effect of excess ^{40}Ar .
- (3) The sample should be sufficiently large so that the fresh part in the interior of the sample might be used for K-Ar dating.

The criterion (3) is required to remove the dirty surfaces in order to exclude the secondary effects. The criterion (1) is the most important requisite in the K-Ar dating and the examination of a sample should be done carefully under macro- and microscopic observations.

In Andean samples, most of which are andesites and dacites, large phenocrysts of plagioclase or biotite with the size of more than a few mm are often observed. Since large phenocrysts are considered to have been formed in a magma reservoir, they are expected to contain the ambient gases in them, resulting in keeping some amount of excess ^{40}Ar . For example, such noble gas components have been identified in large olivine and clinopyroxene phenocrysts (e.g., Kaneoka and Takaoka, 1980). Even plagioclase phenocrysts show the occurrence of excess ^{40}Ar in some cases (e.g., Damon et al., 1967). Hence, it is very important to exclude such phases from samples for K-Ar dating. However it is not easy to separate them completely to exclude the fine fragments. In this study, only those which do not contain large phenocrysts of more than a few mm in size are used for K-Ar dating.

Experimental

From the interior of each block sample, we cut the fresh part in the form of rectangular with about 10 mm in size. Among such rectangular samples, we selected a few pieces of about 2-3 g for Ar analysis and the remains were powdered for K-analysis.

K was analysed with a flame photometer by using Li as an internal standard. Ar was analysed on a Reynolds type mass spectrometer with a radius of 15 cm. ^{38}Ar was used as a tracer for isotope dilution method. K contents for some samples were analysed by the X-ray fluorescence method.

K-Ar ages were calculated by using the constants recommended by Steiger and Jäger (1977). K-analysis includes the uncertainty of 1-1.5%

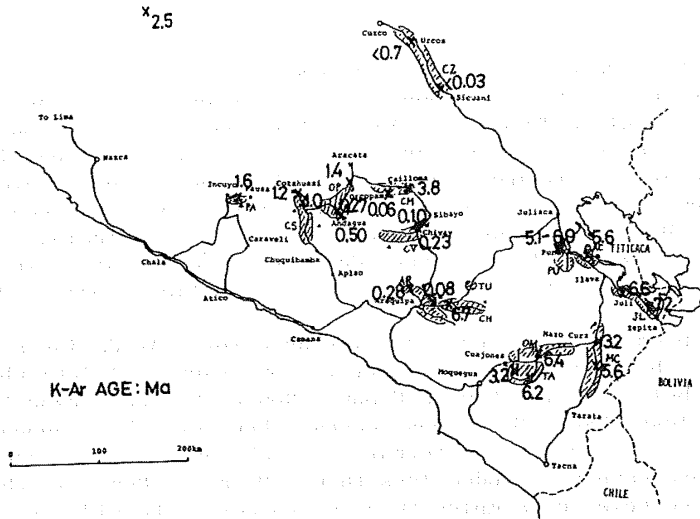


Fig. 3. The results of K-Ar ages determined in the present study. Note that relatively young ages of less than 1 Ma are found for rocks collected from the northwestern part including the vicinity of Arequipa, whereas the samples collected from the southeastern part show the ages of late Tertiary in most cases. Except for one sample from Ayachucho area, these rocks were thought to belong to the Barroso Group.

and Ar-analysis includes those of about 0.5% and 0.2 - 0.3% for $^{40}\text{Ar}/^{36}\text{Ar}$ and $^{40}\text{Ar}/^{38}\text{Ar}$ ratios, respectively. The uncertainty in ages is calculated based on these uncertainties together with the degree of atmospheric contamination.

Results and discussion

The results of K-Ar ages of samples and sampling localities are shown in Fig. 3.

For each sampling area, only samples which fullfill the criteria were selected. Hence, it does not always mean that we have selected typical samples from the area. Even in this case, however, we can at least say that the results shown in Fig. 3 probably reflect some tendency concerning their eruption ages, because they were selected on the basis of common criteria for each area.

In the present study, one of the most conspicuous results is that more than half of samples show the ages of more than 2 Ma, though they were collected as samples of the Barroso Group of Quaternary. Some samples show the ages of more than 5 Ma, which are regarded to be of late Miocene. This results suggest that the ages of the volcanic rocks which are reported to belong to the Barroso Group are not always less than 2 Ma. In effect, Bellon and Lefèvre (1976) also reported two examples in which samples of the Barroso Group show the K-Ar ages of more than 4 Ma. Weibel et al. (1978) reported a K-Ar age of 5.3 Ma for a volcanic rock of probably Barroso Group which was collected at the foot of Coropuna volcano. This case is also raised as an example that the rocks of the Barroso Group do not always show

the ages of Quaternary. Hence, we must be very careful to use the stratigraphically assigned age to infer the eruption age of a sample.

So long as present dated samples are concerned, we have observed some regional difference in the apparent volcanic activity. As shown in Fig. 3, the samples collected from the northwestern part of Arequipa, located in the area around 15 - 17.5°S, 71.5 - 73°W, show the K-Ar ages of less than 1 - 2 Ma, whereas those collected from the eastern part of Arequipa such as the Puno, Juli and Mazo Cruz area show the K-Ar ages of late Tertiary. We have selected samples from each area based on the criteria as mentioned before and have not adopted any other preference. Hence there is a possibility that the main volcanic activity in the southeastern part of southern Peru was older compared with that in the northwestern part such as the Andagua and Arequipa areas. As an example for relatively young age in the southeastern part, a biotite sample in andesite collected from the northwestern foot of Tutupaca volcano is reported to show a K-Ar age of about 0.7 Ma (Tosdal et al., 1979). The sample is located in the Tarata area (TA) in Fig. 3. In the present study, we discarded such samples as included large phenocrysts. One may argue that young samples in the southeastern part in this region might have been systematically dismissed during the procedure. However, we have no reason to believe that relatively young volcanic rocks contain large phenocrysts systematically.

In the present surveyed area, the youngest volcanic activity occurs along the northwestern edge of the Cordillera Occidental. Present results suggest that even in the CZ area which is located at rather inner continental area there occurred very young volcanic activity as shown by the data CZ-02-02 and CZ-04. Although the apparent volcanic activity occurred at similar ages for the northwestern edge of the Cordillera Occidental and the CZ area, the depth of the subducted lithosphere is different between them, which may reflect to the mode of volcanism.

In the northwestern outsuburbs of the Puno area, there are some hills which are composed of shoshonitic rocks. Although they are also believed to belong to the Barroso Group, K-Ar dating results show the ages of about 6 Ma. All samples were collected from different hills and the sample PU-03 shows a little younger ages. However, there is no reason to assume that the hill alone erupted about 0.8 Ma later than the other hills. Since all the other five samples show similar ages of 5.9 ± 0.1 Ma, it is more likely that the shoshonitic rocks were erupted rather in short period. Bellon and Lefèvre (1976) also reported a K-Ar age of 5.7 ± 0.3 Ma for one sample in the Puno area.

Furthermore, an andesite collected at the northwestern part of the lake Titicaca (AC-03) shows an age of about 5.6 Ma and those collected at the southern part of the lake Titicaca indicate the ages of about 7 Ma. Hence, it may be unreasonable to classify them in the Barroso Group.

These results strongly suggest that the stratigraphically assigned ages are not sufficient enough to infer the period of volcanic activity in the central Andes, southern Peru, and their ages should be carefully controlled by radiometric ages.

References

- Baker, M.C.W. (1977) *Geol. Rundsch.*, 66, 455.
Baker, M.C.W. and P. Francis (1978) *Earth Planet. Sci. Lett.*, 41, 175.
Bellon, H. and C. Lefèvre (1976) *C.R. Acad. Sci.*, 283, ser D, 1.
Damon, P.E., A.W. Laughlin and J.K. Percious (1967) *Int. Atomic Energy Agency*, Vienna, 463.
Drake, R.E. (1976) *J. Volcanol. Geotherm. Res.*, 1, 265.

- Farrar, E.H., S.J. Clark, G.S. Haynes, H. Quirt, H. Conn, and M. Zentilli (1970) *Earth Planet. Sci. Lett.*, 10, 60.
- Kaneoka, I. and N. Takaoka (1980) *Science*, 208, 1366.
- Noble, D.C., E.H. McKee, E. Farrar and V. Peterson (1974) *Earth Planet. Sci. Lett.*, 21, 213.
- Schwab, K. and H. Lippolt (1976) *Proc. Symp. on Andean and Antarctic Volcanology Problems*, Santiago, Chile, 698.
- Steiger, R.H. and E. Jäger (1977) *Earth Planet. Sci. Lett.*, 36, 359-362.
- Stewart, J.W., J.F. Evernden and N.J. Snelling (1974) *Geol. Soc. Amer. Bull.*, 85, 1107.
- Thorpe, R.S. and P.W. Francis (1979) *Tectonophys*, 57, 53.
- Tosdal, R.M., E. Farrar, and A.H. Clark (1979) *J. Volcanol. Geother. Res.*, 10, 157.
- Weibel, Von M., M. Frangipane-Gysel and J. Hunziker (1978) *Geol. Rundsch.*, 67, 243.

THE LIST OF FISSION-TRACK AGES (1)

(1970 - 1978)

Yoshiyuki AMANO* and Susumu NISHIMURA**

- * Kadoma-Nishi High School, 29-1, Yanagida-Cho, Kadoma City, Osaka.
** Department of Geology and Mineralogy, Kyoto University, Kyoto.

Since fission-track method was developed by Fleischer et al. (1963), many researchers have been investigated on this method and have got many results.

It is interested in the collection of these data. These data are arranged according to the sampling area. The data of fission-track ages will be collected in this form.

The points of the arrangement of data,

1. The data reported are divided into nine areas of Japan, i.e. Hokkaido, Northern and Southern parts of Tohoku, Kanto, Tokai and Hokushin-etsu (Chubu), Kinki, Chugoku, and Kyushu area.
2. The data are arranged, as follows:

- i) Analyst
- ii) Sample No.
- iii) Fission-track age in M.Y.
- iv) Locality
- v) Geological setting
F. : Formation
G. : Group
- vi) Method
 - a) Material
V.R. : Volcanic rock V.G. : Volcanic glass
T : Tuff
Gr : Granite
GD : Grano-Diorite QD : Quartz-Diorite
Gn : Gneiss
 - b) Minerals and glass
Z : Zircon A : Apatite An : Anthophyllite
H : Hornblende M : Mica
 - c) Method and Etching condition
A : Grain by grain.
B : Grain by grain but calculating by numbers of tracks.
C : Grain by grain using SSTD method.
D : Population method.
E : Replica method.

Etching condition

- 1 : HF + H₂SO₄
- 2 : H₃PO₄
- 3 : HF
- 4 : HNO₃
- 5 : NaOH
- 6 : NaOH + KOH

- vii) Reference

Note : All of these data are calculated by the $\lambda_f = 6.85 \times 10^{-17}$ yr⁻¹, except the data of Ref. (15).

Analyst	Sample No.	F.T.Age (M.Y)	Locality	Geological setting	Method	Ref.	
1. Hokkaido Area							
S. Nishimura	SY74091801	4.2	Kitayuzawa, Usu,	Pliocene	V.R.-Z	1	
	SY74091901-1	1.6	Kitayuzawa, Usu,	Tertiary-Quaternary	V.R.-Z	1	
	SY74091901-2	1.7	Kitayuzawa, Usu,	Tokusyubetu lava	V.R.-Z	1	
	NG73112301	2.1	Nigorikawa, Kayabe,	Simazaki-gawa tuff F.	V.R.-Z	2	
	NG73112302	0.02	Nigorikawa, Kayabe,	Isikura F. Gravel	V.R.-Z	2	
	SK74100703	2.0	Syogingawa, Kayabe	Pliocene-Miocene	V.R.-Z	3	
	TJ74101019	1.9	Nagaoyama, Satuporo	Pleistocene-Pliocene	V.R.-Z	4	
	TJ74101020	8.5	Zyozankei, Satuporo		V.R.-Z	4	
	TJ74101301	15	Toyoha kozan	Zyozankei G.	V.R.-Z	4	
	TJ74101021	5.0	Siraigawa, Satuporo	Asari G. - Yamazawa F.	V.R.-Z	4	
2. Tohoku Area (North)							
Oga Penninsula, Akita Prefecture, Neogene							
S. Nishimura	30	2.8	Yasudanisi	Shibikawa G. pink tuff	T-Z	5	
	33	6.8	Yasudanisi	Wakimoto G. middle tuff	T-Z	5	
	38	7.5	Uryuhigasi	Kitaura G. Kitaura tuff	T-Z	5	
	2	12	Anzenjikita	Funakawa G Anzenji tuff	T-Z	5	
	27	13	Minamihirasawa	Funakawa G.	T-Z	5	
	6	16	nisikurosawa	Nisikurosawa G.	T-Z	5	
	23	20	Hokakejimakita	Daijima G. Welded tuff	T-Z	5	
	24	25	Sugorokuhigasi	Daijima G. pumice-flow	T-Z	5	
	12	26	Kamo	Monzen G. Shinzan Rhyolite	V.R.-Z	5	
	15	62	Akashimahigasi	Adamellite	Gr-z	5	
	S. Tamanyu	OG-6	6.9± 1.4	Anzenji	Funakawa F. Anzenji tuff	T-Z	6
		OG-5	31.2± 4.7	Sugorokuhigasi	Daijima F. pumice-flow	V.R.-Z	6
		OG-4	59.2± 8.7	Kamo	Monzen F. Shinzan Rhyolite	V.R.-Z	6
OG-2		61.2± 9.0	Akasima	Akasima F.	T-Z	6	
OG-3		67.2± 9.9	Akasima	Akasima F. Dacite	V.R.-Z	6	
OG-1		96.1± 13.6	Akasima	Palaeogene basement	Gr.-Z	6	
Hachimantai, Akita and Iwate Prefecture,							
S. Nishimura	HK74092903F	0.07	Yutamatakawa,	Quaternary	V.R.-Z	7	
	HN74081022k	1.6	Sumikawa	Sumikawa lava	V.R. Z	7	
	HN74090426K	1.70	Akakawa	Quaternary or Tertiary	V.R.-Z	7	

Hachimantai, Tamagawa welded tuff							
S. Tamanyu	Yanagizawa	1.3±0.3	Yanagizawa-rindo	Tamagawa-onsen, Akita	T-Z	} 8 8 8 8 8 6 6 6 6 6 6 6 6 6 6 6	
	Hasiba	1.2±0.3	Hasiba, Sizukuishi, Iwate		T-Z		
	Marimori	1.8±0.5	Marimori-rindo, Tamagawa	Tazawako, Akita	T-Z		
	Komatakayo	1.9±0.4	Komatagawa river, Kita-Akita,	Akita	T-Z		
	Iomagari	2.2±0.5	Iomagari, Tamagawa,	Akita	T-Z		
	Flux number were corrected with ratio of Cd by Tamanyu						
	IW-5	16.3± 2.4	Higasi, Kawabe, Akita	Onnagawa F. Tuff (t ₃)	T-Z		
	IW-4	16.4± 2.6	Junction of Sannai r. and Marumai r.	Onnagawa F. Kamisannai tuff	T-Z		
	IW-3	20.5± 3.5	Sugisawa r. Kawabe, Akita	Okuramata F. tuff(O ₂)	T-Z		
	IW-2	21.7± 3.1	Sugisawa r. Kawabe, Akita	Hagikata F. tuff (H ₃)	T-Z		
	IW-1	72.3±11.3	Sugisawa r., Kawabe, Akita	Hagikata F. Rhyolite	V.R.-Z		
	RY-4	6.9± 1.1	Hanayama, Yuta, Iwate	Hanayama F.	T-Z		
	RY-5	7.9± 1.2	Sitomae, Izawa, Iwate	Mizuyama F.	T-Z		
	RY-3	20.9± 3.5	Yuta, Waka, Iwate	Kotunagizawa F.	T-Z		
	RY-2	24.3± 3.6	Yuta, Waka, Iwate	Oishi F. Kawajiri tuff	T-Z		
	RY-1	208 ±30	Koiwazawa, Izawa, Iwate	Paleogen basement	GD-Z		
	S. Nishimura	KNF4	0.2	Kawarageshingi, Akita	Takamatudake lava		V.R.-Z
KNF2		0.32	Kigiyama, Akita	Quaternary	T-Z		
KNF5		0.34	Gosinuma, Akita	Kabutoyama pumice-flow	T-Z		
KNF1		2.1	Oyu Kita, Akita	Neogene-Tertiary	T-Z		
HK74091501		2.0	Simoyu, Aomori	Hakkoda welded tuff	T-Z		
HK74091504		2.1	Tashiro, Aomori	Hakkoda welded tuff	T-Z		
3. Tohoku Area (South)							
S. Nishimura	AN73102921	0.34	Uba spring, Yamagata	Azumayama volcanic rock	V.R.-Z	} 11 11 12 12 12	
	AN73101403	2.2	Itayakozan, Yamagata	Hachimoriyama F.	T-Z		
	TY74091804	0.81	Tuchiyu, Fukushima	Amanuma lava	V.R.-Z		
	TY74092601	0.81	Takayu, Fukushima	Naka Azuma lava	V.R.-Z		
	TY74091601	0.82	Omoiotaki, Azumayama, Fukushima	Takayama lava	V.R.-Z		
Miyagi Prefecture,							
S. Nishimura	KS73101615,	0.02	Uenono, Narugo,	Katanuma quartz andesite	V.R.-Z	} 13 13 13 13	
	KS73101615	0.2	Katanuma, Narugo	Katanuma quartz andesite	V.R.-Z		
	KS73101506	0.35	Ofukazawa, Nargo		V.R.-Z		
	KS74093002	1.5	Arayuzigoku, Narugo	Miyazawa F.	V.R.-Z		

S. Nishimura	KS74100204	1.8	Katayamazigoku, Nargo	Akazawa F.	V.R.-Z	13
	KS73101612	2.2	Sawamegi, Nargo	Kitagawa welded tuff	T-Z	13
	KS73101507	2.3	Karuizawa, Hanayama	Kitagawa welded tuff	T-Z	13
	KS73101616	2.4	Byobuiwa, Narugo	Kitagawa welded tuff	T-Z	13
	KS73101508	9.8	Kunimitoge, Hanayama	Kita-takizawa F.	T-Z	13
S. Tamanyu	SN(1)-15	4.5±0.9)	Hirosegawa, Sendai	Hirosegawa tuff	T-Z	14
		6.0±1.3)				
	SN(1)-14	5.4±1.6)	Hirosegawa, Sendai	Hirosegawa tuff	T-Z	14
		5.8±1.6)				
	SN(1)-12	8.1±1.4)	Misawa, Izumi	Kameoka F.	T-Z	14
		7.7±1.2)				
	SN(1)-13	8.5±1.6)	Tatunokuchi, Sendai	Tatunokuchi F.	T-Z	14
		8.8±1.7)				
	SN(1)- 6	10.4±1.4)	Sendai	Sirasawa F.	T-Z	14
		11.6±1.6)				
	SN(1)-11	10.6±1.5)	Misawa, Izumi	Sirasawa F.	T-Z	14
		11.3±1.7)				
	SN(1)- 4	12.4±1.5)	Aobadai, Sendai	Tunaki F.	T-Z	14
	SN(1)- 8	13.4±1.9)	Akiho, Natori	Sirasawa F.	T-Z	14
		13.6±2.0)				
	SN(1)- 5	13.5±1.6)	Aobadai, Sendai	Tunaki F.	T-Z	14
		14.5±1.8)				
	SN(1)- 9	16.5±2.1)	Dosyo, Izumi	Ozutumi F.	T-Z	14
		14.8±2.0)				
	SN(1)- 3	17.1±2.4)	Sahoyama, Sendai	Hatatachi F.	T-Z	14
	20.5±2.8)					
SN(1)- 7	17.5±2.1)	Nakatani, Sendai	Yumoto F.	T-Z	14	
	17.1±2.0)					
SN(1)- 1	18.4±2.2)	Natorigawa, Sendai	Takadachi Volcanic Rock	V.R.-Z	14	
	18.3±2.1)					
SN(1)-10	19.1±2.5)	Dosyo, Izumi	Ozutumi F.	T-Z	14	
SN(1)- 2	19.5±2.4)	Atagoyama, Sendai	Tukigi F.	T-Z	14	
	14.7±1.8)					

* Flux number were corrected with ratio of Cd by Tamanyu

4. Kanto Area
Kanto Loam

M. Suzuki	4.9±0.5(x10 ⁴)	Taikanyama, Hakone	Tokyo pumice,	V.G.	} (-3) 15 15 15
	6.6±0.6(x10 ⁴)	Taikanyama, Hakone	Oharadai pumice	V.G.	
	7.3±0.4(x10 ⁴)	Sagamihara and	Ontake 1st pumice	V.G.	
	7.7±0.8(x10 ⁴)	Uenohara		V.G.	

Kanto Loam

M. Suzuki	7.8±1.0(x10 ⁴)	} Sagamihara and	} Ontake 1st pumice	V.G.	} 15
	8.2±1.0(x10 ⁴)			} Uenohara	
	9.5±0.5(x10 ⁴)	} Tuchiya, Oiso hill	V.G.		
	8.9±1.3(x10 ⁴)		Simosueyosi loam, pumice	V.G.	
	9.8±1.2(x10 ⁴)		Simosueyosi loam, pumice	V.G.	
	12.8±1.1(x10 ⁴)		Simosueyosi loam, pumice	V.G.	
	11.7±1.0(x10 ⁴)		Simosueyosi loam pumice	V.G.	
13.2±1.0(x10 ⁴)	Simosueyosi loam, pumice	V.G.			

yr.

S. Nishimura	SS74100207	0.05	Setusyokawara, Kusatu, Gunma	Setusyo lava	V.R.-Z	} 16
	SS74100209	0.8	Siraminekozan, Kusatu, Gunma	Matuoazawa lava	V.R.-Z	
	SS74092814	1.8	Manza, Kusatu, Gunma	Takai lava	V.R.-Z	
T. Suzuki	77051001-02TS	65.1±3.2*	Gotanda, Ogawamachi, Saitama	Ogawamachi G. Miocene	GD-Z	} 17
	77051001-01TS	67.4±2.3*	Gotanda, Ogawamachi, Saitama	Ogawamachi G. Miocene	Gr-Z	
	70060906TS	149±9*	Kanisawa, Ogawamachi, Saitama	Kinsyoazan-quartz Diorite	QD-Z	

* Corrected with the etching efficiency of Zircon

5. Chubu Area (Tokai)

S. Nishimura	481225003	2.2	Kameno-ko, Shizuoka	Takegawa G.Hosoya tuff	T-Z	} 18
	481225001	2.8	Iozumihigasi, Shizuoka	Takegawa G.Iozumi tuff	T-Z	
	481226007	5.8	Niino, Shizuoka	Takegawa G.Ariga tuff	T-Z	
	481225001	16	Iozumi-higasi, Shizuoka	Takegawa G.Iozumi tuff	T-Z	
	481226007	18	Niino, Shizuoka	Takegawa G.Ariga tuff	T-Z	
	JGTZ-5	5.1	Takaneyama, Izu, Shizuoka	Sirahama F. Miocene	V.R.-Z	19
J. Nagai		94	Fujioka, Aichi	Gaerome clay	-Z	} 20
		120	Tochihara, Gifu		Gn-Z	

6. Chubu Area (Hokusinetu)

S. Nishimura	NR5	16.0	Nyu mountainland, Fukui	Ito F.Nunogadaki volcanic rock	V.R.-Z	} 21
	NS4	18.6	Nyu mountainland, Fukui	Ito F.Sasagawa volcanic rock	V.R.-Z	
J. Nagai		120	Senjugahara, Tateyama, Toyama	} 175-193m.y. (Rb-Sr)	V.R.-Z	} 20
		150	Senjugahara, Tateyama, Toyama		V.R.-Z	
		250	Senjugahara, Tateyama, Toyama		Gn-Z	

7. Kinki Area

Core sample of Lake Biwa, Kobiwako Group, and Osaka Group

S. Nishimura	BB85	8.0(x10 ⁴ yr.)	200m core Sample, 37m		T-Z	} (B - 1)	22
	BB153	1.1(x10 ⁵ yr.)	200m core Sample, 62m		T-Z		22
	BB195	1.7(x10 ⁵ yr.)	200m core Sample, 82.2m		T-Z		23
	BB239	1.8(x10 ⁵ yr.)	200m core Sample, 99m		T-Z		22
	BB267	2.7(x10 ⁵ yr.)	200m core Sample, 110.0m		T-Z		23
	BB453	4.6(x10 ⁵ yr.)	200m core Sample, 181.2m		T-Z		23
	BB161-d	0.47	1000m core Sample, 386.7-389.3m		T-Z		24
T. Danhara	BE1001	2.12		Kobiwako G. Gamo F. Murasaki tuff	T-Z (A-1)	25	
S. Nishimura	BW2	7.0(x10 ⁵ yr.)		Katata F. Ogoto clay	T-Z (B-1)	23	
			Kono I tuff	2.2	Hino, Gamo, Siga	Kobiwako G. Kono I tuff	T-Z (B-2)
T. Danhara	BE1002	2.23		Gamo F. Kono III tuff	T-Z (A-1)	25	
	BE1004	2.35		Gamo F. Kono II tuff	T-Z (A-1)	25	
S. Nishimura	Sagami tuff	2.9	Sagami, Kooga, Siga	Sagami tuff, 3.0m.y. (Paleomag.)	T-Z	26	
	Masugi tuff	3.1	Kamimasugi, Kooga, Siga	Masugi Tuff, 3.05m.y. (Paleomag.)	T-Z	26	
S. Nishimura		0.37±0.04	Osaka Univ. Toyonaka, Osaka	Osaka G. Kasuri tuff	T-A (B-2)	26	
		0.38±0.03	Osaka Univ. Toyonaka, Osaka	Osaka G. Kasuri tuff	T-An (B-4)	26	
		0.87±0.07	Senrigawa, Toyonaka, Osaka	Osaka G. Azuki tuff	T-H (B-3)	26	
		1.1 ±0.1	Komyoike, Izumi, Osaka	Osaka G. Komyoike tuff	T-Z (B-2)	26	
		1.5 ±0.2	Meisei, Sakai, Osaka	Osaka G. Grey-Maisei tuff	T-Z (B-2)	26	
		2.3 ±0.2	Simakumayama, Toyonaka, Osaka	Osaka G. Simakumayama tuff	T-H (B-3)	26	
		2.4 ±0.3	Simakumayama, Toyonaka, Osaka	Osaka G. Simakumayama tuff	T-Z (B-2)	26	
T. Matuda & T. Danhara		1.6	Fugenji, Tanabe, Kyoto	Osaka G. Fugenji tuff	T-Z (A-1)	27	
		2.2	Fugenji, Tanabe, Kyoto	Osaka G. Higasihata tuff	T-Z (A-1)	27	
J. Nagai		85	Kitasirakawa, Kyoto	99-93 m.y. (Rb-Sr)	Gr-Z (C-2)	20	
S. Nishimura		225	Jito-nisi, Maizuru, Kyoto	Shered granite, Triassic	Gr-Z (B-1)	28	
		420	Tatehara, Ohe, Kyoto	Shered granite, Permian	Gr-Z (B-1)	28	

J. Nagai	91	Kasagi, Nara		Gr-Z (C-2)	20
S. Nishimura	51	Akenobe, Yabu, Hyogo	Post-ore, 52.6my, 57.8my (K-Ar)	V.R-Z	29
	52	Akenobe, Yabu, Hyogo	Post-ore,	V.R.-Z	29
	52	Akenobe, Yabu, Hyogo	Post-ore,	V.R.-Z	29
	52	Ikuno, Asagi, Hyogo	Post-ore,	V.R.-Z	29
	55	Akenobe, Yabu, Hyogo	Post-ore,	V.R.-Z	29
	65	Nakase, Hyogo	Pre-ore	V.R.-Z	29
	70	Ikuno, Asagi, Hyogo	Pre-ore 72.8my. (K-Ar)	V.R.-Z	29
	72	Nakase, Hyogo	Pre-ore	QD-Z	29
	75	Ariga, Haga, Hyogo	Pre-ore	Gr-Z	29
	115	Fudonotaki, Haga, Hyogo	Yakuno metamorphic rock	Gn-Z	29
	83	Rokkozan, Hyogo	96my. (Rb-Sr): Kikozan	G-M (B-3)	30
	85	Rokkozan, Hyogo		G-Z (B-2)	30

8. Chugoku and Sikoku Area

J. Nagai	94	Yasuda, Kisa, Hiroshima	104-111my. (Rb-Sr)	Gr-Z (C-2)	20
	94.2±2.6	Yasuda, Kisa, Hiroshima		Gr-Z (C-2)	20
S. Nishimura	95*	Tai, Yamaguchi	424my (K-Ar), 406my (Rb-Sr)	GD-M (A-3)	30
	400	Tai, Yamaguchi		GD-Z (B-2)	30

* Corrected with length of fission track

9. Kyusyu and Okinawa Area

Pyroclastic flow deposit in South Kyusyu, Pliocene to Late Pleistocene

S. Nishimura	197	2.5(x10 ⁴ yr.) Asahi, Kajiki, Kagosima	Chikuri pyroclastic flow	T-Z (-2)	31
	18	6.3(x10 ⁴ yr.) Daimyoji, Kokubu, Kagosima	L.Pleist.	T-Z (-2)	31
	191	7.2(x10 ⁴ yr.) Shinkawa, Hayato, Kagosima	Shinkawa pyroclastic flow	T-Z (-2)	31
	209-b	0.082 Tamachi, Hitoyosi, Kumamoto	L.Pleist.	T-Z (-1)	32
	728	1.1(x10 ⁵ yr.) Higasi-Urusida, Hitoyosi	Kakuto pyroclastic flow	T-Z (-2)	31
	22	1.9(x10 ⁵ yr.) Shomyoji, Ebino, Miyazaki	Shomyoji F.Kakuto G.	T-Z (-2)	31
	230-8	1.0 Kusakidan, Hiwaki, Kagosima	Nagano F.	T-Z (-1)	32
	230-4	1.0 Kusakidan, Hiwaki, Kagosima	Nagano F.	T-Z (-1)	32
	209-a	1.2 Tamachi, Hitoyosi, Kumamoto	L. pleist.	T-Z (-1)	32
	465	1.2 Yamanokuchi, Iriki, Kagosima	Nagano F.	T-Z (-1)	32
	260-A	1.2 Kiminagawa, Izumi, Kagosima	L.Pleist.	T-Z (-2)	31
	150	1.3 Kiminagawa, Izumi, Kagosima	L.Pleist.	T-Z (-2)	31
	270	1.3 Hiyamizu, Sendai, Kagosima	Sendai pyroclastic flow	T-Z (-1)	32
	132	1.4 Goino, Kagosima, Kagosima	Goino pyroclastic flow	T-Z (-1)	32

S. Nishimura	ST73112901	2.5(x10 ⁴ yr.)	Ibusuki, Kagoshima	Pleistocene	V.R.-Z	33
	ST73112406	2.6(x10 ⁴ yr.)	Yamakawa, Kagoshima	Takeyama lava, Pleist.	V.R.-Z	33
	ST73111507	2.7(x10 ⁴ yr.)	Yamakawa, Kagoshima	Yamakawa lava, Pleist.	V.R.-Z	33
	ST73111311	3.0(x10 ⁴ yr.)	Ibusuki, Kagoshima	Uomidake lava, Pleist.	V.R.-Z	33

Reference

1. Yamaguchi, S., T. Igarashi, Y. Chiba, S. Sato and S. Nishimura (1978) Rept. Geol. Surv. Japan No. 259, 43-84
2. Igarashi, T., K. Sato, T. Ide, S. Nishimura, K. Sumi (1978) Rept. Geol. Surv. Japan No. 259, 85-180
3. Igarashi, T., M. Ishida, N. Okamura, K. Aoki, S. Yamaguchi and S. Nishimura (1978) Rept. Geol. Surv. Japan, No. 259, 181-238
4. Igarashi, T., Y. Furukawa, K. Sugawara, S. Nishimura and K. Okabe (1978) Rept. Geol. Surv. Japan No. 259, 9-42
5. Nishimura, S. and S. Ishida (1972) Jour. Japan. Assoc. Min. Petr. Econ. Geol. 67, 166-168
6. Tamanyu, S. (1978) Jour. Geol. Soc. Japan. 84, 489-503
7. Takashima, I., H. Fuchimoto, Y. Kubota, I. Hayashi and S. Nishimura (1978) Rept. Geol. Surv. Japan. 259, 281-310
8. Tamanyu, S., and S. Sudo (1978) Bull. Geol. Surv. Japan. 29, 159-169
9. Nishimura, S., M. Taniguchi and K. Sumi (1976) Bull. Geol. Surv. Japan. 27, 713-717
10. Nishimura, S., H. Sato and K. Yamada (1977) Bull. Geol. Surv. Japan. 28, 593-595
11. Togashi, U., Y. Kubota, E. Yamada and S. Nishimura (1978) Rept. Geol. Surv. Japan. 259, 415-436
12. Togashi, U., H. Sato, M. Takahazu, Y. Chiba, S. Nishimura and K. Suzuki (1978) Rept. Geol. Surv. Japan. 259, 437-466
13. Yamada, E., H. Okada, S. Nishimura, M. Taniguchi and H. Natori (1978) Rept. Geol. Surv. Japan. 259, 341-376
14. Tamayu, S. (1975) Jour. Geol. Soc. Japan. 81, 233-246
15. Machida, H., and M. Suzuki (1971) Kagaku, 41, No. 5, 263-270
16. Ueno, M., H. Mato, K. Kinbara and S. Nishimura (1978) Rept. Geol. Surv. Japan. No. 259, 467-516
17. Watanabe, K., and T. Suzuki (1978) Anu. Rep. Univ. Tukuba, No. 4 (in press)
18. Nishimura, S. (1975) Tsukumo Earth Science, 10, 1-8
19. Takashima, I., M. Mogi and S. Nishimura (1978) Rept. Geol. Surv. Japan. No. 259, 517-536
20. Nagai, J. (1970) Tsukumo Earth Science, 5, 9-19
21. Hirooka, K., T. Okude and S. Nishimura (1972) Fukui Univ. Kyoiku-faculty, Kiyo, II, 22, 1-15
22. Nishimura, S. and T. Yokoyama (1974) Paleolimnology of Lake Biwa and the Japanese Pleistocene, 2, 38-46
23. Nishimura, S. and T. Yokoyama (1975) Paleolimnology of Lake Biwa and the Japanese Pleistocene, 3, 138-142
24. Takemura, T., S. Nishimura, T. Danhara and T. Yokoyama (1976) Paleolimnology of Lake Biwa and the Japanese Pleistocene, 4, 155-157
25. Yokoyama, T., T. Danhara, Y. Kobata and S. Nishimura (1977) Paleolimnology of Lake Biwa and the Japanese Pleistocene, 5, 44-53
26. Nishimura, S. and S. Sasajima (1970) Earth Science, 24, 222-224
27. Matuda, T. and T. Danhara (1978) Doshisya Univ. Kouchi-gakujyutu-chyosa Iinkai chyosa-shiryu, 13, 33-36
28. Nishimura, S., K. Katura and S. Sasajima (1976) Jour. Geol. Soc. Japan. 82, 413
29. Nishimura, S. (1976) Jour. Japan. Assoc. Min. Petr. Econ. Geol. 71, 323-326

30. Nishimura, S. (1970) Jour. Japan. Assoc. Min. Petr. Econ. Geol. 64, 173-181
31. Nishimura, S. and M. Miyaji (1973) Jour. Japan. Assoc. Min. Petr. Econ. Geol. 68, 225-229
32. Nishimura, S. and M. Miyaji (1976) Jour. Japan. Assoc. Min. Petr. Econ. Geol. 71, 360-362
33. Kamiya, M., S. Nakagawa, S. Nishimura and K. Sumi (1978) Rept. Geol. Surv. Japan. No. 259, 537-578

AUTHOR INDEX

AKIMOTO, Takatoshi	see Onda, Y.	
	see Kikawa, E.	
AMANO, Yoshiyuki and S. Nishimura		117
DHARMA, Agus	see Torii, M.	
DOMEN, Haruo		33, 49, 61, 96
DOMEN, H. and H. Muneoka		36
	also see Muneoka, H.	
FUNAKI, Minoru		80, 88
FUKAO, Yoshio	see Kono, M.	
FURUTA, Toshio	see Onda, Y.	
	see Kikawa, E.	
	see Kobayashi, K.	
HAMANO, Yozo	see Tsunakawa, H.	
	see Kono, M.	
	see Heki, K.	
HEKI, Kosuke, Y. Hamano	and M. Kono	72
	also see Kono, M.	
ISHII, Teruaki	see Kobayashi, K.	
ITO, Haruaki		27
ITO, H., K. Tokieda and Y. Notsu		24
	also see Notsu, Y.	
KANEOKA, Ichiro		111
KIKAWA, E., T. Akimoto, H. Kinoshita and T. Furuta		17
KINOSHITA, Hajimu	see Kikawa, H.	
	see Kono, M.	
KOBAYASHI, Kazuo, T. Furuta and T. Ishii		106
KONO, Masaru, Y. Fukao, Y. Hamano, K. Heki, H. Kinoshita, Y. Onuki, A. Taira, T. Ui and L. Ocola		66
	also see Heki, K.	
MATSUDA, Takaaki	see Otofujii, Y.	
MUNEOKA, Hiroshi and H. Domen		99
	also see Domen, H.	
NAKAJIMA, Tadashi		13
NISHIMURA, Susumu	see Amano, Y.	
NOTSU, Yukio and H. Ito		53
	also see Ito, H.	
OCOLA, Leonidas	see Kono, M.	
ONDA, Yuichi, S. Sugihara, T. Furuta and T. Akimoto		4
ONUSKI, Yoshio	see Kono, M.	
OSHIMA, Osamu		102
OTOFUJII, Yo-ichiro and T. Matsuda		41
SUGIHARA, Shigeo	see Onda, Y.	
TAIRA, Asahiko	see Kono, M.	
TOKIEDA, Katsuyasu	see Ito, H.	
TORII, Masayuki, A. Dharma and T. Yokoyama		1
TOSHA, Toshiyuki		56
TSUNAKAWA, Hideo and Y. Hamano		9
UI, Tadahide	see Kono, M.	
YOKOYAMA, Takuo	see Torii, M.	